AD NUMBER

AD485614

NEW LIMITATION CHANGE

TO

Approved for public release, distribution unlimited

FROM

Distribution authorized to U.S. Gov't. agencies and their contractors; Critical Technology; JUN 1966. Other requests shall be referred to Rome Air Development Center, ATTN: EMLI, Griffiss AFB, NY 13440.

AUTHORITY

RADC ltr dtd 9 Jul 1975

RADC-TR-66-306

PREFERRED-CIRCUIT TECHNIQUES FOR REFLECTION-TYPE PARAMETRIC AMPLIFIERS

David Kaye

TECHNICAL REPORT NO. RADC-TR-66-306
June 1966

Rome Air Development Center
Research and Technology Division
Air Force Systems Command
Griffiss Air Force Base, New York

When US Government drawings, specifications, or other data are used for any purpose other than a definitely related government procurement operation, the government thereby incurs no responsibility nor any obligation whatsoever; and the fact that the government may have formulated, furnished, or in any way supplied the said drawings, specifications, or other data is not to be regarded, by implication or otherwise, as in any manner licensing the holder or any other person or corporation, or conveying any rights or permission to manufacturer, use, or sell any patented invention that may in any way be related thereto.

Do not return this copy. Retain or destroy.

PREFERRED-CIRCUIT TECHNIQUES FOR REFLECTION-TYPE PARAMETRIC AMPLIFIERS

David Kaye

AFLC, GAFB, N.Y., 13 Jul 66-151

FOREWORD

This report was prepared by the Applied Electronics Division of Airborne Instruments Laboratory (AIL), a Division of Cutler-Hammer, Inc., Deer Park, New York as 5591-TDR-2, under Contract No. AF30(602)-3583, Project 4540, Task No. 454002, for the Rome Air Development Center.

The work was performed by the Applied Electronics Division of Airborne Instruments Laboratory by Mr. David Kaye under the direction of Mr. Stanley Becker, Section Head, and Mr. Gerald Kanischak, Group Leader. The author gratefully acknowledges the many helpful discussions with Mr. Robert Steven, Mr. Peter Lombardo, and Mr. James Whelehan of AIL.

RADC Project Engineer was Hollis J. Hewitt, EMCVI-1.

Release of subject report to the general public is prohibited by the Strategic Trade Control Program, Mutual Defense Assistance Control List (revised 6 January 1965), published by the Department of State.

This technical report has been reviewed and is approved.

Approved: Hollis J. Hewitt
HOLLIS J. HEWITT
Task Engineer
Analysis and Prediction Unit

Approved: Samuel D. Zaccari
SAMUEL D. ZACCARI
Chief, Vulnerability Reduction Br
Communications Division

ABSTRACT

This report describes the development and analysis of preferred-circuit techniques for the reduction of certain RFI effects in reflection-type parametric amplifiers.

Emphasis is placed on reducing spurious responses and increasing the saturation power of paramps. Some of the preferred-circuit techniques are incorporated in experimental models, and extensive measurements are reported which support the theoretical predictions of the effects of intermodulation products on paramp performance and the effect of the balanced configuration on spurious responses. Many additional characteristics of the models are described.

TABLE OF CONTENTS

Appendices (Cont) Page

LIST OF ILLUSTRATIONS

1. INTRODUCTION

This report describes the work performed on Contract AF 30(602)-3583 to study interference effects in, and to develop preferred-circuit techniques for, reflection-type parametric amplifiers.

The approach to the development has been to analyze the effect of a preferred-circuit technique on the RFI effects as well as on the desired operating performance characteristics. When this analysis shows promise for improvement in the reduction of RFI effects, and the compromise of desired operating performance is reasonable, the circuit technique is evaluated in practice.

This approach to preferred-circuit development minimizes the amount of cut-and-try experimentatation, because the results of a relatively few circuits can be used to validate a theory. Thus, an overall economy of effort results. Much of the analytical work and all of the relevant measurement results are described in this report.

The interference effects (Appendix I) that are of concern in parametric amplifiers (paramps) are:

1. Spurious responses (intermodulation between the pump and the signal),
2. Saturation of the amplifier by a large input signal,
3. Intermodulation between two input signals,
4. Cross modulation between two input signals,
5. Desensitization of the amplifier by an interfering input signal,
6. Gain-recovery time of the amplifier after a desensitizing pulse of interfering signal.

Preferred-circuit techniques have been developed on this program which reduce interference effects 1 and 2 of the above list. In addition, techniques are suggested to improve amplifier performance with respect to interference effects 3, 4, 5, and 6.

Spurious responses due to intermodulation between the pump and the signal are the major RFI problem in paramps, and the greater part of the theoretical analysis in this report is devoted to this problem. A rigorous analysis is presented which shows the worst-case effect of spurious responses upon the major performance parameters (gain-bandwidth product, and noise temperature) in a single-diode paramp.

Analysis is presented which demonstrates the advantage of a balanced paramp configuration for spurious-response reduction, and the worst-case effect of spurious responses upon the major performance parameters in a balanced paramp is demonstrated.

Another performance parameter that is of interest in a paramp is its tunability without drawing bias current and thereby degrading the noise temperature.

Two experimental balanced paramps were designed and built in the 900-MHz range. One amplifier was used as a control for experiments while, in the other, several preferred-circuit techniques were incorporated and tested. Data on the interference effects and the performance of each amplifier are given in this report.

2. THEORY OF OPERATION OF REFLECTION-TYPE PARAMETRIC AMPLIFIER

A reflection-type parametric amplifier can be thought of as a transmission line terminated in a negative resistance. Consider a uniform transmission line of characteristic impedance Z_0 terminated in a resistor of resistance R. The reflection coefficient Γ at the input of the line is:

$$\Gamma = \frac{R - Z_0}{R + Z_0} \tag{1}$$

Therefore, for a positive resistance R,

$$|\Gamma| \leq 1$$

Since the power gain of a transmission line terminated in some impedance is given by:

$$G = |\Gamma|^2 \tag{2}$$

and for this case

$$G \leq 1$$

a positive resistance terminating a transmission line results in a power loss rather than a power gain.

If the same transmission line is terminated in a negative resistor of resistance -R, the reflection coefficient at the input of the line is given by:

$$\Gamma = \frac{-R-Z_0}{-R+Z_0} \tag{3}$$

Therefore, for a negative resistance,

$$|\Gamma| \geq 1$$

The power gain in this case is

$$G \geq 1$$

and it can be seen that a negative resistance terminating a uniform transmission line results in a power gain rather than a power loss.

The actual expression for the mid-band power gain of a reflection-type paramp can be obtained from equation II-58 in Appendix II by not allowing sum-frequency propagation ($K_3 = \infty$)

$$|\Gamma_o|^2 = \left| \frac{1 - K_o - \frac{M^2}{f_1 f_2 (1+K_2)}}{1 + K_o - \frac{M^2}{f_1 f_2 (1+K_2)}} \right|^2 \qquad (4)$$

where $|\Gamma_o|$ = mid-band voltage gain

f_1 = signal frequency

f_2 = idler frequency

K_o = the ratio of the generator output resistance to the varactor-junction series resistance

K_2 = the ratio of the external idler-circuit resistance to the varactor-junction series resistance

M = a varactor figure of merit, defined by equation II-57 in Appendix II.

The derivations in Appendices II, III, IV, VI, VII, and VIII are based on a characterization of the varactor as a time-varying elastance rather than a time-varying capacitance. Capacitance notation is commonly used in the literature, (references 1, 2, 3, 4, and 5). Although either

characterization can be used, there is an advantage in using the time-varying elastance.

To show the advantage of the use of elastance rather than capacitance, a computer study was performed on the equations of the capacitance and elastance for the varactors which were used in the experimental amplifiers. Figure 1 is a curve of manufacturer's data on junction capacitance versus voltage for the two D5270 silicon graded-junction varactors used in the experimental amplifiers.

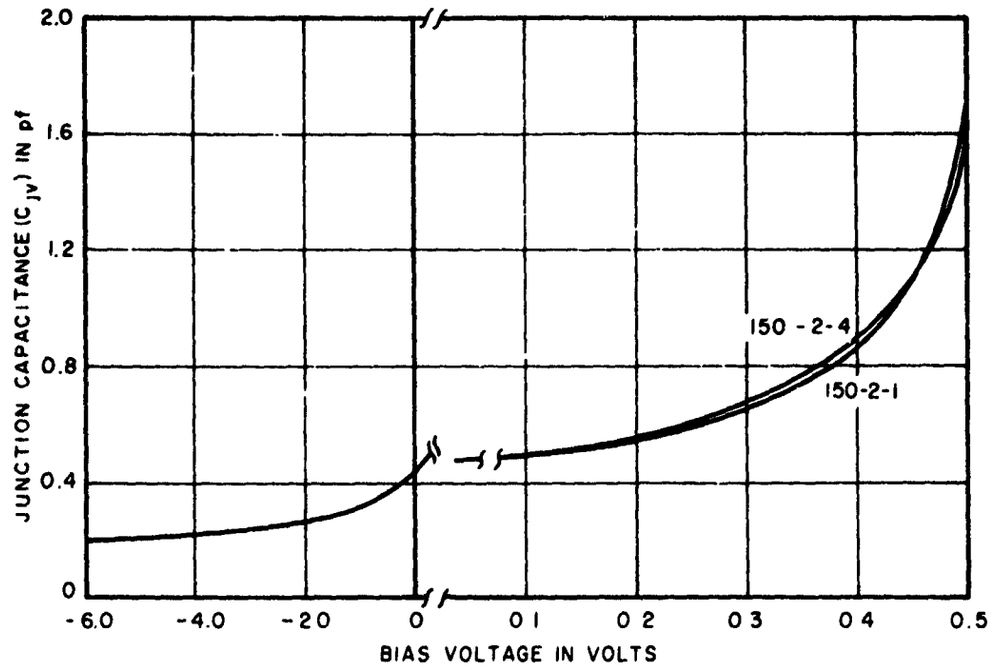

FIGURE 1. JUNCTION CAPACITANCE VERSUS BIAS VOLTAGE FOR SYLVANIA D5270 VARACTORS

The varactors are considered to be pumped by a cosinusoidally varying source, and a computer program was written which gave the Fourier series of the capacitance versus time curve of each varactor. The capacitance-voltage curves are then inverted, and the Fourier series of the elastance-versus-time curves are computed. The following data are the computer results.

VARACTOR D5250 (150-2-1)

$$C(t) = .3403 + .1777\cos\omega t + .1151\cos 2\omega t + .1002\cos 3\omega t + .08634\cos 4\omega t + .08076\cos 5\omega t + .07464\cos 6\omega t + .07093\cos 7\omega t + .06682\cos 8\omega t$$

$$S(t) = 3.449 - 1.167\cos\omega t - .3139\cos 2\omega t - .2668\cos 3\omega t - .1533\cos 4\omega t - .1434\cos 5\omega t - .1039\cos 6\omega t - .09872\cos 7\omega t - .0732\cos 8\omega t$$

VARACTOR D5270 (150-2-4)

$$C(t) = .3387 + .1776\cos\omega t + .1179\cos 2\omega t + .1021\cos 3\omega t + .08853\cos 4\omega t + .08285\cos 5\omega t + .07596\cos 6\omega t + 07222\cos 7\omega t + .06861\cos 8\omega t$$

$$S(t) = 3.4730 - 1.159\cos\omega t - .3393\cos 2\omega t - .2705\cos 3\omega t - .1546\cos 4\omega t - .1526\cos 5\omega t - .1017\cos 6\omega t - .09691\cos 7\omega t - .07851\cos 8\omega t$$

The computed equations above show that the elastance series converges more rapidly than the capacitance series and that, therefore, the assumption $S_n = 0$ where $n = 2, 3\ldots$ is much better than the assumption that $C_n = 0$ where $n = 2, 3, \ldots$ Thus, an approximation using the elastance analysis for a given finite number of terms is more nearly exact than an approximation using the capacitance analysis.

Further illustration of this point is achieved by feeding the C(t) and S(t) series back into the computer and asking for the C(t) and S(t) curves to be plotted. Figures 2 and 3 give the C(t) curve and the inverted S(t) curve, as computed from eight Fourier coefficients, and compare them with the theoretical C(t) curve. It is clear from these comparisons that the S(t) analysis yields a curve that is much closer to the theoretical.

Equations, 5 and 6 are found in the literature (reference 6) for the voltage gain-bandwidth product and noise temperature of a single-diode

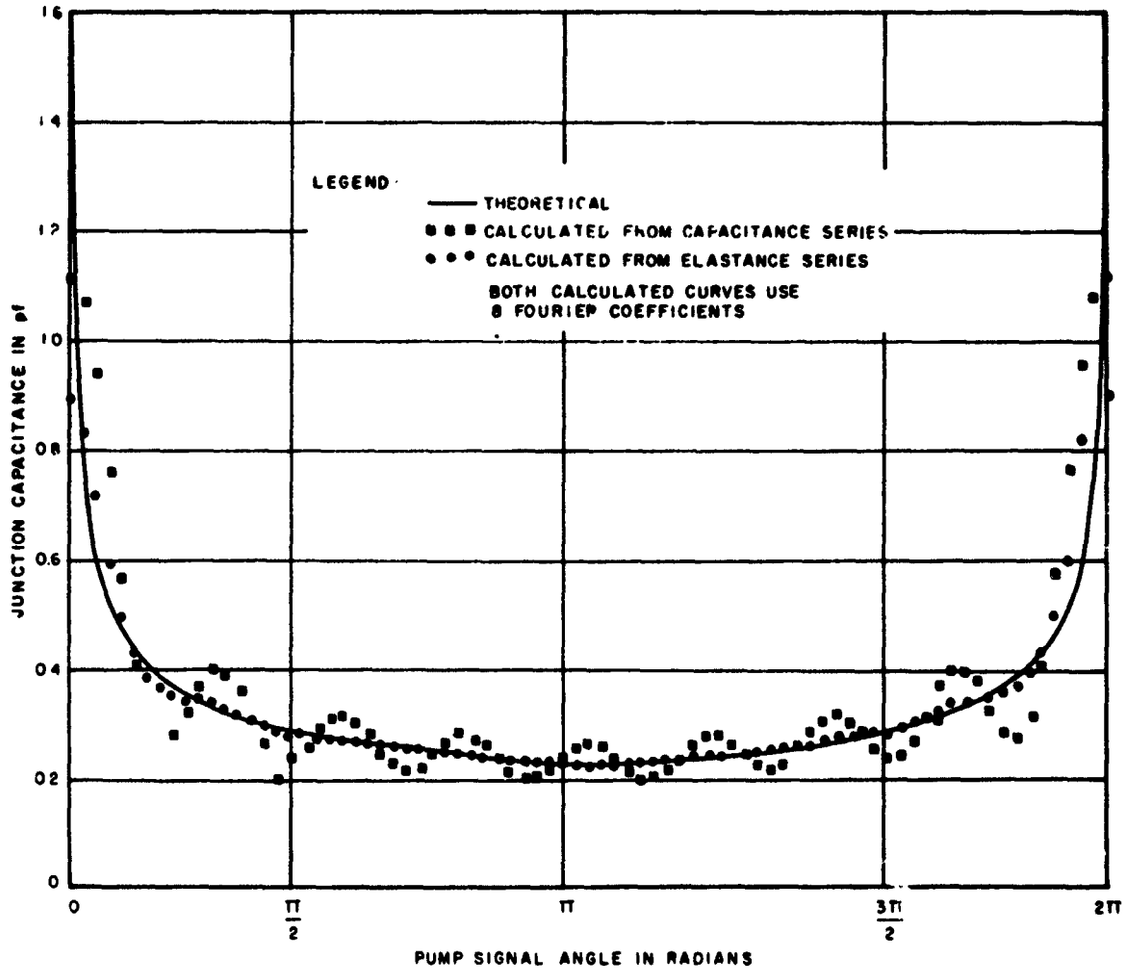

FIGURE 2. CALCULATED TIME-VARYING CAPACITANCE FOR VARACTOR NO. 150-2-1

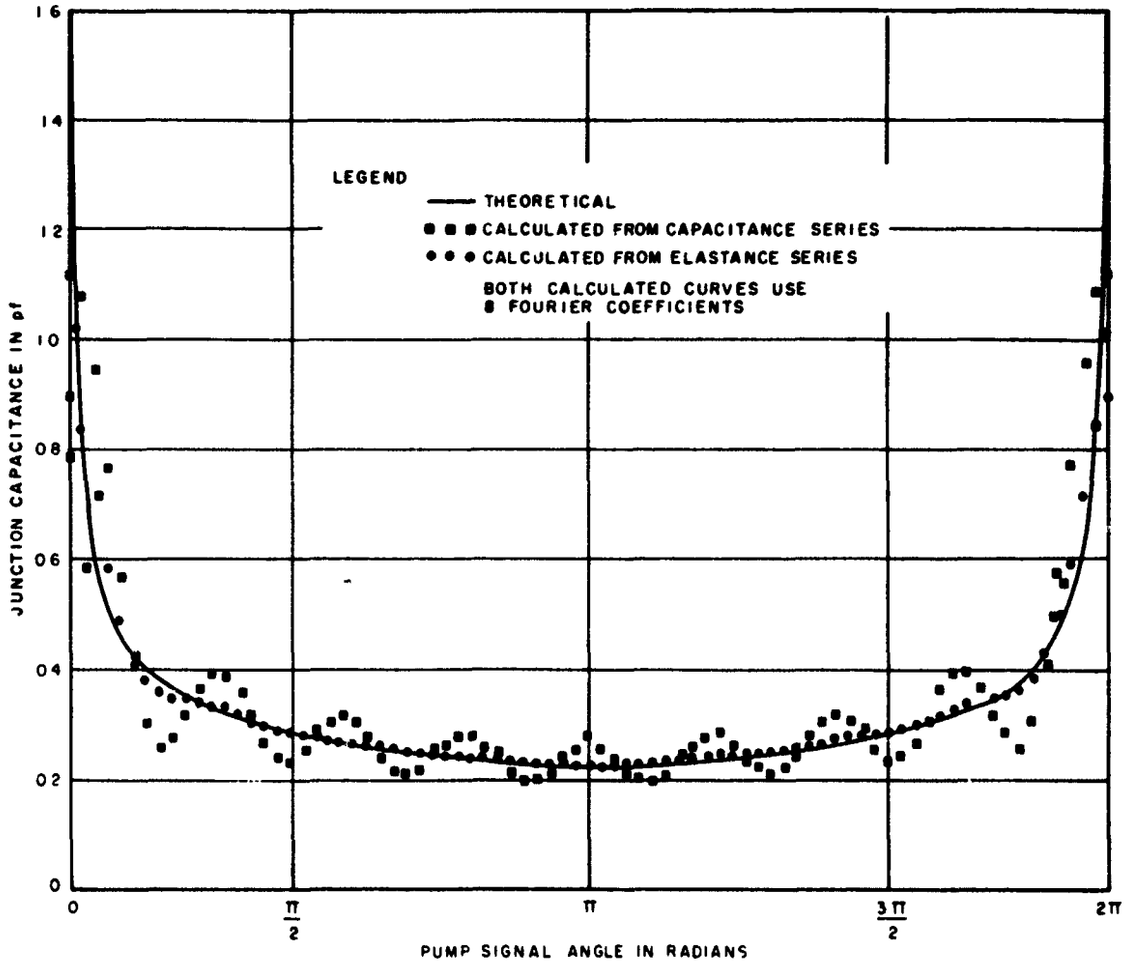

FIGURE 3. CALCULATED TIME-VARYING CAPACITANCE FOR VARACTOR NO. 150-2-4

reflection-type parametric amplifier. The gain-bandwidth product and the noise temperature are the most important performance relations for a single-diode reflection-type parametric amplifier.

The voltage gain-bandwidth product is:

$$|\Gamma_o| \quad X_{3db} = \left[1 - \frac{f_1 f_2}{M^2}\right]\left[\frac{2 f_1}{Q_1 + Q_2 \frac{f_1}{f_2}}\right] \tag{5}$$

where Q_1 = signal circuit loaded Q

Q_2 = idler circuit loaded Q

X_{3db} = 3-db bandwidth of the amplifier

The normalized effective noise temperature is:

$$\frac{T_e}{T_o} = \frac{\frac{f_1 f_2}{M^2} + \frac{f_1}{f_2}}{1 - \frac{f_1 f_2}{M^2}} \tag{6}$$

where T_e = effective noise temperature of the amplifier in degrees K

T_o = ambient of the amplifier in degrees K

Spurious responses due to intermodulation between the pump and the signal are the major RFI problem in paramps. Therefore, a rigorous analysis is performed which shows the worst-case effect of spurious responses on the major performance parameters in a single-diode reflection-type paramp (Appendices II, III, and IV).

The worst-case effect is that of sum-frequency (pump frequency plus signal frequency) propagation in the varactor. Equations 7 and 8 describe the voltage gain-bandwidth product and the noise temperature of a single-diode reflection-type parametric amplifier with sum-frequency

propagation and arbitrary loading at the sum and difference frequencies.

$$|\Gamma_o|_{X_{3db}} = \left[\frac{2}{1 + \frac{1}{K_o}}\right] \left[\frac{B_1}{1 + \frac{B_1}{B_2}[U] - \frac{B_1}{B_3}[V]}\right] \qquad (7)$$

where

$$U = \frac{1}{1 - \frac{f_2(1 + K_2)}{f_3(1 + K_3)}}$$

$$V = \frac{1}{\frac{f_3(1 + K_3)}{f_2(1 + K_2)} - 1}$$

B_1, B_2, B_3 = loaded bandwidths at f_1, f_2, f_3, respectively

K_3 = the ratio of the circuit resistance at the external sum frequency to the varactor-junction series resistance

f_3 = sum frequency (pump + signal).

$$T_e = \frac{T_o}{K_o}\left[1 + \frac{M^2}{f_2^2(1 + K_2)} + \frac{M^2}{f_3^2(1 + K_3)}\right] \qquad (8)$$

When sum-frequency propagation is suppressed ($K_3 = \infty$) and no external idler loading ($K_2 = 0$) is used, equations 7 and 8 reduce to equations 5 and 6, respectively.

A comparison of equation 7 with equation 5 (Appendix III) shows that, under certain conditions, the gain-bandwidth product is degraded (made smaller) by sum-frequency propagation. The conditions are that K_o, B_1 and B_2 are assumed to be the same with or without sum-frequency propagation, and B_3 is greater than B_2.

A comparison of equation 8 with equation 6 (Appendix IV) shows that sum-frequency propagation increases the effective noise temperature of the amplifier

Theory (Appendix V and reference 7) demonstrates that, if a balanced varactor configuration is used, spurious responses that are propagated out of the signal port and are generated by odd harmonics of the pump. are suppressed. Furthermore, spurious responses that are propagated in the idler circuit and generated by even-order harmonics of the pump, are suppressed.

Since a balanced configuration presents these advantages, an analysis was performed of the worst-case effect of spurious responses upon the major performance parameters in a balanced reflection-type paramp (Appendices VI, VII, and VIII). The resulting relations were exactly the same as those derived for a single-diode paramp.

3. PREFERRED-CIRCUIT TECHNIQUES

A. INTRODUCTION

The preferred-circuit modifications are aimed at reducing two particular types of RFI:

1. Intermodulation between the pump and the signal that yields spurious-response signals which are propagated out the signal port of the amplifier.
2. Saturation of the paramp by an input signal.

Three physical modifications are incorporated in the preferred circuit.

B. BALANCED-DIODE CONFIGURATION

A balanced-diode configuration (reference 8) with Sylvania D5270 varactors is used in both the preferred circuit (Figure 4) and the control circuit (Figure 5). Figure 6 illustrates the phasing of the pump and the signal in a balanced-diode configuration.

Certain spurious responses, which are propagated out of the signal port, are suppressed because of the balanced configuration. The responses that are suppressed are those generated by odd harmonics of the pump, since the diodes are excited in-phase by the signal and 180 degrees out-of-phase by the pump (Appendix V and reference 7).

Comparison of items 1 and 7, 3 and 8, and 5 and 9 in Column A of Table I demonstrates that the spurious responses generated by the fundamental of the pump are suppressed. These responses would normally be at a higher power level than those generated by the second harmonic of the pump. Figure 7 illustrates the test setup for spurious-response measurements.

FIGURE 4. PREFERRED CIRCUIT PARAMETRIC AMPLIFIER

It can also be shown, in the same manner, that spurious responses, which are propagated in the idler circuit and generated by even-order harmonics of the pump, are suppressed.

A 3-db increase in the input saturation level of the paramp is also achieved, since the two diodes each handle only half the input power.

C. LOCATION OF VARACTORS IN PUMP WAVEGUIDE

The pump waveguide is perpendicular to the signal circuit, and the varactors are placed in a lower impedance area in the reduced-height waveguide. There are three advantages to this configuration: varactor loading, pump-source matching, and varactor and waveguide impedance matching.

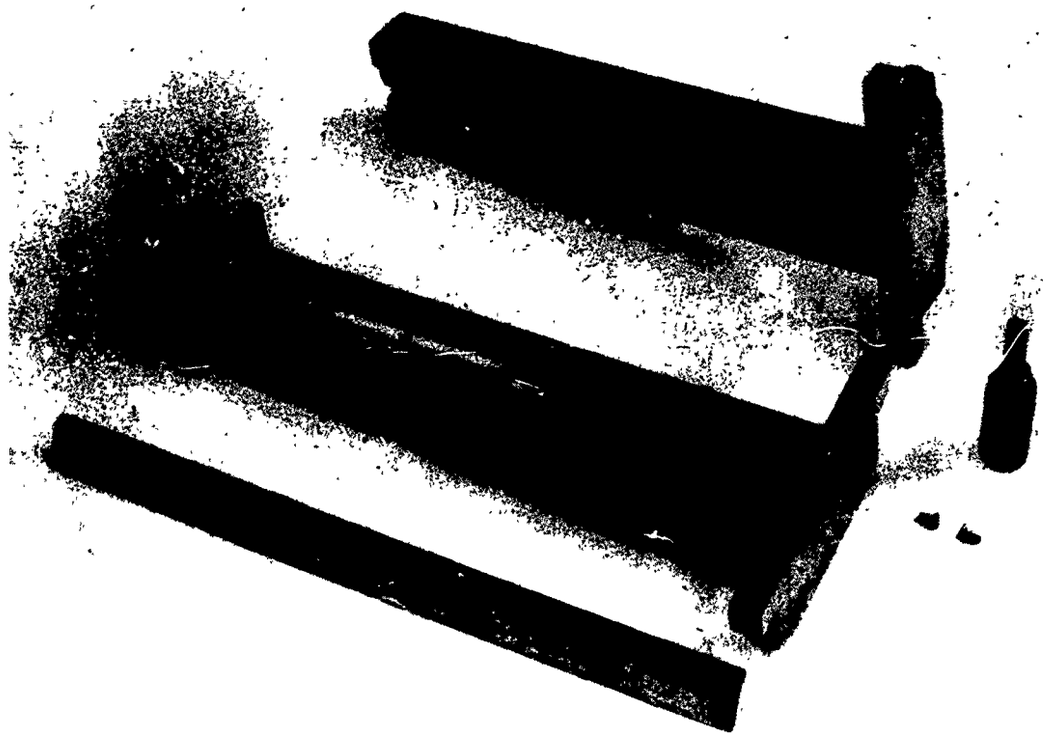

FIGURE 5. CONTROL PARAMETRIC AMPLIFIER

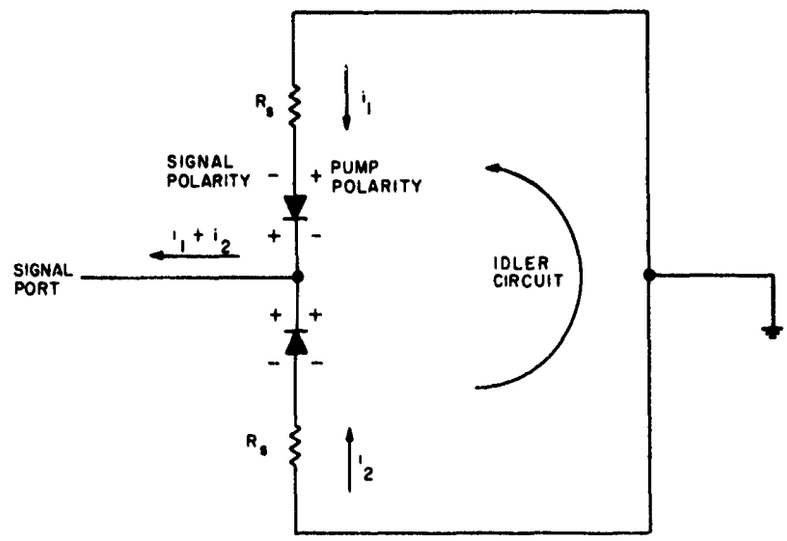

FIGURE 6. BALANCED-DIODE CONFIGURATION

TABLE I

INTERMODULATION (SPURIOUS) OUTPUTS PROPAGATED OUT OF THE SIGNAL PORT OF THE PREFERRED-CIRCUIT PARAMETRIC AMPLIFIER

			A	B	C
Item	Frequency Relation	IM Frequency (MHz)	IM Output Short at Position For Best Pump Match, No filter (dbm)	IM Output Short at Best Pump Match Position, Filter in (dbm)	IM Output Short Set For IM Suppression, Filter in (dbm)
1.	$f_p - f_s$	8,265	-51.5	-68.0	-72.9
2.	$f_p - \frac{1}{2} f_s$	8,720	-44.0	-50.0	-64.5
3.	f_p	9,175	-29.0	-35.0	-38.0
4.	$f_p + \frac{1}{2} f_s$	9,630	-52.0	-63.0	-75.0
5.	$f_p + f_s$	10,085	-61.5	-63.9	-66.5
6.	$2f_p - 2f_s$	16,530	-57.0		
7.	$2f_p - f_s$	17,440	-41.0		
8.	$2f_p$	18,350	-23.0		
9.	$2f_p + f_s$	19,260	-38.0		
10.	$2f_p + 2f_s$	20,170	< -80		

f_p = pump frequency = 9175 MHz. f_s = signal frequency = 910 MHz at a level of -50 dbm.

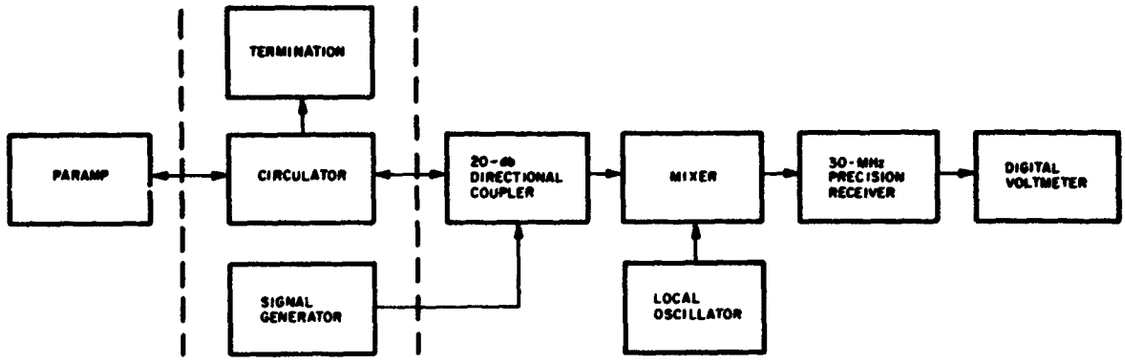

FIGURE 7. TEST SET-UP FOR SPURIOUS-RESPONSE MEASUREMENTS

1. VARACTOR LOADING

A movable short circuit (Figure 4) is provided behind the varactors, on the side opposite the pump, which enables optimization of both saturation and intermodulation between the pump and the signal by varying the loading across the varactors at the intermodulation frequencies.

Since the low-impedance waveguide between the movable short circuit and the varactors is a transmission line, the position of the short circuit determines the impedance that is reflected at the plane of the varactors and, therefore, the loading on the varactors.

When the loading is adjusted so that spurious responses at a certain frequency have a very high impedance in the propagation path, spurious responses at that frequency are suppressed, and an improvement is achieved in both gain-bandwidth product and noise figure. Columns B and C in Table I show the suppression of spurious responses, which propagate down the signal line at various frequencies, when the short-circuit position is optimized.

At the optimum short position, about a 9-db improvement in the saturation level of the amplifier is achieved. With the short position

optimized and the amplifier tuned to 900 MHz with 20-db insertion gain, the input saturation level for a 1-db decrease in gain is -36 dbm. When the short is moved from the optimum position, the input saturation level is typically about -45 dbm for 1-db a decrease in gain.

2. PUMP SOURCE MATCHING

The movable short circuit is also used for better impedance matching of the paramp to the pump source. However, the short position for best pump matching is not necessarily the optimum short position for the suppression of spurious responses.

3. VARACTOR AND WAVEGUIDE IMPEDANCE MATCHING

The varactors are placed in a position where the real part of the characteristic impedance of the waveguide is closer to the real part of the varactor impedance. This results in a better impedance match and, consequently, greater instantaneous bandwidth and tunability over a wider frequency range. At some frequencies as much as an 80 to 90 percent increase in gain-bandwidth product is achieved.

The gain-bandwidth product of a parametric amplifier is not constant as a function of either gain or frequency. Voltage gain-bandwidth products for the control amplifier range between 89 and 270 MHz. The preferred-circuit range is 157 to 447 MHz. In addition, the tunability of the amplifier improved (from 80 MHz for the control amplifier to 115 MHz for the preferred circuit amplifier).

Figure 8 shows the test setup for accurate measurement of the bandpass characteristic of a paramp from which the gain-bandwidth product is determined. Figures 9 and 10 show the bandpass characteristics of the preferred circuit and the control amplifier, respectively.

D. BAND-REJECT FILTER

A broadband band-reject filter is incorporated in the signal circuit (Figure 4) to keep intermodulation frequencies produced by the pump

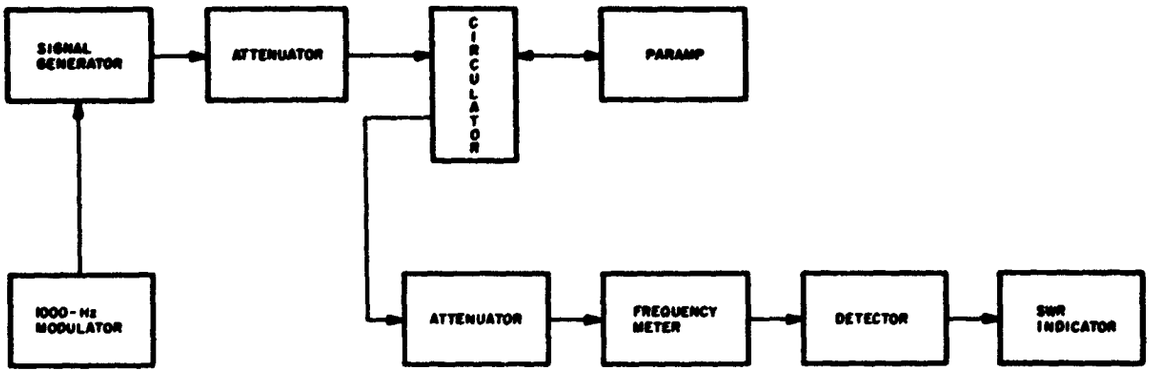

FIGURE 8. TEST SET-UP FOR GAIN-BANDWIDTH MEASUREMENT

and signal from propagating out of the signal port of the paramp and into the associated circuits. Columns A and B in Table I show the suppression of spurious responses when the filter is incorporated in the preferred circuit.

The amount of rejection depends on the number of elements of the filter. The preferred circuit has a two-element filter that is designed to reject spurious responses which are generated by the fundamental frequency of the pump. Spurious responses that are generated by the second harmonic of the pump frequency can also be suppressed by using a band-reject filter. This was not attempted, because the experimental paramp mount was not large enough.

E. ADDITIONAL PREFERRED-CIRCUIT TECHNIQUES

Seven additional preferred-circuit techniques are available for the purpose of increasing the input saturation level of the paramp. Figure 11 illustrates the test setup for measurement of the saturation characteristic of a paramp. Figures 12 and 13 show the saturation characteristics of the control amplifier and the final preferred-circuit amplifier, respectively.

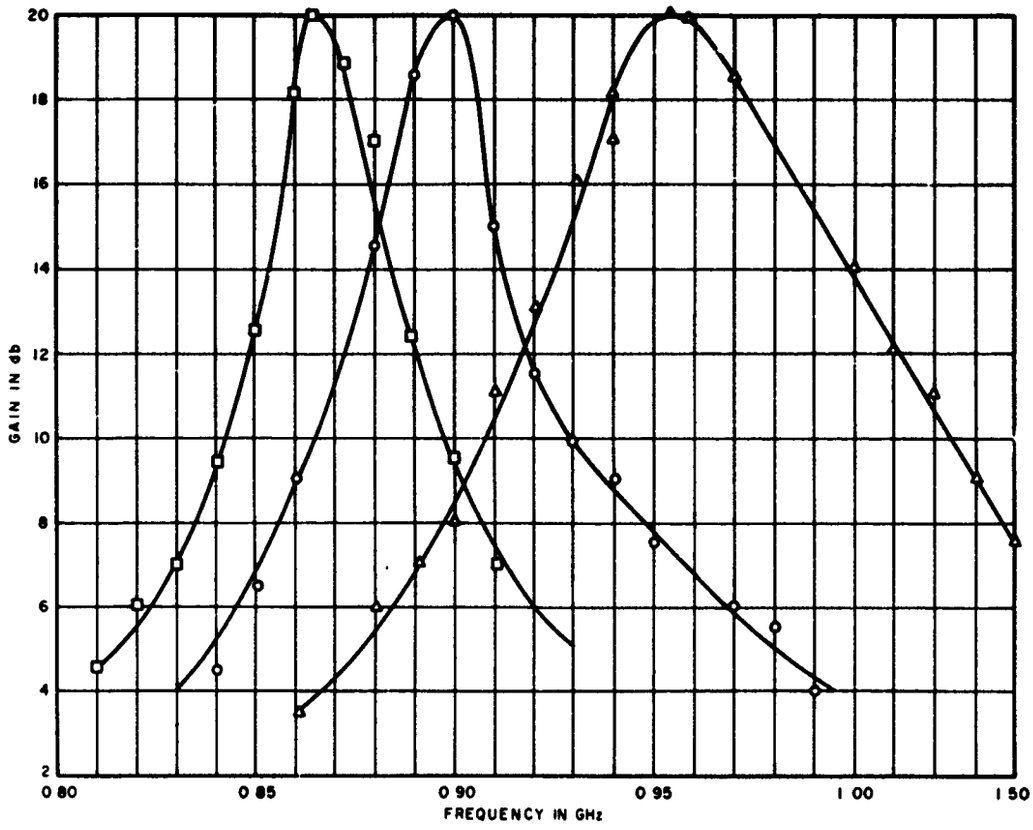

FIGURE 9. PREFERRED-CIRCUIT BANDPASS CHARACTERISITC

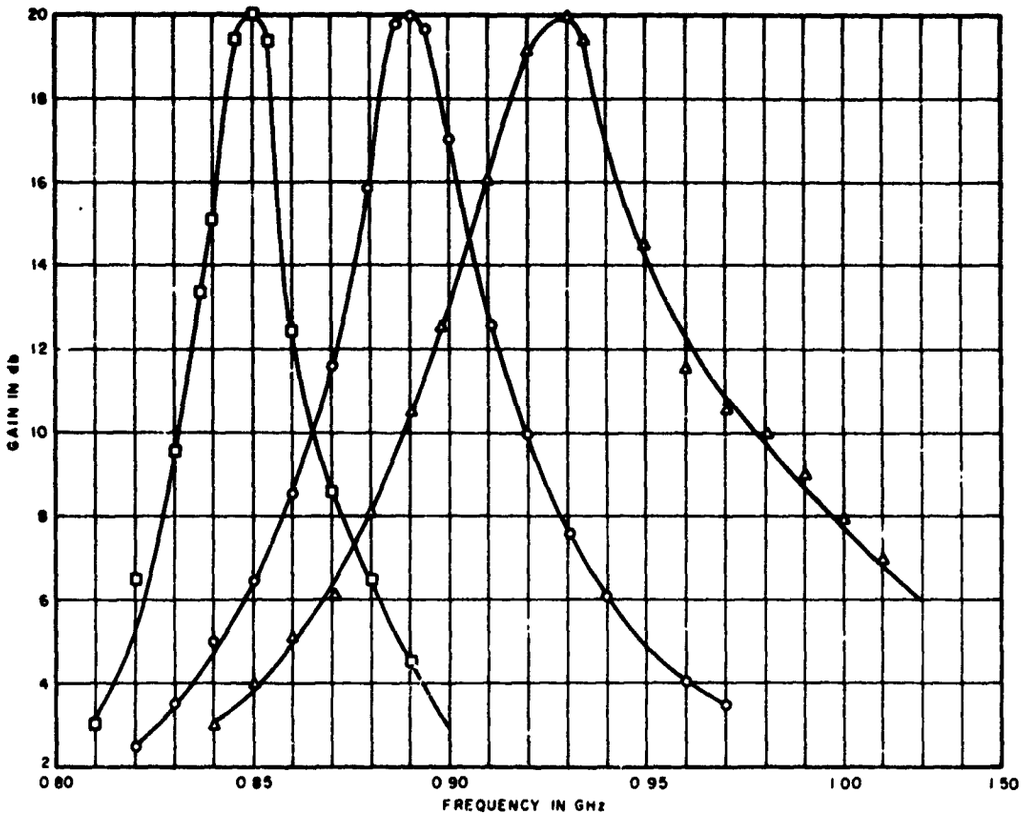

FIGURE 10. CONTROL-AMPLIFIER BANDPASS CHARACTERISTIC

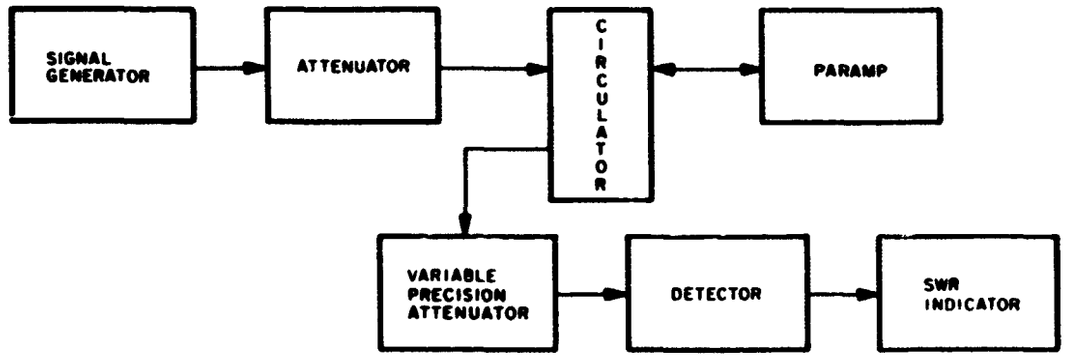

FIGURE 11. TEST SETUP FOR SATURATION MEASUREMENT

1. OPTIMUM PUMP FREQUENCY

An optimum pump frequency can be found which yields the best saturation characteristic. The basis for this technique is the fact that, since initial saturation involves a detuning effect, a certain amount of compensatory detuning can initially be built into an amplifier so that a large input signal will result in better tuning of the paramp circuits. This technique was tried, and an increase of from 4 to 6 db in the input saturation level of the preferred circuit was achieved. To use this technique, however, the range over which the amplifier can be tuned will be reduced.

2. LOWER-GAIN OPERATION

Lower-gain operation results in a higher input saturation level. An X-db decrease in gain, however, does not necessarily yield an X-db increase in input saturation level.

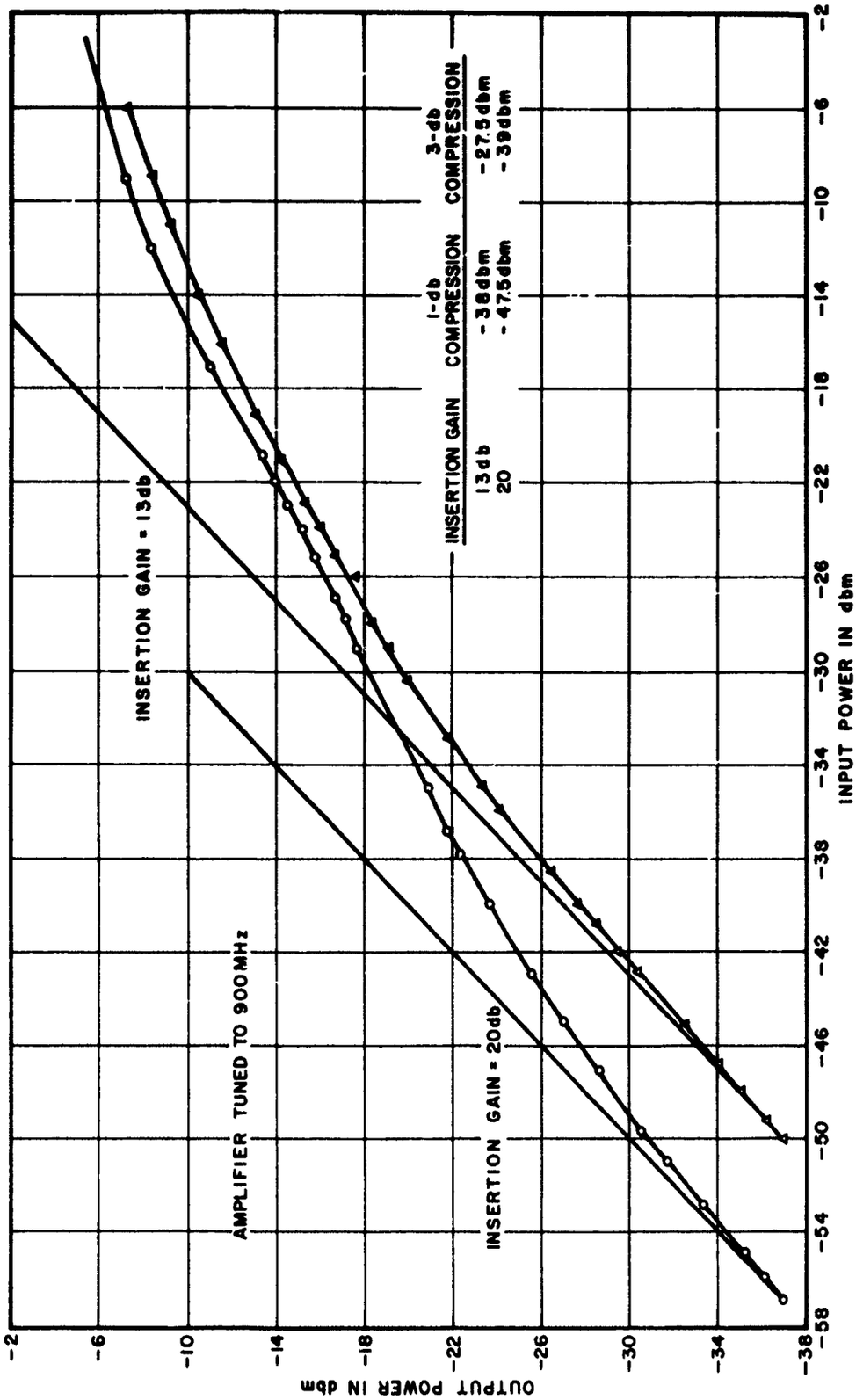

FIGURE 12. SATURATION CHARACTERISTIC OF CONTROL AMPLIFIER

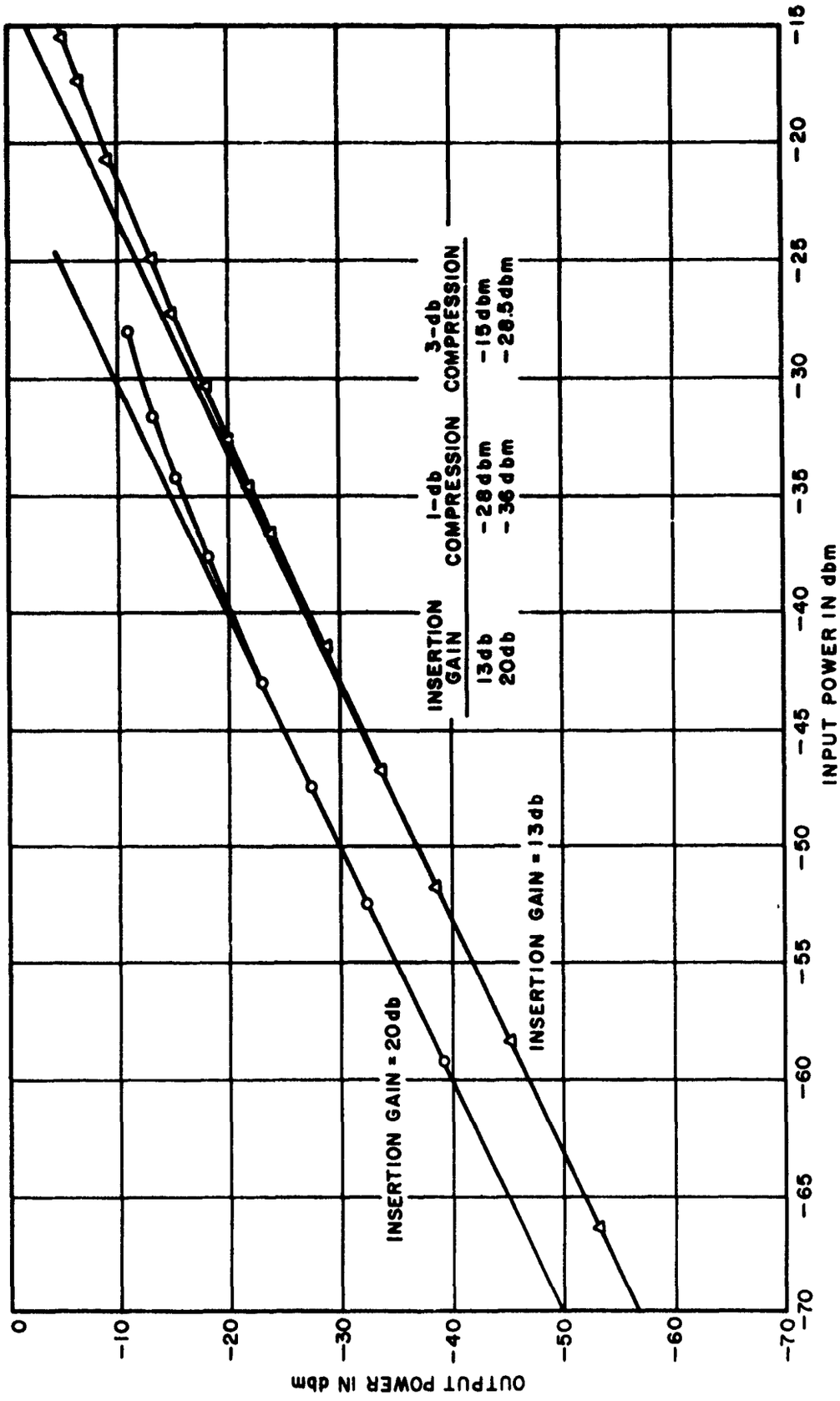

FIGURE 13. SATURATION CHARACTERISTIC OF PREFERRED CIRCUIT

3. IDLER CIRCUIT RESISTANCE

Increasing the resistance in the idler circuit has three effects:

a. Higher input-saturation level,
b. Higher noise temperature,
c. More pump power required for same amount of gain.

The trade-off of noise temperature limits the usefulness of this technique, because, low noise temperature is generally the reason for using a paramp as an RF amplifier.

4. USE OF VARACTORS WITH ABRUPT JUNCTIONS

The use of abrupt-junction varactors, rather diffused-junction varactors, theoretically will yield an improvement in the input saturation level (reference 9).

5. USE OF VARACTORS WITH HIGH REVERSE-BREAKDOWN VOLTAGE

The use of varactors with a high reverse-breakdown voltage allows the varactors to be biased at a greater negative voltage level. Thus, a greater input signal can be impressed upon the varactors without driving them into forward conduction or reverse breakdown.

6. USE OF VARACTORS WITH LARGE JUNCTION CAPACITANCE

The use of varactors with as large a junction capacitance as possible results in higher power-handling capability and greater input-saturation level (reference 10).

7. USE OF VARACTORS WITH LOW FIGURE OF MERIT

The use of varactors with as low an M (figure of merit) as possible is another consideration. Since, for a given series resistance, M is inversely proportional to junction capacitance, and since large junction capacitance is desirable, a higher saturation level is obtained. Similarly, for a given junction capacitance, M is inversely proportional to the varactor series resistance and a higher series resistance is desirable. However,

lower M results in a noise temperature trade-off, because the higher the M the lower the noise temperature (Appendix IV).

4. ADDITIONAL DATA

Further useful measurements were made on the paramps: noise temperature, cross modulation between two input signals, desensitization, intermodulation between two input signals, and gain-recovery time.

A. NOISE TEMPERATURE

The noise temperatures of both circuits were measured with the amplifiers tuned to 900 MHz at four different gain levels. Table II compares the noise temperature and corresponding noise figure of the preferred circuit and the control amplifier at each gain level.

The better noise-temperature results of the preferred circuit support the theory developed in Appendices IV and VIII in that they are attributable to the more nearly optimum terminations presented across the varactors at intermodulation frequencies which are generated by the pump and the signal. The discrepancy at 23-db gain is due to the fact that the gain of the paramp is approaching the isolation of the circulator. Figure 14 illustrates the test setup for noise-figure measurement.

B. CROSS MODULATION

Under the following preferred-circuit conditions,

1. amplifier tuned to 900 MHz (Figure 9),
2. 20-db mid-band insertion gain,
3. interfering signal at 920 MHz (100-percent modulated),
4. desired signal at 900 MHz (CW),

the interfering-signal level for 1-percent cross modulation is -59 dbm for a -50 dbm desired signal level.

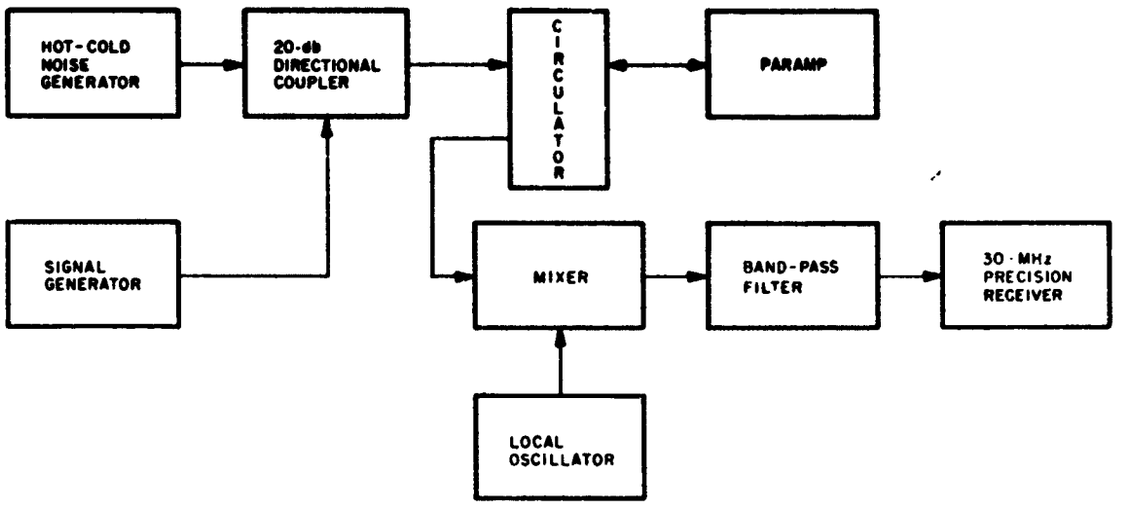

FIGURE 14. TEST SETUP FOR NOISE-TEMPERATURE MEASUREMENT

The maximum cross modulation achieved was 83 percent for an interfering signal of -23 dbm. These figures were also typical of the control amplifier. Figure 15 illustrates the test setup for cross modulation measurement.

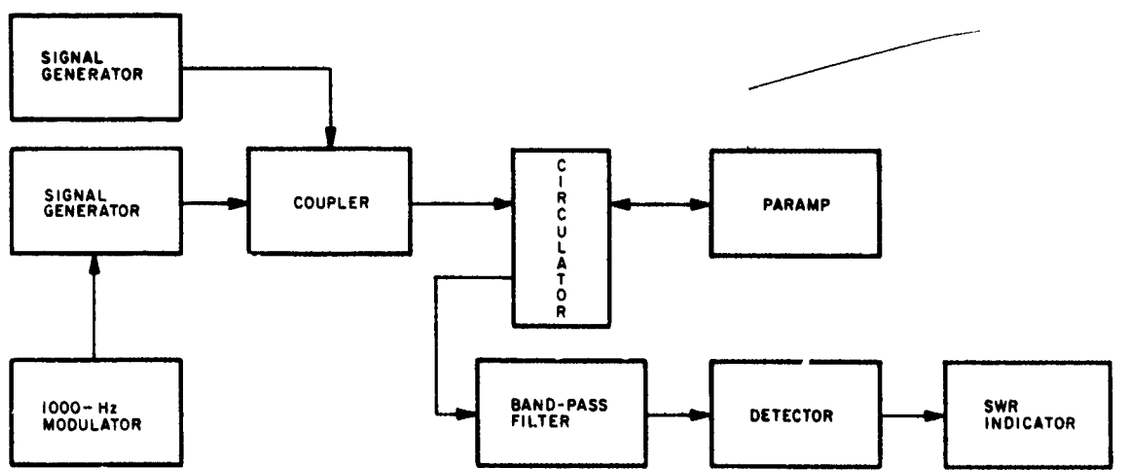

FIGURE 15. TEST SETUP FOR CROSS-MODULATION MEASUREMENT

TABLE II

NOISE PERFORMANCE OF PARAMETRIC-AMPLIFIER CIRCULATOR COMBINATIONS

Control Circuit			Preferred Circuit	
Gain (db)	Noise Figure (db)	Noise Temp (^{o}K)	Noise Figure (db)	Noise Temp (^{o}K)
13	2.35	209	1.77	145
16	2.28	200	1.82	150
20	2.18	191	1.92	161
23	1.85	154	1.89	158

Both amplifiers tuned to 900 MHz.

Figure 16 is a plot of cross modulation versus interfering-signal level for the preferred-circuit paramp. The initial change in the slope of the curve is not a common characteristic. The reason for this effect is not evident at the present time.

Suggestions for further techniques for the reduction of intermodulation and for the reduction of cross modulation are in Section V of this report.

C. DESENSITIZATION

Under the following preferred-circuit conditions,

1. amplifier tuned to 900 MHz (Figure 9),
2. 20-db mid-band insertion gain,
3. interfering signal at 920 MHz (CW),
4. desired signal at 900 MHz (100-percent modulated),

the level of the interfering signal for 1-db desensitization is -36 dbm for a -50 dbm desired-signal level.

The level of the interfering signal for 3-db desensitization is -30 dbm for a -50 dbm desired-signal level. For 13-db insertion gain and -50 dbm desired-signal level the interfering-signal levels for 1 db and 3 db of desensitization are -32 dbm and -26 dbm, respectively. These figures are also typical of the control amplifier.

Figure 17 illustrates the test setup for desensitization measurement. Figures 18 and 19 give desensitization versus interfering-signal level, with a desired signal frequency of 900 MHz and an interfering-signal frequency of 920 MHz, for the control and preferred-circuits, respectively. Figures 20 and 21 give desensitization versus interfering-signal level, with a desired-signal frequency of 945 MHz for the control and preferred circuits, respectively.

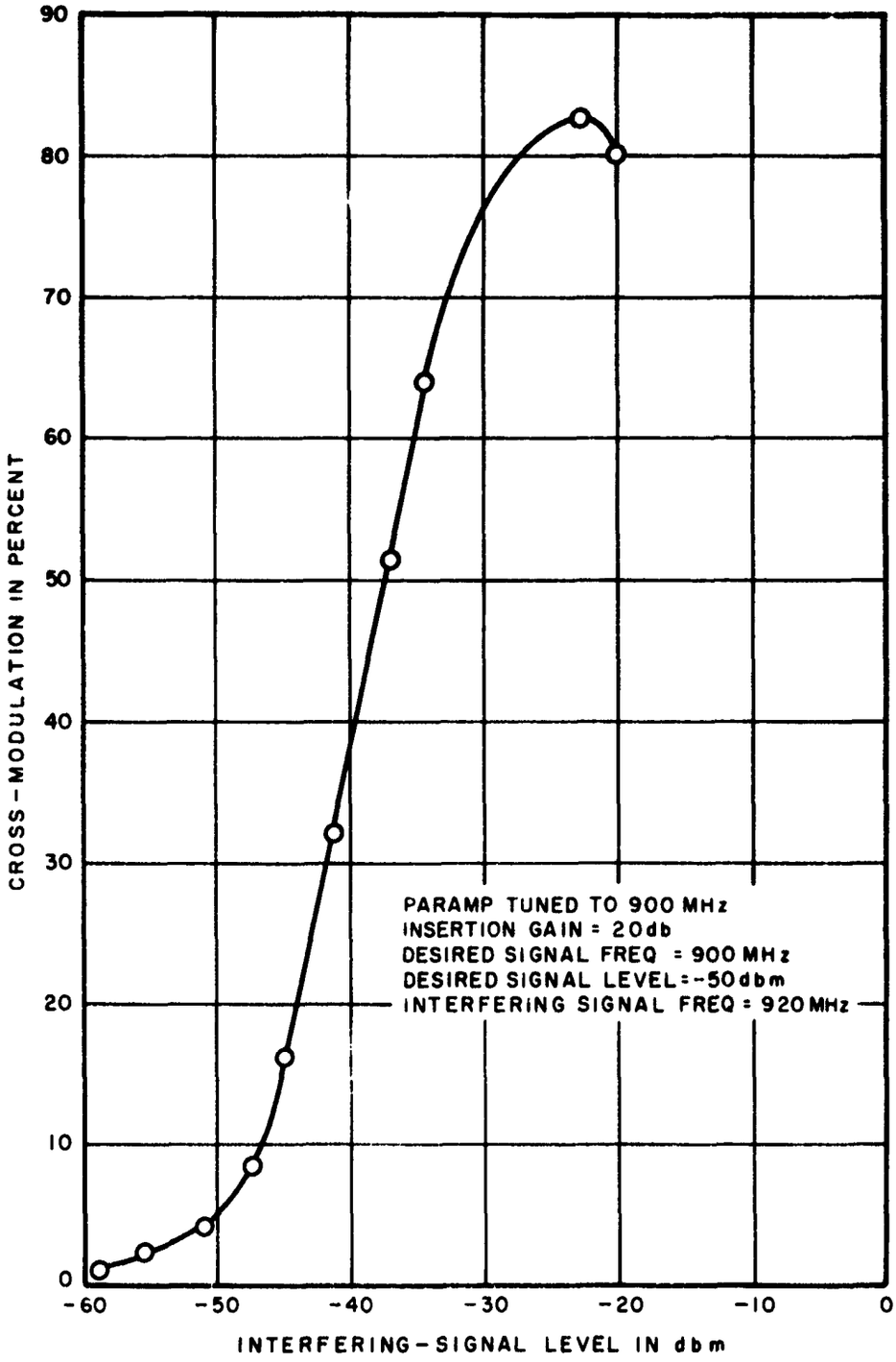

FIGURE 16. CROSS-MODULATION CHARACTERISTIC OF PREFERRED-CIRCUIT PARAMP

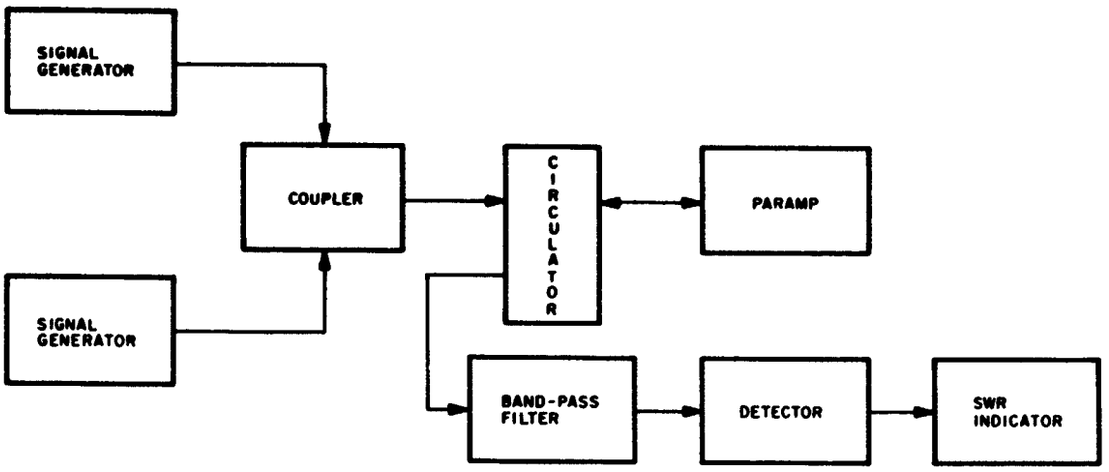

FIGURE 17. TEST SETUP FOR DESENSITIZATION MEASUREMENT

D. INTERMODULATION

Under the following conditions for the preferred circuit:

1. amplifier tuned to 900 MHz, (Figure 9),
2. 20-db mid-band insertion gain,
3. interfering signal at 920 MHz (CW),
4. desired signal at 900 MHz (CW),

the intermodulation constants (K's) given by equation 9, are listed in Table III.

$$P_{mn} = mP_1 + nP_2 + K_{mn} \qquad (9)$$

where

P_1 = output power of input signal f_1 in dbm

P_2 = output power of input signal f_2 in dbm

P_{mn} = intermodulation output power (in dbm) at frequency $mf_1 \pm nf_2$

K_{mn} = constant associated with the particular intermodulation product.

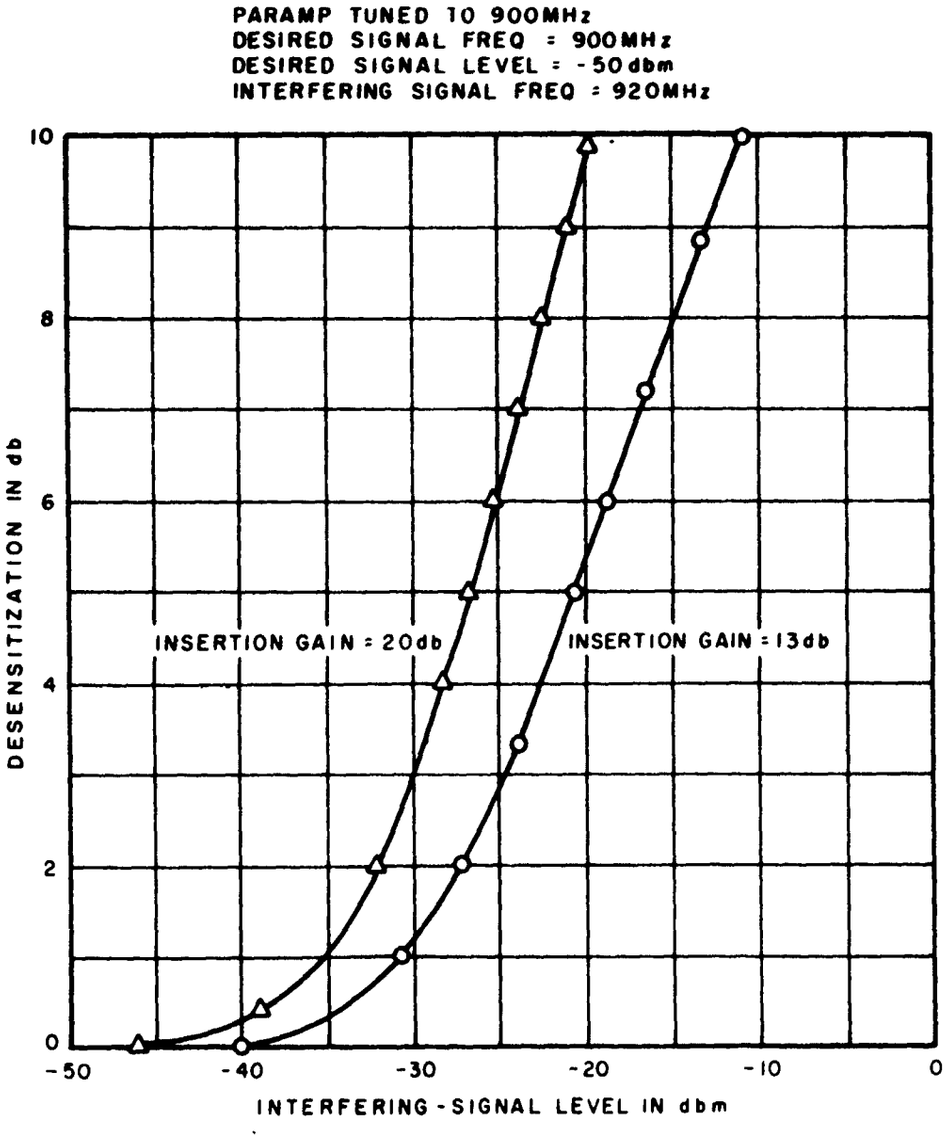

FIGURE 18. DESENSITIZATION VERSUS INTERFERING-SIGNAL LEVEL FOR CONTROL AMPLIFIER TUNED TO 900 MHz

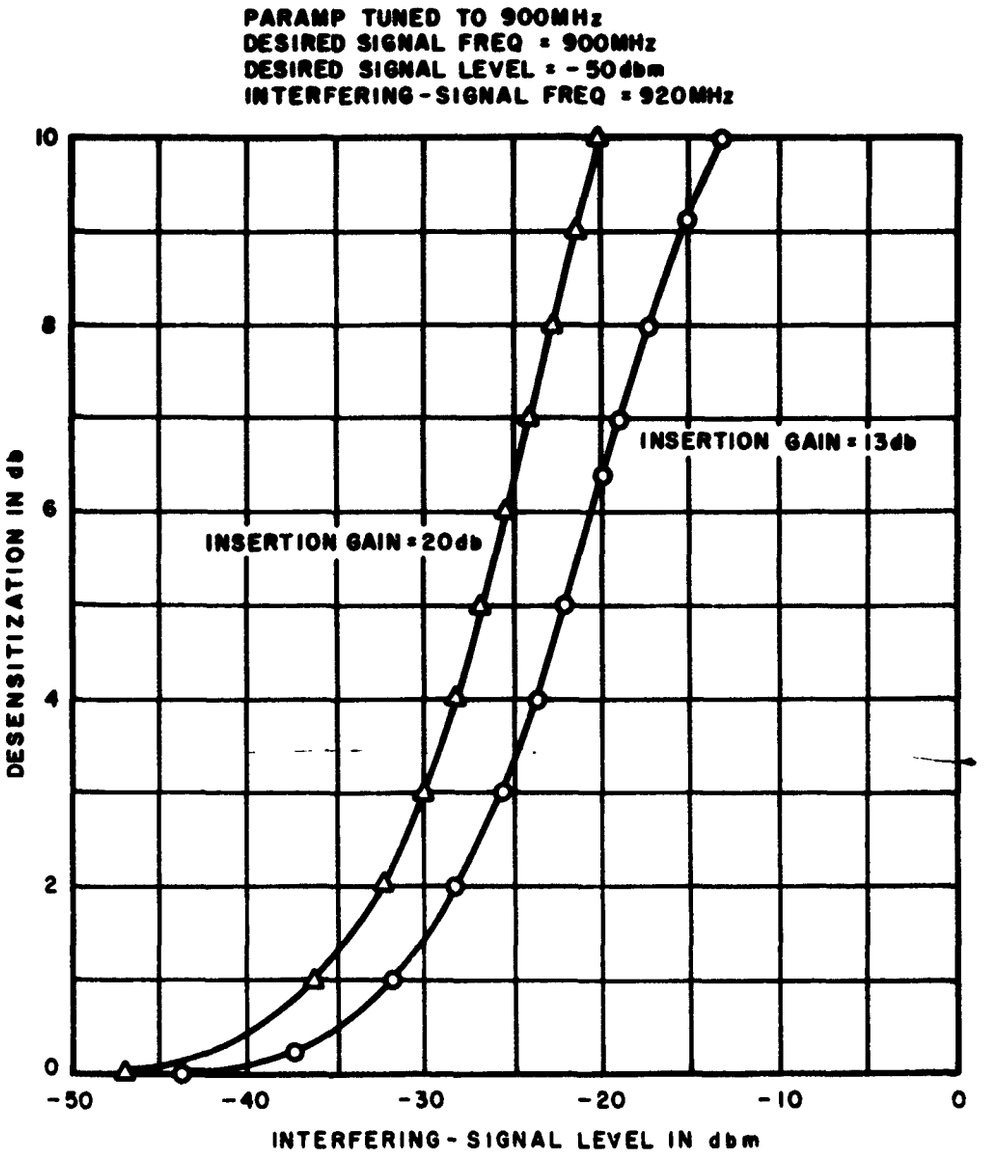

FIGURE 19. DESENSITIZATION VERSUS INTERFERING-SIGNAL LEVEL FOR PREFERRED-CIRCUIT AMPLIFIER TUNED TO 900 MHz

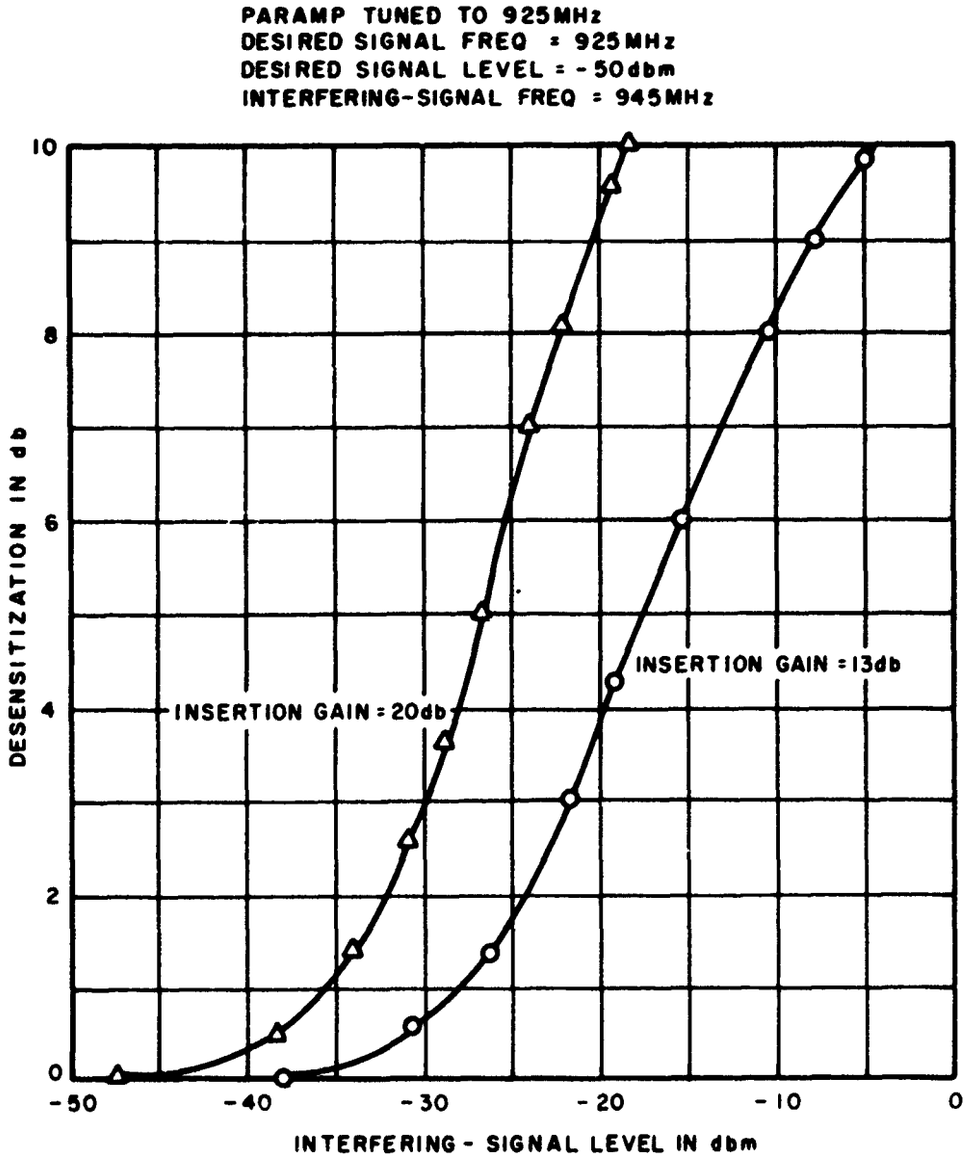

FIGURE 20. DESENSITIZATION VERSUS INTERFERING-SIGNAL LEVEL FOR CONTROL AMPLIFIER TUNED TO 925 MHz

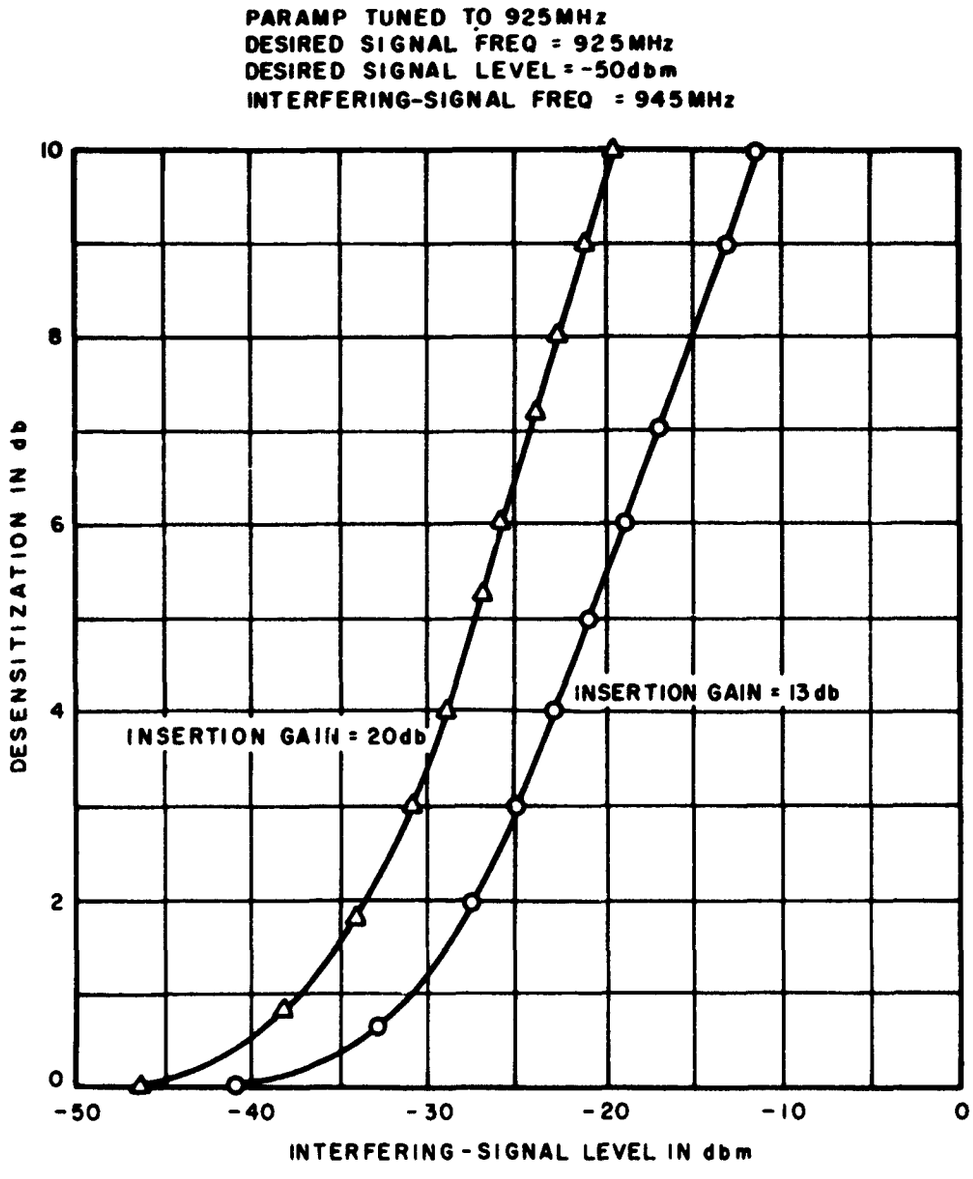

FIGURE 21. DESENSITIZATION VERSUS INTERFERING-SIGNAL LEVEL FOR PREFERRED-CIRCUIT AMPLIFIER TUNED TO 925 MHz

TABLE III

INTERMODULATION CONSTANTS ASSOCIATED WITH TWO INPUT SIGNALS

Constant	Value (dbm)
K_{21}	0
K_{23}	+3.5
K_{43}	+17

20-db insertion gain at 900 MHz

f_{des} = frequency of desired signal = 900 MHz

f_{int} = frequency of interfering signed = 920 MHz

The constants listed are typical of both the preferred circuit and the control amplifier. Figure 22 illustrates the test setup for intermodulation measurement. Figures 23 through 27 give the third-, fifth-, and seventh-order intermodulation data for the preferred-circuit amplifier.

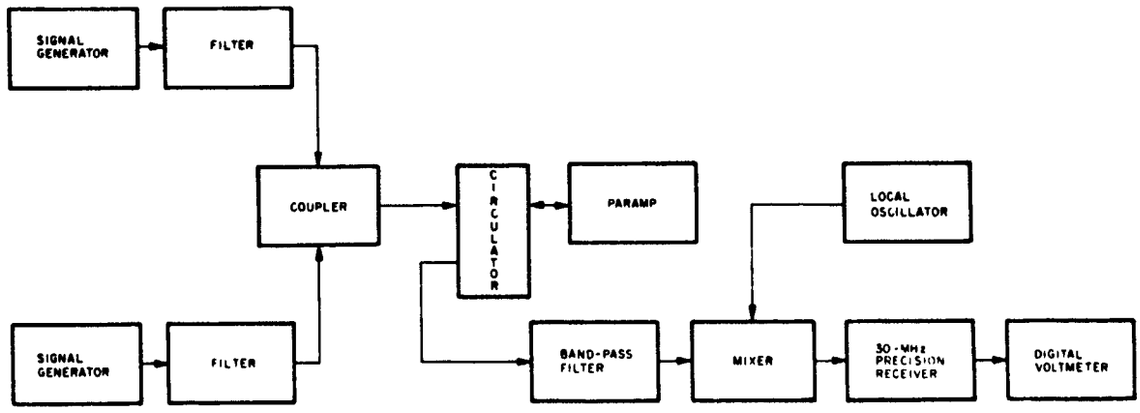

FIGURE 22. TEST SETUP FOR INTERMODULATION MEASUREMENTS

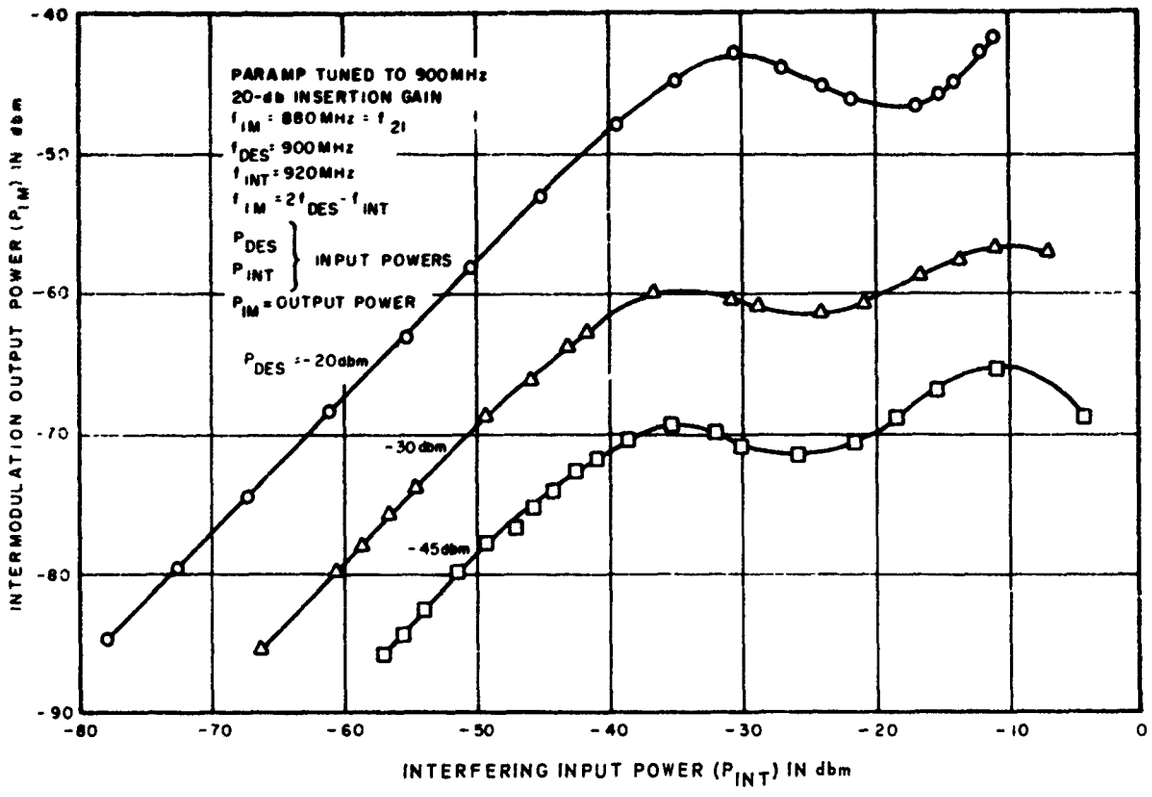

FIGURE 23. THIRD-ORDER INTERMODULATION AT 20-DB GAIN

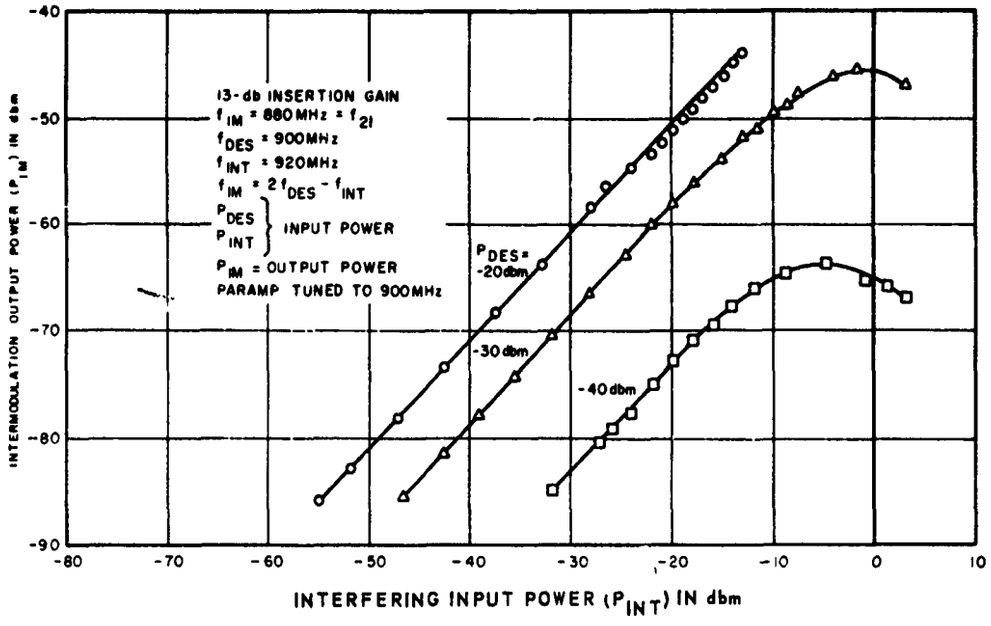

FIGURE 24. THIRD-ORDER INTERMODULATION AT 13-DB GAIN

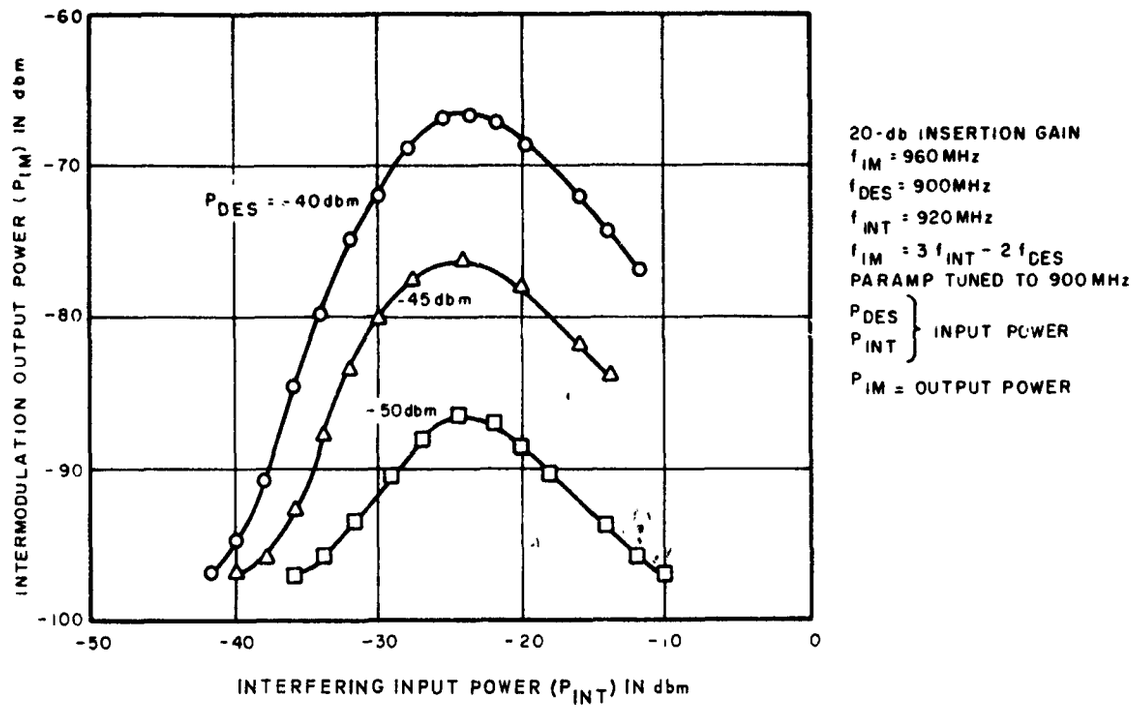

FIGURE 25. FIFTH-ORDER INTERMODULATION AT 20-DB GAIN

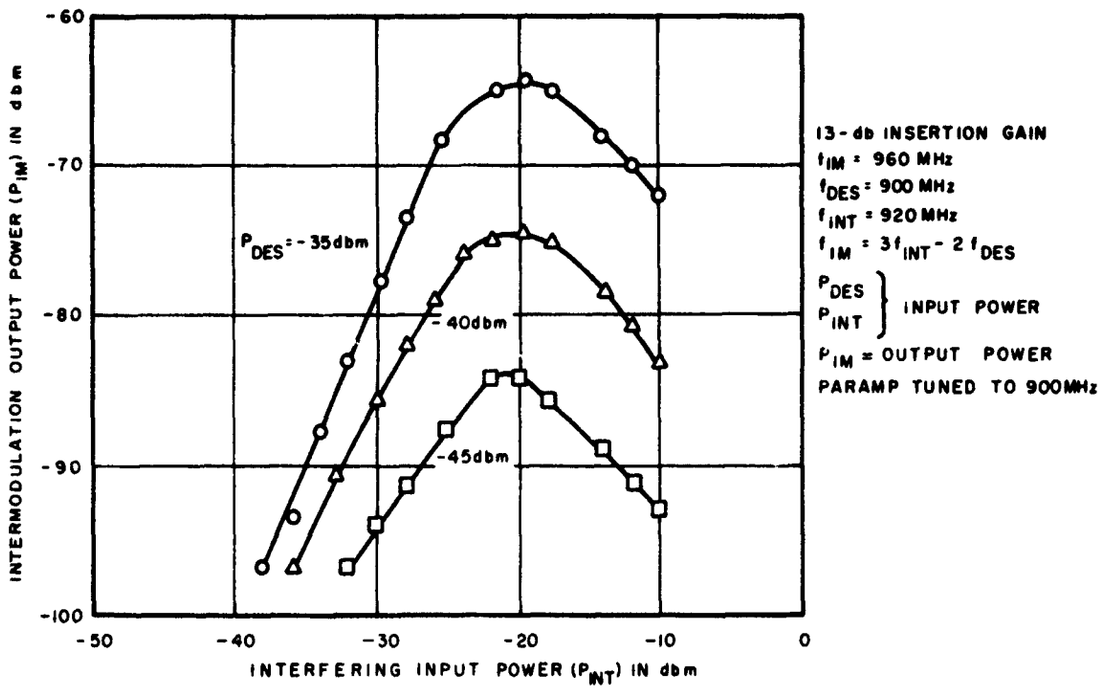

FIGURE 26. FIFTH-ORDER INTERMODULATION AT 13-DB GAIN

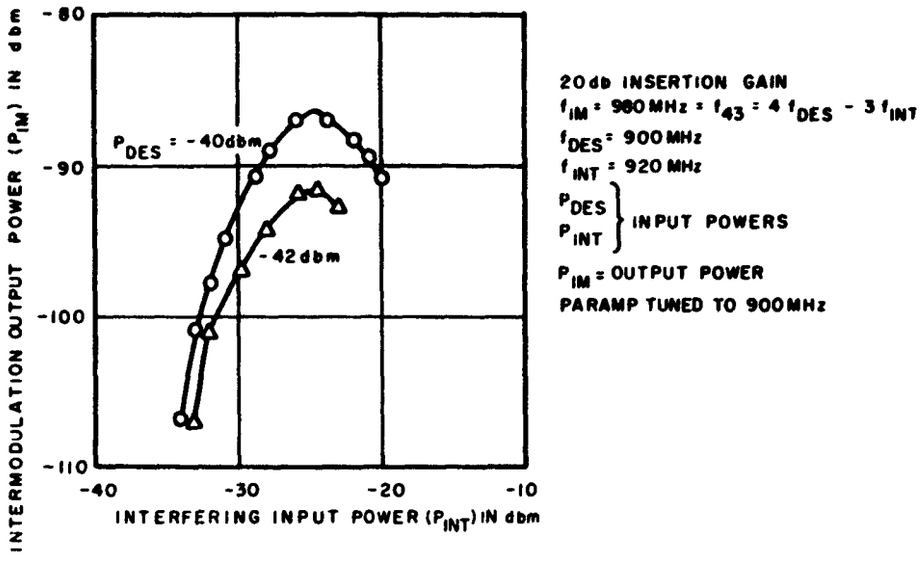

FIGURE 27. SEVENTH-ORDER INTERMODULATION AT 20-DB GAIN

E. GAIN-RECOVERY TIME

A pulse of energy is introduced into the preferred circuit which drives the paramp well into saturation, and the time necessary for the paramp to return to its initial gain, (at the tuned frequency) after the pulse is removed, is measured.

The gain-recovery time for the preferred circuit is less than 1 μsec, which is the limit of the measurement equipment used. It is reasonable to expect that this is also typical of the control amplifier. Figure 28 illustrates the test setup for gain-recovery time measurement.

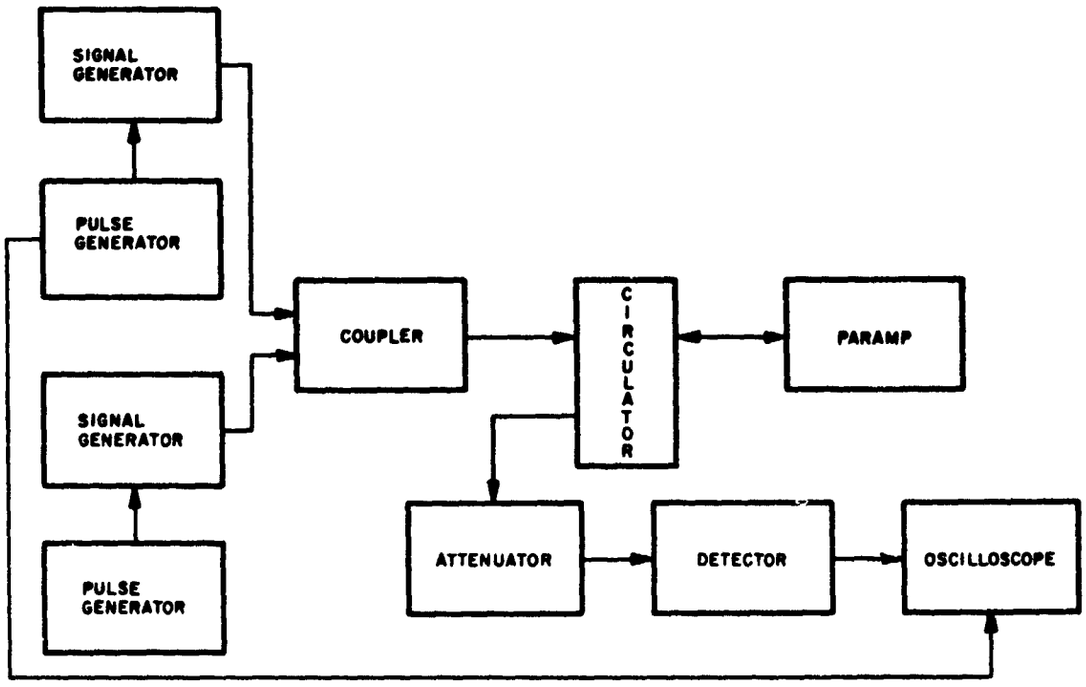

FIGURE 28. TEST SETUP FOR GAIN-RECOVERY TIME MEASUREMENT

5. RECOMMENDATIONS

Other preferred-circuit techniques are suggested in this section which might yield reduction in intermodulation and cross-modulation between two input signals. Experiments were not performed on this project using these techniques due to the cost limitations of the overall program.

From reference 7, it can be shown that intermodulation between two input signals would be reduced if a balanced configuration of varactors was used where the varactors are excited 180 degrees out-of-phase by the signal. Physical realization of this requires that the varactors be biased independently.

Independent biasing can also be used to better match the characteristics of the varactors being used, which should result in better cancellation of intermodulation products. From reference 11, cross modulation can be related to third-order intermodulation and, therefore, better third-order intermodulation performance also implies better cross-modulation performance.

Large quantities of varactors can be arranged in a matrix configuration yielding a substantial increase in the saturation power of the paramp. This technique might present substantial technical difficulties in physical realization.

6. CONCLUSIONS AND SUMMARY

This report has demonstrated a number of techniques useful in the reduction of the following RFI phenomena in reflection-type parametric amplifiers:

a. Spurious responses (intermodulation between the pump and the signal),
b. Saturation of the amplifier by a large input signal,
c. Intermodulation between two input signals,
d. Cross-modulation between two input signals.

Spurious responses has been considered to be the most important RFI phenomenon in parametric amplifiers. A rigorous analysis has been presented which illustrates the deleterious effect of spurious responses upon the gain, the gain-bandwidth product, and the noise temperature of both single-diode and balanced reflection-type paramps. The balanced-paramp performance analysis was required because of the theoretical justification of the use of a balanced configuration for spurious-response reduction.

Some of the RFI reduction techniques were incorporated into an experimental paramp which was called a preferred circuit. Another experimental paramp was built without many of the preferred circuit features to serve as an experimental control. Measurements were made which justified the theoretical analysis and also provided further information about the performance and RFI characteristics of each amplifier. All data led to the conclusion that each preferred-circuit modification incorporated in the experimental model not only improved the RFI characteristics of the paramp but also either improved or did not seriously harm the conventional paramp performance.

Further recommendations were offered for a logical extension of this work. These recommendations each require major design work but promise significant advances in the state the art.

7. CITED REFERENCES

1. H. E. Rowe, "Some General Properties of Nonlinear Elements II," Proc IRE, May 1958.
2. L. Blackwell and K. Kotzebue, Semiconductor-Diode Parametric Amplifiers, Prentice-Hall, 1961.
3. D. B. Anderson and J. C. Aukland, "Transmission-Phase Relations of Four-Frequency Parametric Devices," IRE Trans on MTT, November 1961.
4. K. Kurokawa and M. Uenohara, "Minimum Noise Figure of the Variable Capacitance Amplifier," Bell System Tech Journal, May 1961.
5. P. P. Lombardo and E. W. Sard, "Low-Noise Microwave Reactance Amplifiers with Large Gain-Bandwidth Products," 1959 Wescon Convention Record, Part 1.
6. P. Lombardo, State of the Art of Parametric Amplifiers, Airborne Instruments Laboratory, Feb. 1964.
7. D. Kaye, "Derivation of Intermodulation Outputs of Two General Nonlinear Elements in a Balanced Mixer Array," Proc IEEE, Vol 53, No. 11, November 1965.
8. J. Kliphuis, "Parametric Amplifier with Balanced Self-Resonant Diodes," U.S. Patent No. 3, 150, 941, issued October 1, 1963, to Cutler-Hammer, Inc.
9. B. Bossard et al, "Interference Reduction Techniques for Receivers, Interim Final Report," RCA Report Number CR-64-419-9, 31 July 1964, Radio Corp. of America for U.S. Army Electronics Laboratory on Contract No. DA-36-039-AMC-02345(E).
10. B. Bossard et al, "Interference Reduction Techniques for Receivers," Quarterly Report No. 5, RCA Report Number CR-65-419-3, 26 Nov-

ember 1963, Radio Corp. of America for U.S. Army Electronics Laboratory on Contract No. DA-36-039-AMC--2345(E).

11. O. Hinckelmann et al, "Interference Analysis of New Components and Circuits," Technical Documentary Report No. RADC-TDR-64-161, May 1964, Airborne Instruments Laboratory for Rome Air Development Center on Contract No. AF 30(602)-2919.
12. S. Becker et al, "Interference Analysis of New Components and Circuit Techniques," Technical Documentary Report No. RADC-TDR-62-221, May 1962, Airborne Instruments Laboratory for Rome Air Development Center on Contract No. AF 30(602)-2384.
13. P. Penfield Jr and R. P. Rafuse, Varactor Applications, MIT Press, 1962.

8. BIBLIOGRAPHY

Anderson, D.R. and Leon, B.J., "Nonlinear Distortion and Truncation Errors in Frequency Converters and Parametric Amplifiers," IEEE Trans on Circuit Theory, Vol. CT-12, No. 3, Sept. 1965. Considers the errors involved in analysis due to use of linear instead of nonlinear model.

Burckhardt, C.B., "Analysis of Varactor Frequency Multipliers for Arbitrary Capacitance Variation and Drive Level," BSTJ, April 1965. General multiplier analysis.

Crook, D.E., "A Simplified Technique for Measuring High Quality Varactor Parameters," Solid State Design, Aug. 1965. Describes cutoff frequency measurements.

Deloach, B.C., "A New Microwave Measurement Technique to Characterize Diodes and an 800-GC Cutoff Frequency Varactor at Zero Volts Bias," IEEE Trans. on Microwave Theory and Techniques, Vol. MTT-12, Jan 1964 Describes an experimental technique.

Diamond, B.L., "Idler Circuits in Varactor Frequency Multipliers," IEEE Trans on Circuit Theory, Vol, CT-10, March 1963. Presents a general large-signal analysis of frequency multiplication with lossy, abrupt-junction varactors.

Eng, S.T., "Characterization of Microwave Variable Capacitance Diodes," IRE Trans on Microwave Theory and Techniques, Vol. MTT-9, No. 1, Jan. 1961. Describes three measurement techniques.

Gemulla, W.J. and Wilds, R.B., "Vulnerability of Semiconductor Receiver RF Elements to Signal Environments," Technical Memorandum No. EDL - M480, 20 July 1962. Sylvania Electric Products for US Army Signal Re-

search and Development Laboratory. Paramp section showed location of primary spurious responses in an S-band single-diode paramp.

Greene, J.C. et al., "Final Progress Report on Application of Semiconductor Diodes to Microwave Low-Noise Amplifiers and Harmonic Generators," Report No. 5872-1, 15 July 1957, Airborne Instruments Lab for US Army Signal Engineering Laboratories, Contract No. DA-36-039-sc-78161. Theory for maximum achievable voltage gain-fractional bandwidth product of one-and two-port differences - frequency paramps.

Green, J.C. and Sard, E.W., "Optimum Noise and Gain-Bandwidth Performance for a Practical One-Port Parametric Amplifier," Proc. IRE, Vol. 48, No. 9, Sept. 1960, Derives expressions called out in the title.

Hayasi, S. and Kurokawa, T., "A Balanced-Type Parametric Amplifier," IRE Trans. on Microwave Theory and Techniques, Vol. MTT-10, May, 1962. Uses capacitive susceptance matrix representation to show that theoretical noise-figure and gain-bandwidth product are the same for a balanced as for a single-diode parametric amplifier.

Hudson, A.C., "Varactor Self-Resonance in Parametric Amplifiers," Proc. IEEE, Vol. 51, Sept. 1963. Shows the dependence of necessary varactor loading on self-resonant frequency.

Hyltin, T., "Varactor Packaging and Paramp Performance," Microwaves, July 1962. Discusses the problem of stray reactances introduced by the varactor package.

Keywell, F., "On the Resonant-Cavity Method for Measurement of Varactors," IRE Trans. on Microwave Theory and Techniques, Vol. MTT-10, Nov. 1962. Describes method to measure the cutoff frequency of high-Q varactors if the law of capacitance variation is known.

Ku, W.H., "A Broad-Banding Theory for Varactor Parametric Amplifiers - Part 1, "IEEE Trans. on Circuit Theory, Vol. CT-11, No. 1, March 1964. Describes a rigorous synthesis method.

Ku, W.H., "A Broad-Banding Theory for Varactor Parametric Amplifiers - Part 2," IEEE Trans. on Circuit Theory, Vol. CT-11, No. 1, Same comment as for Part 1.

Kuh, E.S., "Theory and Design of Wide-Band Parametric Converters," Proc. of IRE, Vol. 50, No. 1, January 1962. Linear time-varying capacitance analysis of paramp.

Kurokawa, K., "Use of Passive Circuit Measurements For Adjustment of Variable Capacitance Amplifiers," Bell System Monograph 4089, Jan. 1962. Paramp adjustments made from impedance measurements.

Leeson, D.B., "Capacitance and Charge Coefficients for Varactor Diodes," Proc. IRE, Vol. 51, Aug. 1962. Gives closed-form solution in terms of Gamma functions.

Leon, B.J. and Anderson, D.R., "The stability of Pumped Nonlinear Reactance Circuits," IEEE Trans, on Circuit Theory, Vol. CT-10, December 1963. Discusses stability criteria in a network where the quiescent state is a driven state.

Lombardo, P., "Nitrogen-Cooled Low-Noise Parametric Amplifier Using Indium Antimonide Varactors," RADC Technical Report, August 1965, Airborne Instruments Lab for Rome Air Development Center on Contract No. AF 30(602)-3373. Interesting evaluation of indium antimonide varactors.

Lombardo, P.P. and Sard, E.W., "Low-Noise Microwave Reactance Amplifiers with Large Gain-Bandwidth Products," Wescon Convention Record, Pt 1, 1959. Derives conditions for large gain-bandwidth paramps.

Manley, J.M. and Rowe, H. E., "Some General Properties of Nonlinear Elements- Part I, General Energy Relations Proc. IRE, Vol. 44, No. 7, July, 1956. Original derivation of the Manley-Rowe power-frequency relationships.

Matthaei, G. L., "A Study of the Optimum Design of Wide-Band Parametric Amplifiers and Up-converters," IRE Trans. on Microwave Theory and Techniques, Vol. MTT-9, January, 1961. Describes use of multiple-resonator filters as coupling networks in single-diode parametric amplifier.

McManamon, P., "Future Aerospace System Electromagnetic Interference Control Approaches Investigation," ASD Technical Report 61-637, Nov. 1961, Armour Research Foundation for Wright-Patterson Air Force Base, Communications Laboratory. Paramp section reviews AIL work and suggests that further work should be done.

Mumford, W.W., "Some Notes on the History of Parametric Transducers," Proc. IRE, Vol 48, No. 5, May, 1960. Bibliography of early references on parametric amplifiers.

Olson, F.A., "The Large-Signal Properties of Microwave Cavity Type Parametric Circuits," SEL Report No. 315-1, Feb 8, 1960. Discusses saturation in parametric amplifiers, parametric frequency converters, and parametric limiters.

Penfield, P., JR., "Fourier Coefficients of Power-Law Devices," Jour of Franklin Inst., Feb. 1962. Complete analysis of the evaluation integral.

Penfield, P. Jr., "Note on Fourier Coefficients of Power-Law Devices," Proc. IEEE, Vol. 53, May 1965. More on Fourier coefficients of power-law devices.

Powell, R.J., "Intercept System Dynamic Range Enhancement, First Technical Note," RADC-TDR-62-475, Sept 1962, Sylvania, for Rome Air Development Center on Contract No. AF 30(602)-2721. Discusses the dynamic range of parametric devices.

Powell, R.J. et al., "Intercept System Dynamic Range Enhancement, Second Technical Note," RADC-TDR-63-91, Jan 1963, Sylvania, for Rome Air Force Development Center on Contract No. AF 30(602)-2721. Dynamic range of parametric devices.

Reed, J.R., "Spurious Free Dynamic Range in Wideband High Sensitivity Amplifiers," Microwave Journal, Vol. 8, No. 9, Sept 1965. Gives rule-of-thumb considerations for calculation of spurious free dynamic range.

Reid, E.D., "Diode Parametric Amplifiers; Principles and Experiments," BELL Monograph 3784, 1961. Elementary paramp theory.

Salzberg, B., "Masers and Reactance Amplifiers - Basic Power Relations," Proc. IRE, Vol. 45, No. 11, Nov. 1957. Describes a derivation of the Manley-Rowe power relations.

Siegel, K., "Anomalous Reverse Current in Varactor Diodes," Proc. IRE, Vol 45, No. 6, June 1960. Discusses the phenomenon of reverse current measured for DC bias voltages very much closer to forward conduction than to reverse breakdown.

Siegel, K., "Comparative Figures of Merit for Available Varactor Diodes," Proc. IRE, Vol. 49, No. 4, April 1961. Discuss nonlinearity ratio (ϵ_1/ϵ_0) and M of diodes.

Sleven, R.L., "Octave Tuning Parametric Amplifiers," Microwave Journal, Vol V, No. 10, Oct. 1962. Describes the design of amplifiers from 1 to 2 GHz. and 2 to 4 GHz.

Uhlir, A., "The Potential of Semiconductor Diodes in High-Frequency Communications," Proc. IRE, Vol 46, No. 6, June 1958. Describes properties of varactor diodes.

Vice, D.G., "Parametric Amplifier Noise Analysis," IEEE Trans. on Microwave Theory and Techniques, Vol. MTT-13, March 1965. Demonstrates the effect on the noise figure of changing the series resistance in the idler circuit.

Whelehan, J.J. et al., "Final Report on Development of Tunable C-Band Reactance Amplifiers," AIL report No. 1124-1-4, August 1962, Airborne Instrument Lab for US Army Signal Research and Development Laboratories

on Contract No. DA-36-039-sc-87405. Evaluates tuning procedures and varactors for use in stable, low-noise, tunable paramps.

White, D. H., "Long Range Communications Interference Study," RADC-TDR-360 Vol. III, Nov. 1962, Melpar Inc. Made measurements of pulse-type interference on a Raytheon Model PNS-2 paramp.

-------Varactor Handbook, Sylvania, 1965. Brief general discussion of varactors.

APPENDIX I
INTRODUCTION TO MAJOR INTERFERENCE EFFECTS

A. INTERMODULATION AND HARMONIC DISTORTION

Intermodulation is the process that produces signals of a given frequency at the output of a device when two signals of different frequencies are fed at the input. The frequencies of the intermodulation products are related to the input signal frequencies by the equation

$$f_{mn} = mf_1 \pm nf_2 \qquad \text{(I-1)}$$

where

f_{mn} = undesired intermodulation frequencies,

f_1 = frequency of first input signal,

f_2 = frequency of second input signal,

$m,n = 0, 1, 2, 3 \ldots\ldots$

The levels of the intermodulation products are given by the relation:

$$P_{mn} = mP_1 + nP_2 + K_{mn} \qquad \text{(I-2)}$$

where

P_{mn} = intermodulation product level in dbm,

P_1 = level of first input signal referred to output of device in dbm,

P_2 = level of second input signal referred to output of output of device in dbm,

K_{mn} = constant depending on device in dbm.

When either n = 0 or m = 0, only one input signal is present, and the output frequencies are harmonically related to the input frequency. This can be seen by substituting either m = 0, or n = 0 into equations I-1 and I-2.

These harmonically related outputs are generally referred to as harmonic distortions. Although intermodulation generally implies that the output signals are not harmonically related to the input, it should be apparent that harmonics are a special case of the intermodulation equation.

The intermodulation constants are related to the device nonlinearity. In general, the constant associated with an intermodulation of order m + n is related to the nonlinearity of order m + n. For example, a third-order intermodulation with m = 2 and n = 1 would be defined by:

$$P_{21} = 2P_1 + P_2 + K_{21} \qquad \text{(I-3)}$$

where the order is m + n = 3 and K_{21} is related to (the third-order coefficient of the power-series transfer function of the device).

The coefficients of nonlinearity and, therefore, the intermodulation constants depend on the device operating point. For example, in a parametric amplifier, the coefficients will depend upon the bias voltage. Therefore, the intermodulation and harmonic output levels will vary with bias voltage in a parametric amplifier.

The presence of intermodulation or harmonic distortion violates the rule of additivity for linear devices. A graphic representation of intermodulation is shown in Figure I-1.

B. SATURATION

A device is said to be in saturation when the device gain changes as a result of the magnitude of the input signal. Thus, a device in the saturation region of operation does not obey the rule of homogeneity and is, therefore, nonlinear. When a device is driven into the saturation region, distortion of the signal waveform usually occurs, and an increase of input signal results in a decrease in the gain provided by the device.

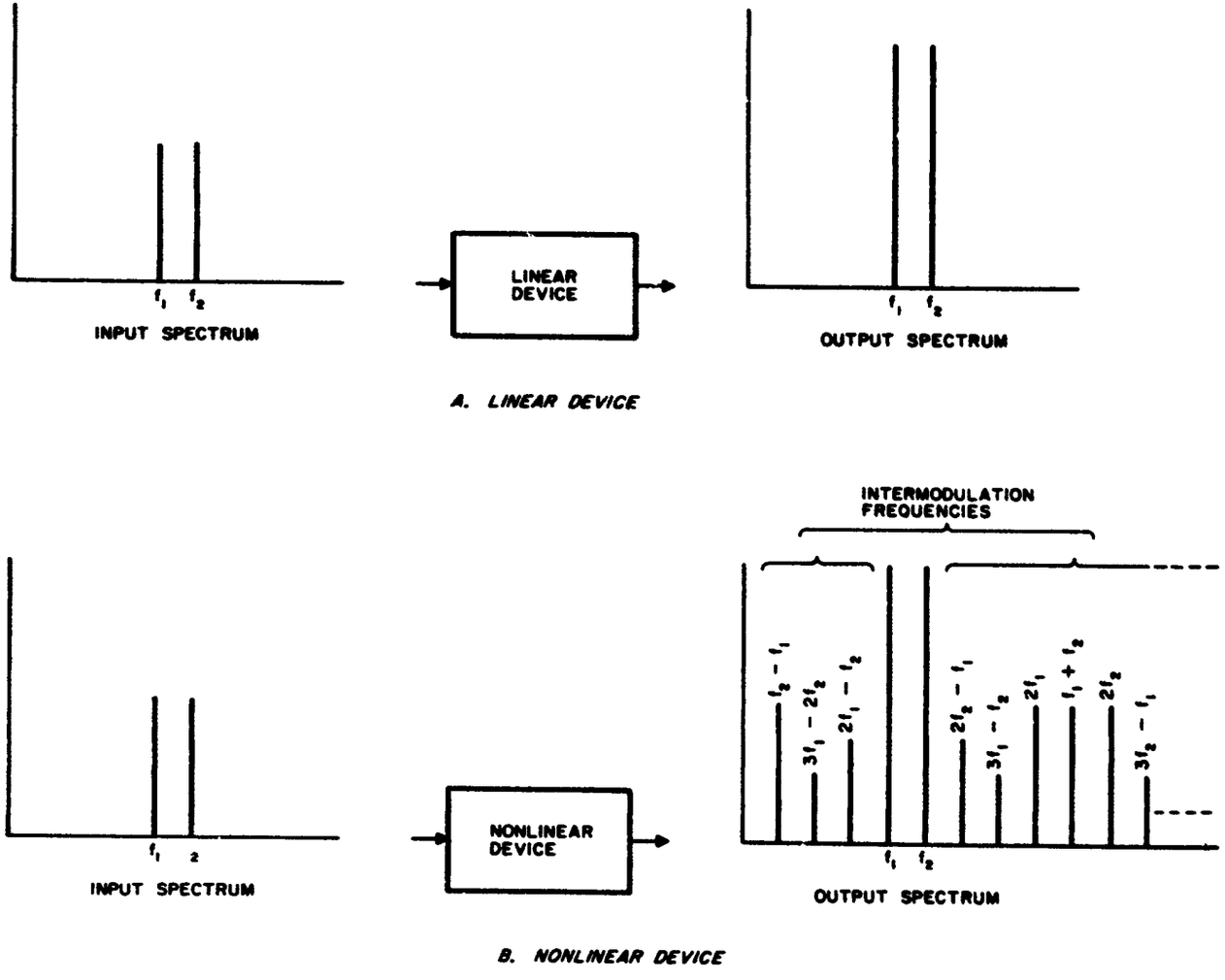

FIGURE I-1. GRAPHIC REPRESENTATION OF INTERMODULATION

The saturation level is usually determined by plotting an input-output characteristic for the device as shown in Figure I-2. Saturation is defined at various input signal levels, depending on the situation. In solid-state amplifiers, saturation is defined as the level at which gain is reduced by 1 db. For traveling-wave tube amplifiers, saturation is usually defined as that input signal level where maximum output power is obtained.

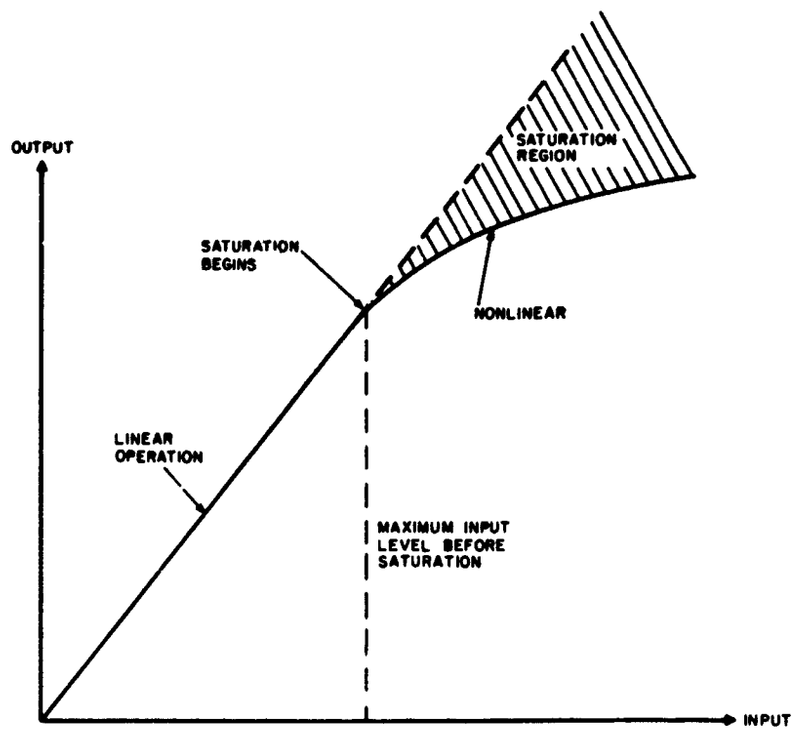

FIGURE I-2. INPUT-OUTPUT CHARACTERISTIC ILLUSTRATING SATURATION

C. CROSS MODULATION

Cross modulation is the transfer of modulation from one signal to another. That is, with two input signals (f_1, an unmodulated signal and f_2, a modulated signal), the modulation will be transferred from signal f_2 to signal f_1. It is not necessary to specify f_1 as an unmodulated signal, but the cross modulation is more apparent if f_1 is unmodulated.

In the following discussion, f_1 is assumed to be unmodulated and is referred to as the desired signal; the modulated signal can be considered to be the interfering signal even though both signals may be desired and only the transfer of modulation is undesired. If cross modulation occurs, the device does not obey the rule of additivity and is therefore nonlinear. A pictorial representation of cross modulation is shown in Figure I-3.

It has been shown (reference 12) that cross modulation can be related to the third-order curvature of the device transfer characteristic by the following equation:

$$m_k = \frac{3\frac{a_3}{a_1} V_I^2 m_I}{1 + \frac{3}{4}\frac{a_3}{a_1}\left[V_D^2 + 2V_I^2\left(1 + \frac{1}{2} m_I^2\right)\right]} \qquad \text{(I-4)}$$

where

m_k = cross-modulation index,

m_I = modulation index of interfering signal,

V_I = peak voltage of interfering signal,

V_D = peak voltage of desired signal,

a_1 = first-order coefficient of power series transfer function,

a_3 = third-order coefficient of power series transfer function.

When the interfering signal is much larger than the desired signal, equation I-4 can be simplified. It is also useful to consider the case where $m_I = 1$, which is for an interfering signal that is 100-percent modulated (the worst case). Then equation (I-4) becomes:

$$m_k = \frac{3\frac{a_3}{a_1}V_I^2}{1 + \frac{9}{4}\frac{a_3}{a_1}V_I^2} \qquad \text{(I-5)}$$

Equation I-5 defines cross modulation as a function only of the interfering signal and the first two odd-order coefficients. For V_I much less than unity, equation (I-5) states that m_k is proportional to V_I^2 or to P_I. As V_I becomes very large, m_k increases to a limiting value of 1.33. This mathematical limit is never achieved in practice.

Thus, m_k is proportional to P_I over some region and then, as P_I is increased, m_k approaches a constant maximum value.

The equation for cross modulation below the saturation region can be expressed in terms of the interfering signal power in dbm as follows (reference 11):

$$M = P_I + K \qquad \text{(I-6)}$$

where

$M = 10 \log \frac{m_k}{m_I}$ = cross-modulation ratio in db,

P_I = interfering signal output power in dbm,

K = cross-modulation constant in dbm.

When plotted against the interfering signal power in dbm, equation (I-6) is a straight line with a slope of one.

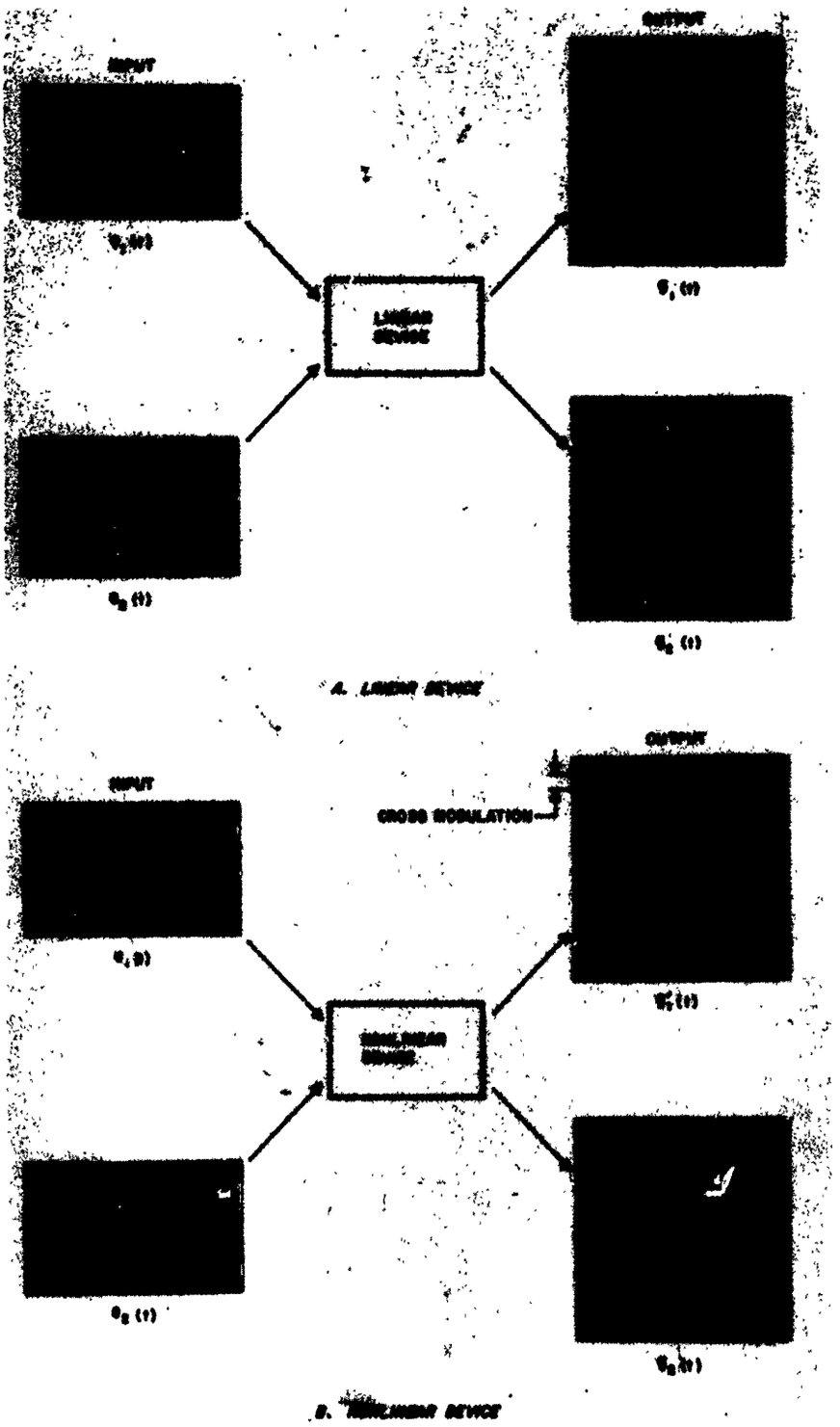

FIGURE I-3. GRAPHIC REPRESENTATION OF CROSS MODULATION

APPENDIX II

SMALL SIGNAL ANALYSIS OF MID-BAND GAIN OF PARAMETRIC AMPLIFIER WITH SUM-FREQUENCY PROPAGATION

To determine the effect of the various possible intermodulation frequencies on the performance parameters (noise figure, gain bandwidth product) of a reflection-type parametric amplifier, a method similar to that of Rowe (reference 1) will be used. This analysis will depart from Rowe, however, in that it will treat the varactor as a time-varying elastance rather than a time-varying capacitance.

The voltage v across the varactor is some function of charge q:

$$v = f(q) \tag{II-1}$$

v_p and q_p are the pump-frequency components of voltage and charge, respectively, including harmonics.

When no signal is present:

$$v_p = f(q_p) \tag{II-2}$$

A signal is introduced that is small, compared to the magnitude of the pump voltage, ... Δv and Δq are the signal components of voltage and charge, respectively.

$$\Delta v \ll v_p$$

and

$$\Delta q \ll q_p$$

Since

$$v = f(q)$$

then

$$\frac{dv}{dq} = f'(q) = \frac{df(q)}{dq} \tag{II-3}$$

Since

$$v = v_p + \Delta v \tag{II-4}$$

and

$$q = q_p + \Delta q$$

and equation II-2 has been made a condition, then

$$f'(q) = f'(q_p) \tag{II-5}$$

When a small signal is introduced,

$$\Delta v = f'(q_p)\, \Delta q \tag{II-6}$$

The term $f'(q_p)$ can be treated as a time-varying elastance, because:

$$v(t) = S(t)q(t) \tag{II-7}$$

and

$$\frac{\Delta v}{\Delta q} = S(t) = f'(q) = f'(q_p) \tag{II-8}$$

S(t) is periodic at the pump frequency and can be written in the form of a Fourier Series.

$$S(t) = \sum_{n=-\infty}^{\infty} S_n \, e^{jn\omega_p t} \qquad \text{(II-9)}$$

where

$$S_n = \frac{1}{2\pi} \int_0^{2\pi} S(t) \, e^{-jn\omega_p t} \, d(\omega_p t) \qquad \text{(II-10)}$$

and

$$S_n = S_{-n}^* \qquad \text{(II-11)}$$

From the standpoint of the signal, the nonlinear elastance can be thought of as a linearly variable elastance whose time variation is determined by the nonlinearity of the varactor and the pump waveform. Since the time origin is arbitrary, it can be chosen such that S_1 is positive and real.

Therefore,

$$S_1 = S_{-1} \qquad \text{(II-12)}$$

For a worst-case analysis, assume that the largest possible intermodulation frequency signal can flow through the varactor. Therefore, assume that current can flow through the varactor at only four frequencies: the signal, the pump, the (pump + signal), and the (pump - signal) frequencies.

At all other frequencies an open circuit will be impressed across the varactor by an ideal filter. Since equation II-4 gives an expression for the total charge, Δq is made up of components of only the signal, sum (pump + signal), and difference (pump - signal) frequencies, and can be written:

$$\Delta q = Q_1 e^{j\omega_1 t} + Q_1^* e^{j\omega_1 t} + Q_2 e^{-j\omega_2 t} + Q_2 e^{j\omega_2 t} + Q_2^* e^{-j\omega_2 t} + Q_3 e^{j\omega_3 t} + Q_3^* e^{-j\omega_3 t} \qquad \text{(II-13)}$$

where

ω_1 = signal frequency

ω_2 = difference frequency

ω_3 = sum frequency

$\omega_n = 2\pi f_n$

Although currents cannot flow at any other than the specified frequencies, voltages are produced, due to the nonlinearity of the varactor, at all harmonic mixing (intermodulation) frequencies of the pump and the signal.

Therefore,

$$\Delta v = \sum_{m=-\infty}^{\infty} \sum_{n=-\infty}^{\infty} V_{m,n} e^{j(m\omega_p + n\omega_1)t} \qquad \text{(II-14)}$$

Equation II-14 can be rewritten:

$$\Delta v = V_1 e^{j\omega_1 t} + V_1^* e^{-j\omega_1 t} + V_2 e^{j\omega_2 i} + V_2^* e^{-j\omega_2 t} + V_3 e^{j\omega_3 t} + V_3^* e^{-j\omega_3 t}_{+\ldots} \qquad \text{(II-15)}$$

Equation II-9 can be rewritten:

$$S(t) = S_o + S_1 e^{j\omega_p t} + S_{-1} e^{-j\omega_p t} + S_2 e^{j2\omega_p t} + S_{-2} e^{-j2\omega_p t} + \ldots + S_n e^{jn\omega_p t}$$

$$+ S_{-n} e^{-jn\omega_p t} \qquad \text{(II-16)}$$

Since $\Delta v = S(t)\,\Delta q$, equations II-13 and II-16 can be multiplied together and equated to the right hand side of equation II-15. This will give a relation which is reducible to a matrix form:

$$\left[S_o + S_1 e^{j\omega_p t} + S_{-1} e^{-j\omega_p t} + S_2 e^{j2\omega_p t} + S_{-2} e^{-j\omega_p t} + \ldots \right]$$

$$\cdot \left[Q_1 e^{j\omega_1 t} + Q_1^* e^{-j\omega_1 t} + Q_2 e^{j\omega_2 t} + Q_2^* e^{-j\omega_2 t} + Q_3 e^{j\omega_3 t} + Q_3^* e^{-j\omega_3 t} \right]$$

$$= V_1 e^{+j\omega_1 t} + V_1^* e^{-j\omega_1 t} + V_2 e^{+j\omega_2 t} + V_2^* e^{-j\omega_2 t} + V_3 e^{+j\omega_3 t} + V_3^* e^{-j\omega_3 t} + \ldots \quad \text{(II-17)}$$

In the following analysis all elastance terms of the form S_n where n = 3, 4, 5,..., will be neglected.

Equating the coefficients of the exponentials in equation II-17.

Exponential	Equations of Coefficients	
$e^{j\omega_1 t}$	$V_1 = S_o Q_1 + S_1 Q_2^* + S_{-1} Q_3$	(II-18)
$e^{-j\omega_1 t}$	$V_1^* = S_o Q_1^* + S_1 Q_3^* + S_{-1} Q_2$	(II-19)
$e^{j\omega_2 t}$	$V_2 = S_o Q_2 + S_1 Q_1^* + S_2 Q_3^*$	(II-20)
$e^{-j\omega_2 t}$	$V_2^* = S_o Q_2^* + S_{-1} Q_1 + S_{-2} Q_3$	(II-21)
$e^{j\omega_3 t}$	$V_3 = S_o Q_3 + S_1 Q_1 + S_2 Q_2^*$	(II-22)
$e^{-j\omega_3 t}$	$V_3^* = S_o Q_3^* + S_{-1} Q_1^* + S_{-2} Q_2$	(II-23)

From equations II-18 through II-23 two matrix relations result that are merely complex conjugates of each other:

Matrix I (from equations II-18, II-21, and II-22:

$$\begin{bmatrix} V_1 \\ V_2^* \\ V_3 \end{bmatrix} = \begin{bmatrix} S_o & S_1 & S_{-1} \\ S_{-1} & S_o & S_{-2} \\ S_1 & S_2 & S_o \end{bmatrix} \begin{bmatrix} Q_1 \\ Q_2^* \\ Q_3 \end{bmatrix} \quad \text{(II-24)}$$

Matrix II (from equations II-19, II-20, and II-23:

$$\begin{bmatrix} V_1^* \\ V_2 \\ V_3^* \end{bmatrix} = \begin{bmatrix} S_o & S_{-1} & S_1 \\ S_1 & S_o & S_2 \\ S_{-1} & S_{-2} & S_o \end{bmatrix} \begin{bmatrix} Q_1^* \\ Q_2 \\ Q_3^* \end{bmatrix} \qquad \text{(II-25)}$$

Either equation II-24 or II-25 can be used in the following analysis. Matrix I will be used in this analysis.

Since $I = j\omega Q$ and $I^* = -j\omega Q^*$, equation II-24 can be rewritten:

$$\begin{bmatrix} V_1 \\ V_2^* \\ V_3 \end{bmatrix} = \begin{bmatrix} \frac{-j\,S_o}{\omega_1} & \frac{jS_1}{\omega_2} & \frac{-jS_{-1}}{\omega_3} \\ \frac{-jS_{-1}}{\omega_1} & \frac{jS_o}{\omega_2} & \frac{-jS_{-2}}{\omega_3} \\ \frac{-jS_1}{\omega_1} & \frac{jS_2}{\omega_2} & \frac{-jS_o}{\omega_3} \end{bmatrix} \begin{bmatrix} I_1 \\ I_2^* \\ I_3 \end{bmatrix} \qquad \text{(II-26)}$$

Equation II-26 has the form of an impedance matrix:

$$\begin{bmatrix} V_1 \\ V_2^* \\ V_3 \end{bmatrix} = \begin{bmatrix} Z_{11} & Z_{12} & Z_{13} \\ Z_{21} & Z_{22} & Z_{23} \\ Z_{31} & Z_{32} & Z_{33} \end{bmatrix} \begin{bmatrix} I_1 \\ I_2^* \\ I_3 \end{bmatrix} \qquad \text{(II-27)}$$

The paramp can be considered to be a three - port device with an arbitary loading at ω_2 and ω_3. Also, port 1 can be considered to support only ω_1, port 2 to support only ω_2, and port 3 to support only ω_3, due to the built in isolation of one port from each of the others. The three-port paramp can be represented schematically as:

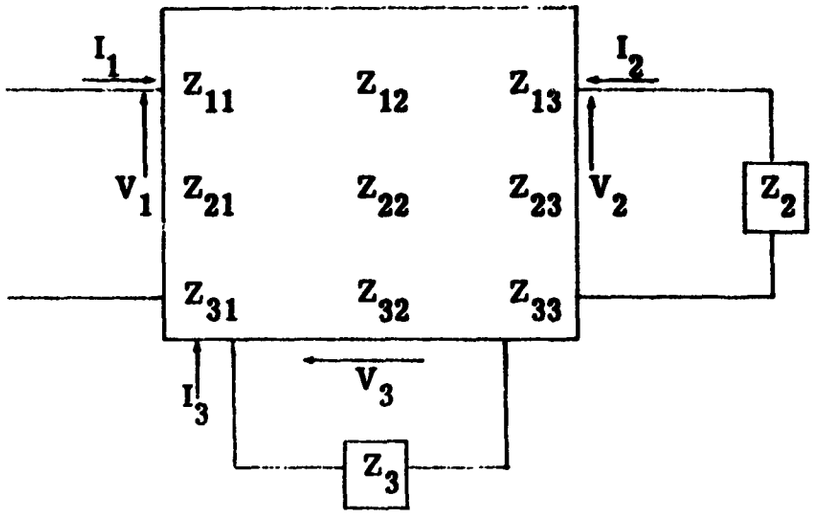

The loading (Z_2 and Z_3) can be taken into the matrix in the following way:

$$\begin{bmatrix} V_1 \\ O \\ O \end{bmatrix} = \begin{bmatrix} Z_{11} & Z_{12} & Z_{13} \\ Z_{21} & Z_{22}+Z_2 & Z_{23} \\ Z_{31} & Z_{32} & Z_{33}+Z_3 \end{bmatrix} \begin{bmatrix} I_1 \\ I_2^* \\ I_3 \end{bmatrix} \qquad \text{(II-28)}$$

The input impedance of this device is

$$Z_{in} = \frac{V_1}{I_1} \qquad \text{(II-29)}$$

Solving for I_1:

$$I_1 = \frac{V_1 \left\{ \left[(Z_{22}+Z_2)(Z_{33}+Z_3) \right] - Z_{23}Z_{32} \right\}}{\left((Z_{11})(Z_{22}+Z_2)(Z_{33}+Z_3) + Z_{12}Z_{23}Z_{31} + Z_{13}Z_{21}Z_{32} \right.} \qquad \text{(II-30)}$$
$$\left. - Z_{13}Z_{31}(Z_{22}+Z_2) - Z_{11}Z_{23}Z_{32} - Z_{12}Z_{21}(Z_{33}+Z_3) \right)$$

Therefore, Z_{in} can be written:

$$Z_{in} = \frac{V_1}{I_1} = \frac{\left\{ \begin{array}{l} Z_{11}(Z_{22} + Z_2)(Z_{33} + Z_3) + Z_{12}Z_{23}Z_{31} + Z_{13}Z_{21}Z_{32} \\ - Z_{13}Z_{31}(Z_{22} + Z_2) - Z_{11}Z_{23}Z_{32} - Z_{12}Z_{21}(Z_{33} + Z_3) \end{array} \right\}}{(Z_{22} + Z_2)(Z_{33} + Z_3) - Z_{23}Z_{32}} \quad \text{(II-31)}$$

$$Z_{in} = Z_{11} - \frac{Z_{12}\left[Z_{21} - \frac{Z_{23}Z_{31}}{(Z_{33} + Z_3)}\right]}{\left[(Z_{22} + Z_2) - \frac{Z_{23}Z_{32}}{(Z_{33} + Z_3)}\right]} - \frac{Z_{13}\left[Z_{31} - \frac{Z_{21}Z_{32}}{(Z_{22} + Z_2)}\right]}{\left[(Z_{33} + Z_3) - \frac{Z_{23}Z_{32}}{(Z_{22} + Z_2)}\right]} \quad \text{(II-32)}$$

It is now necessary to specify the loading at the difference (ω_2) and sum (ω_3) frequency ports. The loading in each case is a reactance that resonates with the self-impedance at the port in series with a resistance. The resistance is a series combination of:

1. the series resistance R_D of the varactor,
2. the finite resistance of the reactive element,
3. any additional resistive loading.

The second and third resistances are combined and denoted by R_L.

Thus, at the ω_2 port,

$$Z_{22} + Z_2 = (R_D + R_{L2}) + \frac{jS_o}{\omega_2} - jX_2. \quad \text{(II-33)}$$

Let X_2 be of the form ωL_2. At resonance,

$$Z_{22} + Z_2 = R_D + R_{L2}$$

but, to get the input impedance in a form which takes a small detuning into account, the following derivation is necessary:

$$Z_{22} + Z_2 = (R_D + R_{L2}) + j\left(\frac{S_o}{\omega} - \omega L_2\right) \qquad \text{(II-34)}$$

At resonance,

$$S_o = \omega_2^2 L_2 \qquad \text{(II-35)}$$

Therefore

$$Z_{22} + Z_2 = (R_D + R_{L2}) + j\left(\frac{\omega_2^2 L_2}{\omega} - \omega L_2\right) \qquad \text{(II-36)}$$

Defining,

$$Q_2 = \frac{\omega_2 L_2}{R_L + R_{L2}} \qquad \text{(II-37)}$$

$$Z_{22} + Z_2 = R_{L2} + R_D \left[1 + jQ_2\left(\frac{\omega_2}{\omega} - \frac{\omega}{\omega_2}\right)\right] \qquad \text{(II-38)}$$

Let

$$\delta = \frac{\omega - \omega_2}{\omega_2} \qquad \text{(II-39)}$$

Therefore

$$Z_{22} + Z_2 = R_{L2} + R_D \left[1 - jQ_2\delta\left(\frac{2 + \delta}{1 + \delta}\right)\right] \qquad \text{(II-40)}$$

For the narrow-band approximation of $1 \gg \delta$, equation II-40 reduces to:

$$Z_{22} + Z_2 = R_{L2} + R_D \left[1 - jQ_2\delta 2\right] \qquad \text{(II-41)}$$

Substituting equation II-37 back intc equation II-41

$$Z_{22} + Z_2 = R_D + R_{L2} - j\omega_2 L_2 \delta 2$$

$$Z_{22} + Z_2 = R_D + R_{L2} - j2L_2 (\omega - \omega_2) \qquad \text{(II-42)}$$

Let

$$\Delta\omega_2 = \omega - \omega_2 \qquad \text{(II-43)}$$

and substitute equation II-43 into equation II-42:

$$\boxed{Z_{22} + Z_2 = R_D + R_{L2} - j2L_2 \Delta\omega_2} \qquad \text{(II-44)}$$

The above derivation can also be performed for port 3, and the result is:

$$\boxed{Z_{33} + Z_3 = R_D + R_{L3} + j2L_3 \Delta\omega_3} \qquad \text{(II-45)}$$

Letting

$$R_D + R_{L3} = R_{33} \text{ and } R_D + R_{L2} = R_{22} \qquad \text{(II-46)}$$

and substituting equations II-44 and II-45 and the appropriate elastance notation back into the input impedance expression (equation II-32), and expression for the input impedance of a paramp under a narrow-band approximation results:

$$Z_{in} = Z_{11} - \left\{ \frac{\dfrac{S_1^2}{\omega_1\omega_2} - \dfrac{jS_1^2S_2}{\omega_1\omega_2\omega_3(R_{33}+j2\Delta\,\omega_3L_3)}}{R_{22}-j2\Delta\,\omega_2L_2 - \dfrac{S_2^2}{\omega_2\omega_3\,(R_{33}+j2\Delta\,\omega_3L_3)}} \right\} + \left\{ \frac{\dfrac{S_1^2}{\omega_1\omega_3} + \dfrac{jS_1^2S_2}{\omega_1\omega_2\omega_3\,(R_{22}-j2\Delta\,\omega_2L_2)}}{R_{33}+j2\Delta\,\omega_3L_3 - \dfrac{S_2^2}{\omega_2\omega_3\,(R_{22}-j2\Delta\,\omega_2L_2)}} \right\} \qquad \text{(II-47)}$$

According to experimental data obtained on a number of varactors, S_2 is very small compared with S_1. Therefore, the further approximation is made that:

$$S_2 \approx 0$$

Equation II-47 then simplifies to:

$$Z_{in} = Z_{11} - \frac{S_1^2/\omega_1\omega_2}{R_{22} - j2\Delta\omega_2L_2} + \frac{S_1^2/\omega_1\omega_3}{R_{33}+j2\Delta\omega_3L_3} \qquad \text{(II-48)}$$

The paramp which equation II-48 describes is of the form:

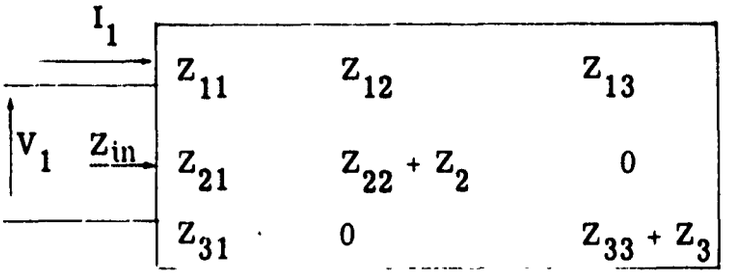

In a real paramp mount, the signal passes through a circuit tuned to the signal frequency at port 1. The tuned circuit is made up of a very-low-loss inductance in series with the self-impedance of the varactor at port 1. The resistance introduced will be considered small compared with the series resistance of the varactor junction. The above situation is characterized by:

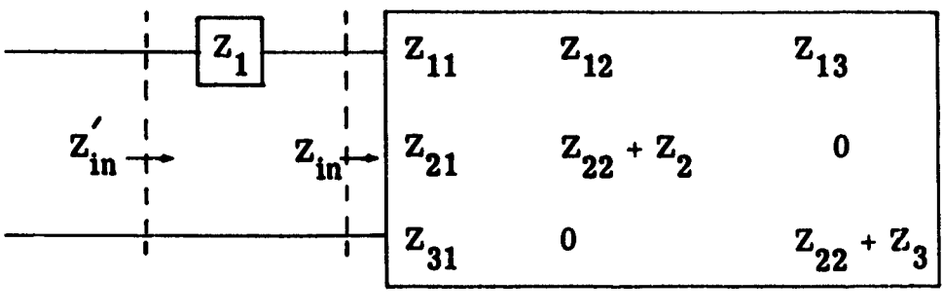

Impedance Z_1 can be taken into the matrix in the same manner as Z_2 and Z_3, resulting in the following:

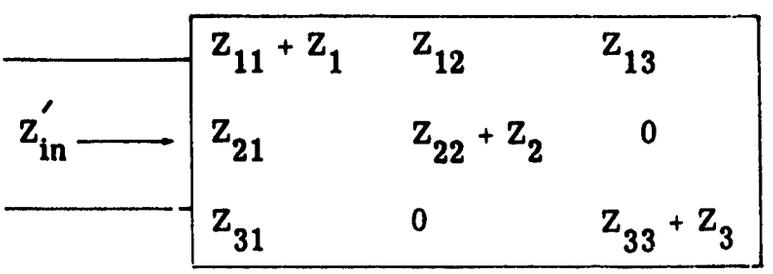

Also impedance $Z_{11} + Z_1$ can be rewritten to take into account a small detuning:

$$Z_{11} + Z_1 = R_D + j2\Delta\omega_1 L_1 \qquad \text{(II-49)}$$

Z'_{in} can now be written:

$$Z'_{in} = R_D + j2\Delta\omega_1 L_1 - \frac{S_1^2/\omega_1\omega_2}{R_{22} - j2\Delta\omega_2 L_2} + \frac{S_1^2/\omega_1\omega_3}{R_{33} + j2\Delta\omega_3 L_3} \qquad \text{(II-50)}$$

From equation II-50 the mid-band gain of the parametric amplifier can easily be derived.

Assuming that the paramp is driven from a purely resistive generator of resistance R_g, the voltage gain is given by:

$$|\Gamma_o| = \frac{|V_r|}{|V_i|} = \left| \frac{Z'_{in,\,m} - R_g}{Z'_{in,\,m} + R_g} \right| \qquad \text{(II-51)}$$

where $|\Gamma_o|$ = mid-band voltage gain

V_r = reflected voltage

V_i = incident voltage

$Z'_{in,\,m}$ = mid-band input impedance (when all ports are at resonance)

$$\boxed{Z'_{in,\,m} = R_D - \frac{S_1^2}{R_{22}\omega_1\omega_2} + \frac{S_1^2}{R_{33}\omega_1\omega_3}} \qquad \text{II-52)}$$

$$|\Gamma_o| = \left| \frac{R_D - R_g - \dfrac{S_1^2}{R_{22}\omega_1\omega_2} + \dfrac{S_1^2}{R_{33}\omega_1\omega_3}}{R_D + R_g - \dfrac{S_1^2}{R_{22}\omega_1\omega_2} + \dfrac{S_1^2}{R_{33}\omega_1\omega_3}} \right|$$

Dividing through by R_D,

$$|\Gamma_o| = \left| \frac{1 - \dfrac{R_g}{R_D} - \dfrac{S_1^2}{R_D R_{22}\omega_1\omega_2} + \dfrac{S_1^2}{R_D R_{33}\omega_1\omega_3}}{1 + \dfrac{R_g}{R_D} - \dfrac{S_1^2}{R_D R_{22}\omega_1\omega_2} + \dfrac{S_1^2}{R_D R_{33}\omega_1\omega_3}} \right|$$

Let

$$K_o = \frac{R_g}{R_D} \tag{II-53}$$

$$K_2 = \frac{R_{L2}}{R_D} \tag{II-54}$$

and

$$K_3 = \frac{R_{L3}}{R_D} \tag{II-55}$$

$$\left|\Gamma_o\right| = \left| \frac{1 - K_o - \dfrac{S_1^2}{\omega_1\omega_2 R_D^2(1+K_2)} + \dfrac{S_1^2}{\omega_1\omega_3 R_D^2(1+K_3)}}{1 + K_o - \dfrac{S_1^2}{\omega_1\omega_2 R_D^2(1+K_2)} + \dfrac{S_1^2}{\omega_1\omega_3 R_D^2(1+K_3)}} \right| \tag{II-56}$$

In the literature, and in common use in industry, is the figure of merit M of a varactor (reference 13). An expression for M is given in equation II-57.

$$\boxed{M = \frac{S_1}{2\pi R_D}} \tag{II-57}$$

Substituting equation II-57 into equation II-56 yields a usable expression for the mid-band voltage gain of a four-frequency paramp.

$$\boxed{\left|\Gamma_o\right| = \left| \frac{1 - K_o - \dfrac{M^2}{f_1 f_2(1+K_2)} + \dfrac{M^2}{f_1 f_3(1+K_3)}}{1 + K_o - \dfrac{M^2}{f_1 f_2(1+K_2)} + \dfrac{M^2}{f_1 f_3(1+K_3)}} \right|} \tag{II-58}$$

From the expression for the mid-band voltage gain of the paramp (equation II-58), it is clear that the amplifier can have gain ($|\Gamma_o| > 1$) only if the following condition is satisfied:

$$\boxed{\frac{M^2}{f_1 f_2 (1+K_2)} > 1 + \frac{M^2}{f_1 f_3 (1+K_3)}} \qquad \text{(II-59)}$$

Thus, equation II-59 is the condition for gain in the paramp if the sum frequency is allowed to propagate.

The condition for gain (equation II-59) can be used to show the effect of sum-frequency propagation on the ability to vary the idler loading under a constant M condition.

The preferred-circuit amplifier has the following parameters:

$$M^2 = 125 \times 10^{18}\ \text{Hz}^2,$$

$$f_1 = .900\ \text{GHz}$$

$$f_2 = 8.275\ \text{GHz},$$

$$f_3 = 10.075\ \text{GHz}.$$

The range of K_2 for perfect sum-frequency propagation ($K_3 = 0$) can be found from:

$$\frac{M^2}{f_1 f_2 (1+K_2)} > 1 + \frac{M^2}{f_1 f_3} \qquad \text{(II-60)}$$

$$K_2 < \frac{\frac{M^2}{f_1 f_2}}{1 + \frac{M^2}{f_1 f_3}} - 1 \qquad \text{(II-61)}$$

Substituting the amplifier parameters into equation II-61:

$$K_2 < \frac{\frac{125}{(.9)(8.275)}}{1 + \frac{125}{(.9)(10.075)}} - 1$$

$$K_2 < .141$$

The range of K_2 for no sum-frequency propagation ($K_3 = \infty$) can be found from:

$$\frac{M^2}{f_1 f_2 (1+K_2)} > 1 \qquad \text{(II-62)}$$

$$K_2 < \frac{M^2 - f_1 f_2}{f_1 f_2} \qquad \text{(II-63)}$$

Substituting the amplifier parameters into equation II-63:

$$K_2 < \frac{125 - (.9)(8.275)}{(.9)(8.275)}$$

$$K_2 < 15.85$$

Thus, the range of K_2 for no sum-frequency propagation is much greater than the range of K_2 with sum-frequency propagation.

APPENDIX III

DERIVATION OF GAIN-BANDWIDTH PRODUCT FOR A PARAMETRIC AMPLIFIER WITH SUM-FREQUENCY PROPAGATION

Since the narrow-band approximation was used in deriving the input impedance of this paramp (Appendix II), a high gain condition will be used to derive a usable gain-bandwidth expression.

To maximize the gain, the denominator of the mid-band gain expression (equation II-58 in Appendix II) should approach zero:

$$1 + K_o - \frac{M^2}{f_1 f_2 (1+K_2)} + \frac{M^2}{f_1 f_3 (1+K_3)} \approx 0$$

$$1 + K_o = \frac{M^2 \left[1 - \frac{f_2 (1+K_2)}{f_3 (1+K_3)} \right]}{f_1 f_2 (1+K_2)} \qquad \text{(III-1)}$$

$$\boxed{\frac{M^2 \left[1 - \frac{f_2 (1+K_2)}{f_3 (1+K_3)} \right]}{f_1 f_2 (1+K_2)(1+K_o)} \approx 1} \qquad \text{(III-2)}$$

Equation III-2 is the high gain condition under which this analysis will continue.

The input or signal circuit of the paramp will be considered to be a single-tuned resonant circuit, and the shape of the gain-versus-frequency curve will be considered to be that of a single-tuned resonant circuit. The 3-db bandwidth points occur when the phase angle of the expression for the input impedance of the loaded signal circuit is ± 45 degrees from the center-frequency phase angle.

The signal circuit is excited from a source impedance of R_g and, therefore, the input impedance of the loaded signal circuit Z_s is:

$$Z_s = R_g + Z'_{in} = \alpha + j\beta \qquad \text{(III-3)}$$

The 3-db bandwidth occurs when $\alpha = \beta$.

The expression for Z'_{in} will now be put in a more convenient form:

$$Z'_{in} = R_D + j2\Delta\omega_1 L_1 - \frac{S_1^2/\omega_1\omega_2}{R_{22} - j2\Delta\omega_2 L_2} + \frac{S_1^2/\omega_1\omega_3}{R_{33} + j2\Delta\omega_3 L_3}$$

$$Z'_{in} = R_D + j2\Delta\omega_1 L_1 + \left\{ \frac{\frac{S_1^2 R_{22}}{\omega_1\omega_3} - \frac{S_1^2 R_{33}}{\omega_1\omega_2} - j\left[\frac{S_1^2 2\Delta\omega_3 L_3}{\omega_1\omega_2} + \frac{S_1^2 2\Delta\omega_2 L_2}{\omega_1\omega_3}\right]}{(R_{22} - j2\Delta\omega_2 L_2)(R_{33} + j2\Delta\omega_3 L_3)} \right\} \qquad \text{(III-4)}$$

Evaluating the denominator of the bracketed expression:

$$(R_{22} - j2\Delta\omega_2 L_2)(R_{33} + j2\Delta\omega_3 L_3) = R_{22} + R_{33} + 4\Delta\omega_2\Delta\omega_3 L_2 L_3 + j\left[2\Delta\omega_3 L_3 R_{22} - 2\Delta\omega_2 L_2 R_{33}\right]$$

$$= R_{22}R_{33}\left[1 + 4\left(\frac{\Delta\omega_2 L_2}{R_{22}}\right)\left(\frac{\Delta\omega_3 L_3}{R_{33}}\right) + j\left(\frac{2\Delta\omega_3 L_3}{R_{33}} - \frac{2\Delta\omega_2 L_2}{R_{22}}\right)\right] \qquad \text{(III-5)}$$

Since $Q = \frac{\omega L}{R}$ has been defined as the loaded Q, the following notation will now be used:

$$Q_2 = \frac{\omega_2 L_2}{R_{22}} \quad \text{and} \quad Q_3 = \frac{\omega_3 L_3}{R_{33}} \qquad \text{(III-6)}$$

equation III-5 can now be rewritten:

$$(R_{22} - j2\Delta\omega_2 L_2)(R_{33} + j2\Delta\omega_3 L_3) = R_{22}R_{33}\left\{1 + 4Q_2\frac{\Delta\omega_2}{\omega_2}\ Q_3\frac{\Delta\omega_3}{\omega_3} + j\left[2Q_3\ \frac{\Delta\omega_3}{\omega_3} - 2Q_2\ \frac{\Delta\omega_2}{\omega_2}\right]\right\} \qquad \text{(III-7)}$$

Over a narrow band,

$$4Q_2Q_3\ \frac{\Delta\omega_2}{\omega_2}\ \frac{\Delta\omega_3}{\omega_3} << 1$$

Therefore equation III-7 becomes:

$$(R_{22} - j2\Delta\omega_2 L_2)(R_{33} + j2\Delta\omega_3 L_3) = R_{22}R_{33}\left[1 + j\left(2Q_3\ \frac{\Delta\omega_3}{\omega_3} - 2Q_2\ \frac{\Delta\omega_2}{\omega_2}\right)\right] \qquad \text{(III-8)}$$

Substituting equation III-8 into equation III-4:

$$Z'_{in} = R_D + j2\Delta\omega_1 L_1 + \left\{\frac{\frac{S_1^2 R_{22}}{\omega_1\omega_3} - \frac{S_1^2 R_{33}}{\omega_1\omega_2} - j\left[\frac{S_1^2 2\Delta\omega_3 L_3}{\omega_1\omega_2} + \frac{S_1^2 2\Delta\omega_2 L_2}{\omega_1\omega_3}\right]}{R_{22}R_{33}\left[1 + j\left(2Q_3\ \frac{\Delta\omega_3}{\omega_3} - 2Q_2\ \frac{\Delta\omega_2}{\omega_2}\right)\right]}\right\} \qquad \text{(III-9)}$$

or

$$Z'_{in} = R_D + j2\Delta\omega_1 L_1 + \left\{\frac{\frac{S_1^2}{\omega_1\omega_3 R_{33}} - \frac{S_1^2}{\omega_1\omega_2 R_{22}} - j\left[\frac{S_1^2 2\Delta\omega_3 L_3}{\omega_1\omega_2 R_{22}R_{33}} + \frac{S_1^2 2\Delta\omega_2 L_2}{\omega_1\omega_3 R_{22}R_{33}}\right]}{1 + j\left(2Q_3\ \frac{\Delta\omega_3}{\omega_3} - 2\,Q_2\ \frac{\Delta\omega_2}{\omega_2}\right)}\right\}$$

Substituting equation III-6 into equation III-9:

$$Z'_{in} = R_D + j2\Delta\omega_1 L_1 + \left\{\frac{\frac{S_1^2}{\omega_1\omega_3 R_{33}} - \frac{S_1^2}{\omega_1\omega_2 R_{22}} - j\left[\frac{S_1^2 2Q_3\Delta\omega_3}{R_{22}\omega_1\omega_2\omega_3} + \frac{S_1^2 2Q_2\Delta\omega_2}{R_{33}\omega_1\omega_2\omega_3}\right]}{1 + j\left(2Q_3\ \frac{\Delta\omega_3}{\omega_3} - 2Q_2\ \frac{\Delta\omega_2}{\omega_2}\right)}\right\} \qquad \text{(III-10)}$$

Multiplying the numerator and denominator of the fraction in equation III-10 by the complex conjugate of the denominator, and assuming that terms of the form $(\Delta\omega)(\Delta\omega)$ are negligible, yields:

$$Z'_{in} = R_D + j2\Delta\omega_1 L_1 + \frac{S_1^2}{\omega_1\omega_3 R_{33}} - \frac{S_1^2}{\omega_1\omega_2 R_{22}} - j\left[\frac{S_1^2 2Q_2}{R_{22}\omega_1\omega_2}\left(\frac{\Delta\omega_2}{\omega_2}\right) + \frac{S_1^2 2Q_3}{R_{33}\omega_1\omega_3}\frac{\Delta\omega_3}{\omega_3}\right] \quad \text{(III-11)}$$

It is now useful to convert the Z_s.

$$Z_s = R_g + Z'_{in} = R_o + R_g + \frac{S_1^2}{\omega_1\omega_3 R_{33}} - \frac{S_1^2}{\omega_1\omega_2 R_{22}} - j\left[\frac{S_1^2 2Q_2}{R_{22}\omega_1\omega_2}\left(\frac{\Delta\omega_2}{\omega_2}\right) + \frac{S_1^2 2Q_3}{R_{33}\omega_1\omega_3}\left(\frac{\Delta\omega_3}{\omega_3}\right) - \Delta 2\omega_1 L_1\right] \quad \text{(III-12)}$$

Since $K_o = \frac{R_g}{R_D}$ and the unloaded Q of the signal circuit is:

$$Q_{1U} = \frac{\omega_1 L_1}{R_D} \quad \text{(III-13)}$$

equation III-12 can be divided through by R_D and rewritten in the form:

$$\frac{Z_s}{R_D} = 1 + K_o + \frac{S_1^2}{\omega_1\omega_3 R_{33} R_D} - \frac{S_1^2}{\omega_1\omega_2 R_{22} R_D} + j\left[2Q_{1U}\left(\frac{\Delta\omega_1}{\omega_1}\right) - \frac{S_1^2 2Q_2}{R_{22}\omega_1\omega_2}\left(\frac{\Delta\omega_2}{\omega_2}\right) - \frac{S_1^2 2Q_3}{R_{33}\omega_1\omega_3}\left(\frac{\Delta\omega_3}{\omega_3}\right)\right] \quad \text{(III-14)}$$

Since the pump frequency is fixed at ω_p and

$$\omega_2 = \omega_p - \omega_1$$

and

$$\omega_3 = \omega_p + \omega_1$$

an increase in ω_1 yields a decrease in ω_2 and an increase in ω_3. Thus,

$$\Delta\omega = \Delta\omega_1 = -\Delta\omega_2 = \Delta\omega_3 \qquad \text{(III-15)}$$

Substituting equation III-15 into equation III-14:

$$\frac{Z_s}{R_D} = 1 + K_o + \frac{S_1^2}{\omega_1\omega_3 R_{33} R_D} - \frac{S_1^2}{\omega_1\omega_2 R_{22} R_D} + j\left[2Q_{1U}\left(\frac{\Delta\omega}{\omega_1}\right) + \frac{S_1^2 2Q_2}{R_{22}\omega_1\omega_2}\left(\frac{\Delta\omega}{\omega_2}\right)\right.$$

$$\left. - \frac{S_1^2 2Q_3}{R_{33}\omega_1\omega_2}\left(\frac{\Delta\omega}{\omega_3}\right)\right] \qquad \text{(III-16)}$$

Since $\Delta\omega$ represents a deviation to only one side of the resonant frequency, $2\Delta\omega$ is necessary to specify a symmetrical bandwidth. Therefore, let

$$X = 2\Delta f \qquad \text{(III-17)}$$

Since M has been previously defined as $M = \frac{S_1}{2\pi R_D}$, then equation III-17 and the definition of M can be substituted into equation III-16:

$$\frac{Z_s}{R_D} = 1 + K_o + \frac{M^2}{f_1 f_3\left(1 + \frac{R_{L3}}{R_D}\right)} - \frac{M^2}{f_1 f_2\left(1 + \frac{R_{L2}}{R_D}\right)} + j\left[Q_{1U}\left(\frac{X}{f_1}\right) + \frac{M^2 Q_2}{f_1 f_2\left(1 + \frac{R_{L2}}{R_D}\right)}\left(\frac{X}{f_2}\right)\right.$$

$$\left. - \frac{M^2 Q_3}{f_1 f_2\left(1 + \frac{R_{L3}}{R_D}\right)}\left(\frac{X}{f_3}\right)\right] \qquad \text{(III-18)}$$

Since

$$K_2 = \frac{R_{L2}}{R_D}$$

and

$$K_3 = \frac{R_{L3}}{R_D}$$

equation III-18 can be rewritten:

$$\frac{Z_s}{R_D} = 1 + K_o + \frac{M^2}{f_1 f_3 (1+K_3)} - \frac{M^2}{f_1 f_2 (1+K_2)} + jX \left[\frac{Q_{1U}}{f_1} + \frac{M^2}{f_1 f_2 (1+K_2)} \left(\frac{Q_2}{f_2} \right) - \frac{M^2}{f_1 f_3 (1+K_3)} \left(\frac{Q_3}{f_3} \right) \right] \quad \text{(III-19)}$$

As described before, X is the 3-db bandwidth of the paramp if the real part of Z_s equals the imaginary part of Z_s:

$$1 + K_o + \frac{M^2}{f_1 f_3 (1+K_3)} - \frac{M^2}{f_1 f_2 (1+K_2)} = X_{3db} \left[\frac{Q_{1U}}{f_1} + \frac{M^2}{f_1 f_2 (1+K_2)} \left(\frac{Q_2}{f_2} \right) - \frac{M^2}{f_1 f_3 (1+K_3)} \left(\frac{Q_3}{f_3} \right) \right] \quad \text{(III-20)}$$

At this point, a more convenient notation would be the loaded or unloaded bandwidths of the resonant structures at ports 1, 2, and 3 of the paramp. The bandwidth of a single-tuned resonant circuit is related to the Q in the following way:

$$B = \frac{f_o}{Q} \quad \text{(III-21)}$$

where B is either the loaded or unloaded bandwidth, depending upon whether Q is the loaded or the unloaded Q, and f_o is the resonant frequency.

Therefore,

$$B_{1U} = \frac{f_1}{Q_{1U}} \quad \text{(III-22)}$$

$$B_2 = \frac{f_2}{Q_2} \quad \text{(III-23)}$$

and

$$B_3 = \frac{f_3}{Q_3} \quad \text{(III-24)}$$

where B_{1U} is an unloaded bandwidth and B_2 and B_3 are loaded bandwidths.

Substituting equations III-22, III-23, III-24 into equation III-20 yields:

$$1+K_o+\frac{M^2}{f_1f_3(1+K_3)}-\frac{M^2}{f_1f_2(1+K_2)}=X_{3db}\left[\frac{1}{B_{1U}}+\frac{M^2}{f_1f_2(1+K_2)}\left(\frac{1}{B_2}\right)-\frac{M^2}{f_1f_3(1+K_3)}\left(\frac{1}{B_3}\right)\right]$$

The expression for the 3-db bandwidth is,

$$X_{3db}=\frac{1+K_o+\frac{M^2}{f_1f_3(1+K_3)}-\frac{M^2}{f_1f_2(1+K_2)}}{\frac{1}{B_{1U}}+\frac{M^2}{f_1f_2(1+K_2)}\left(\frac{1}{B_2}\right)-\frac{M^2}{f_1f_3(1+K_3)}\left(\frac{1}{B_3}\right)} \qquad \text{(III-25)}$$

Based on the high-gain narrow-bandwidth approximation, the gain-bandwidth product for a paramp of a reflection type is given by multiplying equation III-25 by equation II-58 of Appendix II.

$$|\Gamma_o|\,X_{3db}=\left[\frac{\left|1-K_o-\frac{M^2}{f_1f_2(1+K_2)}+\frac{M^2}{f_1f_3(1+K_3)}\right|}{\left|1+K_o-\frac{M^2}{f_1f_2(1+K_2)}+\frac{M^2}{f_1f_3(1+K_3)}\right|}\right]\left[\frac{1+K_o-\frac{M^2}{f_1f_2(1+K_2)}+\frac{M^2}{f_1f_3(1+K_3)}}{\frac{1}{B_{1U}}+\frac{M^2}{f_1f_2(1+K_2)}\left(\frac{1}{B_2}\right)-\frac{M^2}{f_1f_3(1+K_3)}\left(\frac{1}{B_3}\right)}\right] \qquad \text{(III-26)}$$

$$|\Gamma_o|\,X_{3db}=\frac{\left|1-K_o-\frac{M^2}{f_1f_2(1+K_2)}+\frac{M^2}{f_1f_3(1+K_3)}\right|}{\frac{1}{B_{1U}}+\frac{M^2}{f_1f_2(1+K_2)}\left(\frac{1}{B_2}\right)-\frac{M^2}{f_1f_3(1+K_3)}\left(\frac{1}{B_3}\right)} \qquad \text{(III-27)}$$

Applying the high-gain condition of

$$1 + K_o = \frac{M^2}{f_1 f_2 (1 + K_2)} - \frac{M^2}{f_1 f_3 (1 + K_3)}$$

to the numerator of equation III-27 yields:

$$|\Gamma_o| X_{3db} = \frac{2 K_o}{\frac{1}{B_{1U}} + \frac{M^2}{f_1 f_2 (1 + K_2)} \left(\frac{1}{B_2}\right) - \frac{M^2}{f_1 f_3 (1 + K_3)} \left(\frac{1}{B_3}\right)} \quad \text{(III-28)}$$

Applying the high gain condition of equation III-2 to the denominator of equation III-28 yields:

$$|\Gamma_o| X_{3db} = \frac{2K_o}{\frac{1}{B_{1U}} + \frac{1}{B_2}\left[\frac{1 + K_o}{1 - \frac{f_2 (1 + K_2)}{f_3 (1 + K_3)}}\right] - \frac{1}{B_3}\left[\frac{1 + K_o}{\frac{f_3 (1 + K_3)}{f_2 (1 + K_2)} - 1}\right]} \quad \text{(III-29)}$$

To have all loaded, measurable bandwidths in the final expression, B_{1U} will be converted to a loaded bandwidth by the relation,

$$B_1 = B_{1U} (1 + K_o) \quad \text{(III-30)}$$

Now equation III-29 can be rewritten:

$$|\Gamma_o| X_{3db} = \frac{2 K_o}{(1 + K_o)\left[\frac{1}{B_1} + \frac{1}{B_2\left[1 - \frac{f_2 (1 + K_2)}{f_3 (1 + K_3)}\right]} - \frac{1}{B_3\left[\frac{f_3 (1 + K_3)}{f_2 (1 + K_2)} - 1\right]}\right]} \quad \text{(III-31)}$$

The final expression for the gain-bandwidth product of a single diode reflection-type parametric amplifier is:

$$\boxed{|\Gamma_o| X_{3db} = \left[\frac{2}{1 + \frac{1}{K_o}}\right]\left[\frac{B_1}{1 + \frac{B_1}{B_2}[U] - \frac{B_1}{B_3}[V]}\right]} \quad \text{(III-32)}$$

where $$U = \left[\frac{1}{1 - \frac{f_2}{f_3} \frac{(1 + K_2)}{(1 + K_3)}} \right]$$

and $$V = \left[\frac{1}{\frac{f_3 (1 + K_3)}{f_2 (1 + K_2)}} \right]$$

A check can be made on the validity of equation III-32 for the conventional case of a difference-frequency parametric amplifier with no sum-frequency propagation by showing its equivalence to a known gain-bandwidth relationship.

For this case ($K_3 = \infty$), equation III-32 reduces to:

$$|\Gamma_o| X_{3db} = \left[\frac{2}{1 + \frac{1}{K_o}} \right] \left[\frac{1}{\frac{1}{B_1} + \frac{1}{B_2}} \right]$$

$$= \left[\frac{K_o}{1 + K_o} \right] \left[\frac{2 f_1}{Q_1 + Q_2 \frac{f_1}{f_2}} \right]$$

Using the high-gain condition,

$$|\Gamma_o| X_{3db} = \left[1 - \frac{f_1 f_2}{M^2} (1 + K_2) \right] \left[\frac{2 f_1}{Q_1 + Q_2 \frac{f_1}{f_2}} \right] \qquad \text{(III-33)}$$

Equation III-33 is an expression for the gain-bandwidth product of a difference-frequency paramp, if external idler loading is allowed. Equation III-33 simplifies to the following familiar expression (equation III-34) if external idler loading is non-existent ($K_2 = 0$), thus verifying equation III-32.

$$|\Gamma_o|\, X_{3db} = \left[1 - \frac{f_1 f_2}{M^2}\right]\left[\frac{2 f_1}{Q_1 + Q_2 \frac{f_1}{f_2}}\right] \qquad \text{(III-34)}$$

From equation III-32, the effect of the presence of sum-frequency propagation on the gain-bandwidth product is illustrated in the following example: The parametric amplifier has the following parameters:

$K_o = 2.6$,
f_2 = idler resonant frequency = 8.275 GHz,
f_3 = sum-resonant frequency = 10.075 GHz,
B_1 = signal-circuit loaded bandwidth = 0.200 GHz,
B_2 = idler-circuit loaded bandwidth = 0.680 GHz,
B_3 = sum-circuit loaded bandwidth = 0.150 GHz,
$K_2 = 0$.

Substituting these parameters into equation III-32, the gain-bandwidth product can be calculated for the case of perfect sum-frequency propagation ($K_3 = 0$).

$$|\Gamma_o| X_{3db} = \left[\frac{2}{1 + \frac{1}{2.6}}\right]\left[\frac{.2}{1 + \frac{.2}{.68}\left[\frac{1}{1 - \frac{8.275}{10.075}}\right] - \frac{.2}{1.15}\left[\frac{1}{\frac{10.075}{8.275} - 1}\right]}\right]$$

$$|\Gamma_o| X_{3db} = 0.171 \text{ GHz}$$

When sum-frequency propagation is not allowed ($K_3 = \infty$), the gain-bandwidth product can be recalculated:

$$|\Gamma_o| X_{3db} = \left[\frac{2}{1 + \frac{1}{2.6}}\right]\left[\frac{.2}{1 + \frac{.2}{.68}}\right]$$

$$|\Gamma_o| X_{3db} = 0.223 \text{ GHz}$$

Thus, the gain-bandwidth product is degraded with sum-frequency propagation.

It can be shown that, if K_o, B_1, and B_2 are assumed to be the same, with or without sum-frequency propagation, the gain-bandwidth product is degraded by sum-frequency propagation only if B_3 is greater than B_2.

APPENDIX IV

DERIVATION OF MID-BAND NOISE TEMPERATURE FOR A PARAMETRIC AMPLIFIER WITH SUM-FREQUENCY PROPAGATION

A. INTRODUCTION

The following equivalent circuit is used to calculate the midband noise temperature of the paramp:

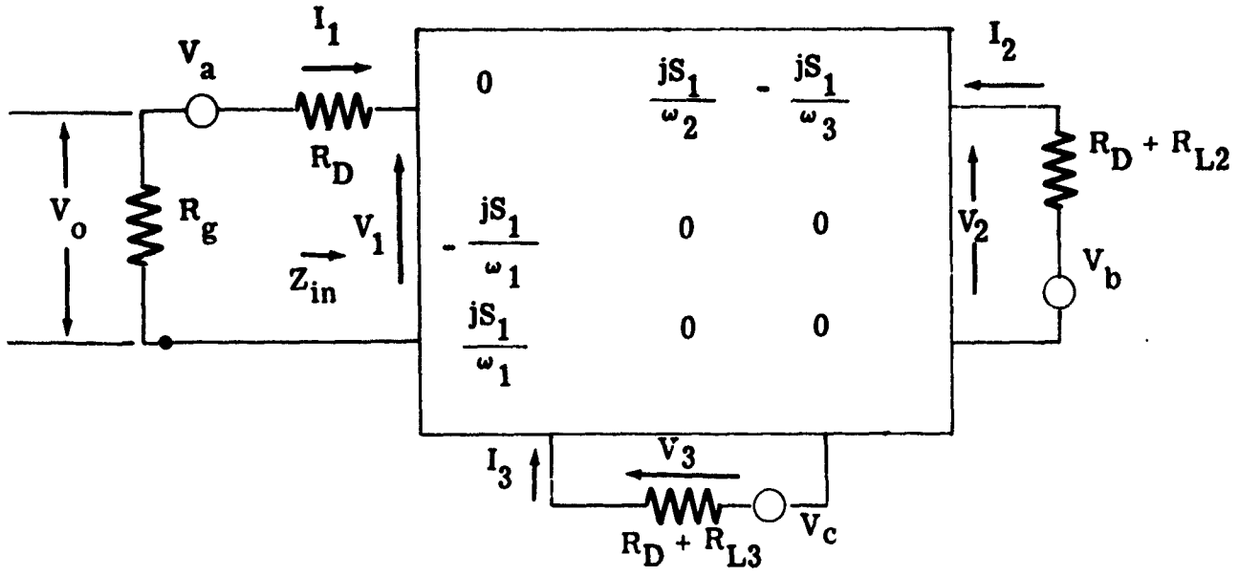

The resistors are ideal and noise free, and the voltage sources are noise-power generators which, in series with the ideal resistors, closely represent real resistors.

The mean-squared amplitudes of the voltage sources in the 3-db bandwidth of the paramp are given by:

$$\overline{|V_a|^2} = 4\,k\,T_o\,R_D\,X_{3db} \qquad \text{(IV-1)}$$

where k - Boltzmann's constant

X_{3db} = 3-db bandwidth of the paramp,

T_o = ambient temperature of the paramp in degrees Kelvin,

$$\overline{|V_b|^2} = 4\,k\,T_o\,(R_D + R_{L2})\;X_{3db} = 4\,k\,T_o\,R_{22}\,X_{3db'} \qquad \text{(IV-2)}$$

and

$$\overline{|V_c|^2} = 4\,k\,T_o\,R_{33}\,X_{3db}. \qquad \text{(IV-3)}$$

The noise output power delivered to a matched load through a circulator, exclusive of the noise contributed by the generator, can be calculated by considering separately the contributions to I_1 of each of the three noise generators and then adding them by linear superposition, since there is no coherence to noise generated by independent generators.

Since the noise generators are random voltage sources, the polarity assigned to them for the purposes of the following calculations is arbitrary.

The equivalent circuit will now be redrawn bringing all of the ideal resistors into the matrix:

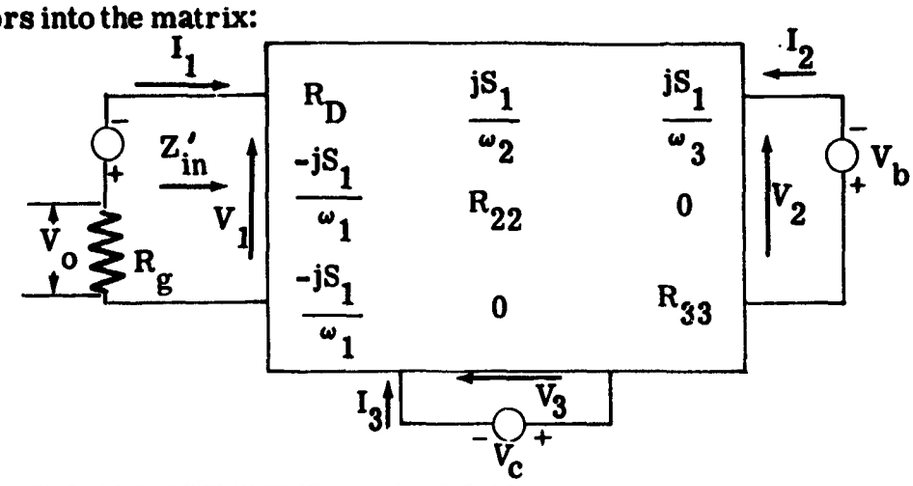

B. NOISE OUTPUT POWER DUE TO V_a

$$V_o = \frac{V_a\,R_g}{R_g + Z'_{in,m}} = \frac{V_a\,R_g}{R_g + R_D - \dfrac{S_1^2}{\omega_1\omega_2 R_{22}} + \dfrac{S_1^2}{\omega_1\omega_3 R_{33}}} \qquad \text{(IV-4)}$$

where $Z'_{in,m}$ = mid-band input impedance,

$$V_o = \frac{V_a\,R_g}{R_D\left[1 + K_o - \dfrac{M^2}{f_1 f_2\,(1 + K_2)} + \dfrac{M^2}{f_1 f_3\,(1 + K_3)}\right]} \qquad \text{(IV-5)}$$

$$|N_{oa}| = \frac{\overline{|V_o|^2}}{|R_g|} = \left| \frac{\overline{|V_a|^2} R_g}{\left(R_g + Z'_{in,m}\right)^2} \right| \qquad \text{(IV-6)}$$

where N_{oa} = noise output power due to V_a.

$$|N_{oa}| = \left| \frac{\overline{|V_a|^2} R_g}{R_D^2 \left[1 + K_o - \frac{M^2}{f_1 f_2 \left(1 + K_2\right)} + \frac{M^2}{f_1 f_3 \left(1 + K_3\right)}\right]^2} \right| \qquad \text{(IV-7)}$$

C. NOISE OUTPUT POWER DUE TO V_b

The network relation expressed in matrix terms is:

$$\begin{bmatrix} -V_o \\ -V_b^* \\ 0 \end{bmatrix} = \begin{bmatrix} R_D & Z_{12} & Z_{13} \\ Z_{21} & R_{22} & 0 \\ Z_{31} & 0 & R_{33} \end{bmatrix} \begin{bmatrix} I_{1b} \\ I_2^* \\ I_3 \end{bmatrix} \qquad \text{(IV-8)}$$

Equation IV-8 will be solved for I_{1b}, using Cramer's Rule:

$$I_{1b} = \frac{\begin{vmatrix} V_o & Z_{12} & Z_{13} \\ -V_b^* & R_{22} & 0 \\ 0 & 0 & R_{33} \end{vmatrix}}{\begin{vmatrix} R_D & Z_{12} & Z_{13} \\ Z_{21} & R_{22} & 0 \\ Z_{31} & 0 & R_{33} \end{vmatrix}}$$

$$I_{1b} = \frac{-V_o R_{22} R_{33} + V_b^* Z_{12} R_{33}}{R_D R_{22} R_{33} - R_{22} Z_{13} Z_{31} - R_{33} Z_{12} Z_{21}}$$

Since

$$V_o = I_{1b} R_g$$

$$I_{1b} = \frac{V_b^* Z_{12} R_{33}}{R_g R_{22} R_{33} + R_D R_{22} R_{33} - R_{22} Z_{13} Z_{31} - R_{33} Z_{12} Z_{21}}$$

(IV-9)

$$I_{1b} = \frac{j V_b^* R_{33} \frac{S_1}{\omega_2}}{R_g R_{22} R_{33} + R_D R_{22} R_{33} + \frac{R_{22} S_1^2}{\omega_1 \omega_3} \frac{R_{33} S_1^2}{\omega_1 \omega_2}}$$

$$I_{1b} = \frac{\frac{j V_b^* S_1}{R_D R_{22} \omega_2}}{\frac{R_g}{R_D} + 1 + \frac{S_1^2}{\omega_1 \omega_3 R_D R_{33}} - \frac{S_1^2}{\omega_1 \omega_2 R_D R_{22}}}$$

$$I_{1b} = \frac{\frac{j V_b^* M}{f_2 R_{22}}}{1 + K_o - \frac{M^2}{f_1 f_2 (1 + K_2)} + \frac{M^2}{f_1 f_3 (1 + K_3)}} \qquad \text{(IV-10)}$$

$$|N_{ob}| = |I_{1b}|^2 R_g = \left| \frac{\overline{|V_b|^2} M^2 R_g}{f_2^2 R_{22}^2 \left[1 + K_o - \frac{M^2}{f_1 f_2 (1 + K_2)} + \frac{M^2}{f_1 f_3 (1 + K_3)} \right]^2} \right|$$

(IV-11)

Similarly,

$$|N_{oc}| = |I_{1c}|^2 R_g = \left| \frac{\overline{|V_c|^2}\ M^2\ R_g}{f_3^2 R_{33}^2 \left[1 + K_o - \frac{M^2}{f_1 f_2 (1+K_2)} + \frac{M^2}{f_1 f_3 (1+K_3)}\right]^2} \right| \quad \text{(IV-12)}$$

By linear superposition,

$$|N_o| = |N_{oa}| + |N_{ob}| + |N_{oc}| \quad \text{(IV-13)}$$

$$|N_o| = \frac{R_g}{\left[1 + K_o - \frac{M^2}{f_1 f_2 (1+K_2)} + \frac{M^2}{f_1 f_3 (1+K_3)}\right]^2} \left[\frac{\overline{|V_a|^2}}{R_D^2} + \frac{\overline{|V_b|^2}\ M^2}{f_2^2 R_{22}^2} + \frac{\overline{|V_c|^2}\ M^2}{f_3^2 R_{33}^2} \right] \quad \text{(IV-14)}$$

Substituting for the noise voltages,

$$|N_o| = \left| \frac{4 k X_{3db} T_o K_o}{\left[1 + K_o - \frac{M^2}{f_1 f_2 (1+K_2)} + \frac{M^2}{f_1 f_3 (1+K_3)}\right]^2} \left[1 + \frac{M^2}{f_2^2 (1+K_2)} + \frac{M^2}{f_3^2 (1+K_3)} \right] \right| \quad \text{(IV-15)}$$

The mid-band effective noise temperature of the paramp (T_e) is defined as,

$$T_e = \frac{|N_o|}{k X_{3db} |\Gamma_o|^2} \quad \text{(IV-16)}$$

Therefore,

$$T_e = \frac{\left[\dfrac{4\,T_o\,K_o}{\left[1 + K_o - \dfrac{M^2}{f_1 f_2 (1+K_2)} + \dfrac{M^2}{f_1 f_3 (1+K_3)}\right]^2}\left[1 + \dfrac{M^2}{f_2^{\,2}(1+K_2)} + \dfrac{M^2}{f_3^{\,2}(1+K_3)}\right]\right]}{\dfrac{\left[1 - K_o - \dfrac{M^2}{f_1 f_2 (1+K_2)} + \dfrac{M^2}{f_1 f_3 (1+K_3)}\right]^2}{\left[1 + K_o - \dfrac{M^2}{f_1 f_2 (1+K_2)} + \dfrac{M^2}{f_1 f_3 (1+K_3)}\right]^2}}$$

$$\boxed{T_e = \frac{4\,T_o\,K_o\left[1 + \dfrac{M^2}{f_2^{\,2}(1+K_2)} + \dfrac{M^2}{f_3^{\,2}(1+K_3)}\right]}{\left[1 - K_o - \dfrac{M^2}{f_1 f_2 (1+K_2)} + \dfrac{M^2}{f_1 f_3 (1+K_3)}\right]^2}} \qquad \text{(IV-17)}$$

Under the high-gain condition of:

$$\frac{M^2}{f_1 f_2 (1+K_2)} - \frac{M^2}{f_1 f_3 (1+K_3)} = 1 + K_o$$

Equation IV-17 reduces to:

$$\boxed{T_e = \frac{T_o}{K_o}\left[1 + \frac{M^2}{f_2^{\,2}(1+K_2)} + \frac{M^2}{f_3^{\,2}(1+K_3)}\right]} \qquad \text{(IV-18)}$$

Equation IV-18 is the expression for the mid-band effective noise temperature of a single-diode reflection-type parametric amplifier when sum frequency propagation is allowed.

The result of equation IV-18 will be checked by deriving from it the familiar difference-frequency noise-temperature relation when no sum frequency is allowed to propagate $K_3 = \infty$.

Equation IV-18 simplifies to:

$$\frac{T_e}{T_o} = \frac{1}{K_o}\left[1 + \frac{M^2}{f_2^{\,2}(1 + K_2)}\right] \qquad \text{(IV-19)}$$

Substituting the high-gain condition back into equation IV-19 yields:

$$\frac{T_e}{T_o} = \frac{f_1 f_2 (1 + K_2)}{M^2 - f_1 f_2 (1 + K_2)}\left[1 + \frac{M^2}{f_2^{\,2}(1 + K_2)}\right]$$

$$= \frac{f_1 f_2^{\,3}(1 + K_2)^2 + M^2 f_1 f_2 (1 + K_2)}{f_2^{\,2}(1 + K_2)M^2 - f_1 f_2^{\,3}(1 + K_2)^2}$$

Simplifying,

$$\boxed{\frac{T_e}{T_o} = \frac{\dfrac{f_1 f_2 (1 + K_2)}{M^2} + \dfrac{f_1}{f_2}}{1 - \dfrac{f_1 f_2 (1 + K_2)}{M^2}}} \qquad \text{(IV-20)}$$

When the external idler loading is diminished to zero $K_2 = 0$ equation IV-20 reduces to the familiar expression (equation IV-21), thus verifying equation IV-18.

$$\boxed{\frac{T_e}{T_o} = \frac{\dfrac{f_1 f_2}{M^2} + \dfrac{f_1}{f_2}}{1 - \dfrac{f_1 f_2}{M^2}}} \qquad \text{(IV-21)}$$

From equation IV-20 it can be seen that, as K_2 is increased, T_e also increases.

The effect of sum-frequency propagation on noise temperature is illustrated in the following example. Let the parametric amplifier have the following parameters:

$M^2 = 125 \times 10^{18}\ GHz^2$

$f_2 = 8.275\ GHz$

$f_3 = 10.075\ GHz$

$K_o = 2.6$

$K_2 = 0$

Substituting these parameters into equation IV-17 with $K_3 = 0$, and since equation IV-18 assumes infinite gain:

$$\frac{T_e}{T_o} = \frac{(4)\ (2.6)\left[1 + \frac{125}{68.3} + \frac{125}{101.5}\right]}{\left[1 - 2.6 - \frac{125}{7.42} + \frac{125}{9.08}\right]^2}$$

$$\frac{T_e}{T_o} = 1.925$$

When there is no sum-frequency propagation $K_3 = \infty$,

$$\frac{T_e}{T_o} = \frac{(4)\ (2.6)\left[1 + \frac{125}{68.3}\right]}{\left[1 - 2.6 - \frac{125}{7.42}\right]^2}$$

$$\frac{T_e}{T_o} = 0.0864$$

The effective noise temperature is related to the noise figure F by the following relation:

$$F = 1 + \frac{T_e}{T_o} \qquad \text{(IV-22)}$$

where

F = noise figure (ratio)

T_e = effective noise temperature in degrees Kelvin

T_o = ambient temperature in degrees Kelvin

APPENDIX V

DERIVATION OF INTERMODULATION OUTPUTS OF PAIR OF GENERAL NONLINEAR ELEMENTS IN BALANCED MIXER ARRAY

Given a general nonlinear element (Z_n) with a current-versus-voltage characteristic as follows:

$$i = \sum_{n=o}^{\infty} A_n v^n \qquad \text{(V-1)}$$

A balanced-mixer array can be set up as in Figure V-1. The currents developed in each nonlinear element can be calculated, and then the current that flows through the load resistor can be found:

$$i_1 = \sum_{n=o}^{\infty} A_n \left(V_2 \cos \omega_2 t + V_1 \cos \omega_1 t\right)^n$$

$$= \sum_{n=o}^{\infty} B_n \cos^n \omega_2 t + \sum_{m=o}^{\infty} C_m \cos^m \omega_1 t \qquad \text{(V-2)}$$

$$+\left(\sum_{p=1}^{\infty} D_p \cos^p \omega_2 t\right)\left(\sum_{q=1}^{\infty} E_q \cos^q \omega_1 t\right)$$

$$i_1 = \left(\sum_{r=o}^{\infty} F_r \cos^r \omega_2 t\right)\left(\sum_{s=o}^{\infty} G_s \cos^s \omega_1 t\right) . \qquad \text{(V-3)}$$

Since every term of the form $\cos^n \omega t$ has harmonic equivalence, equation V-3 can be rewritten:

$$i_1 = \left(\sum_{r=o}^{\infty} H_r \cos r \omega_2 t\right)\left(\sum_{s=o}^{\infty} I_s \cos s \omega_1 t\right) . \qquad \text{(V-4)}$$

Since both nonlinear elements are identical in every respect, but the second element is excited 180 degrees out of phase by ω_2, i_2 can be written as follows:

$$i_2 = \left[\sum_{r=o}^{\infty} H_r \cos r\left(\omega_2 t + 180^o\right)\right]\left[\sum_{s=o}^{\infty} I_s \cos s\,\omega_1 t\right] \qquad \text{(V-5)}$$

The total current that flows through the load is:

$$i_T = i_1 - i_2 = \left(\sum_{r=o}^{\infty} H_r \cos r\,\omega_2 t\right)\left(\sum_{s=o}^{\infty} I_s \cos s\,\omega_1 t\right) - \left[\sum_{r=o}^{\infty} H_r \cos r\left(\omega_2 t + 180^o\right)\right]\left[\sum_{s=o}^{\infty} I_s \cos s\,\omega_1 t\right]$$

Therefore,

$$\boxed{i_T = \left(\sum_{s=o}^{\infty} I_s \cos s\omega_1 t\right)\left\{\left(\sum_{r=o}^{\infty} H_r \cos r\,\omega_2 t\right) - \left[\sum_{r=o}^{\infty} H_r \cos r\left(\omega_2 t + 180^o\right)\right]\right\}} \qquad \text{(V-6)}$$

From equation V-6 it can be seen that, for all r where r is an even integer, i_T does not exist. Therefore, all intermodulation outputs at frequencies of the form,

$$\omega_{IM} = \left|\pm s\,\omega_1 \pm r\,\omega_2\right| \qquad \text{(V-7)}$$

exist for all s but only for odd r.

Although this analysis is done for an ideal case, in the realistic situation of some unbalance, there is still suppression, but not elimination, of intermodulation frequencies which are formed with even-order harmonics of ω_2.

In the case of a paramp, the two diodes are excited in - phase by the signal and 180 degrees out-of-phase by the pump (Figure V-1). The

current i_T is the current that flows through the load resistance in the idler circuit of the paramp. Therefore, power is not dissipated in the load resistance in the idler circuit at intermodulation frequencies that are formed with even-order harmonics of the pump.

If the load is placed in the signal arm of the paramp, as with the circulator coupled output load, the two currents add rather than subtract, and the result is that $i_T = 0$ for all intermodulation frequencies that are formed with odd-order harmonics of the pump. This means that, for perfectly balanced varactors, energy at neither the sum nor the idler frequencies can be propagated out of the signal arm of the paramp.

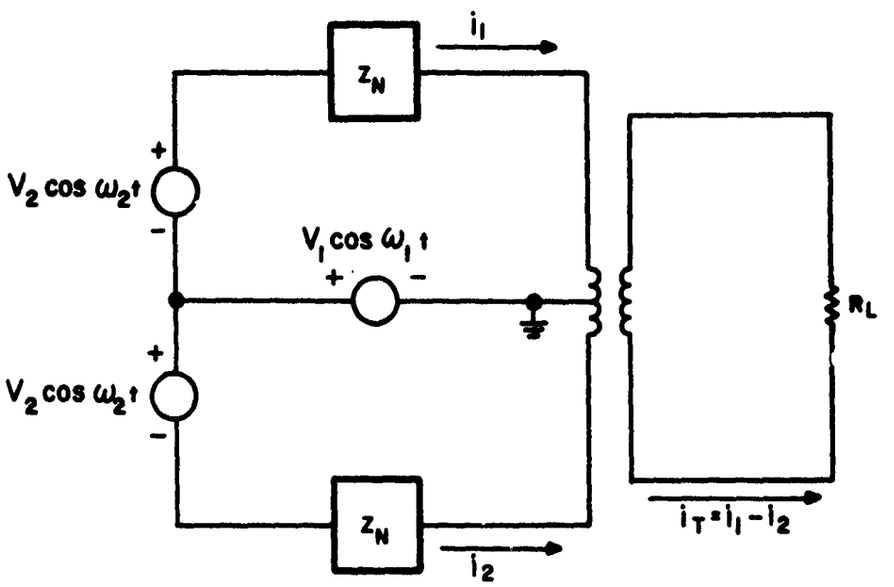

FIGURE V-1. BALANCED-MIXER ARRAY

APPENDIX VI

DERIVATION OF GAIN OF BALANCED REFLECTION-TYPE PARAMETRIC AMPLIFIER

To derive the expressions that describe a balanced paramp, the two varactors must be considered to be in parallel in the signal circuit and in series in each idler circuit (difference-frequency and sum-frequency circuits). The varactors are pumped 180 degrees out of phase with one another, and the effective capacitance in the idler circuits is halved while the inductance and junction resistances are doubled. Therefore, the Q's (Q_2 and Q_3), as defined in Appendix II, are the same as for a single varactor.

In the signal circuit, the capacitance is doubled, the inductance and junction resistances are halved, and the Q (Q_1) of the signal circuit remains constant. Figure VI-1 shows the equivalent circuit of a balanced reflection-type paramp. Figure VI-2 shows the phasing and polarities of the varactors in Figure VI-1.

As in the case of the single-varactor paramp, only the signal difference- and sum-frequencies will be allowed to propagate.

Figure VI-3 represents the balanced configuration in impedance notation.

The currents and voltages associated with the external loads (Z_1, Z_2, and Z_3) are found in the following manner:

$$I_1 = I_1' + I_1'' \qquad \text{(VI-1)}$$

$$V_1 = V_1' = V_1'' \qquad \text{(VI-2)}$$

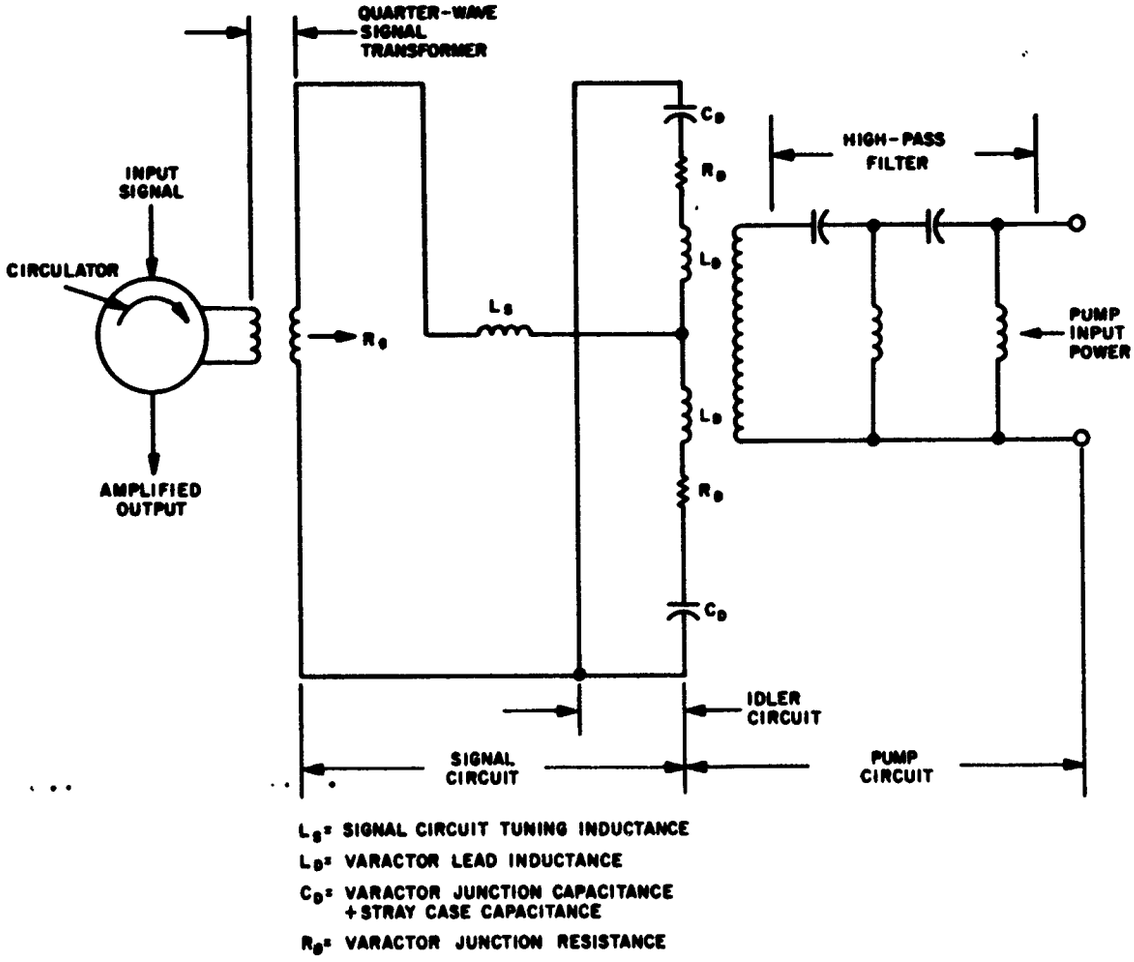

FIGURE VI-1. EQUIVALENT CIRCUIT OF A BALANCED REFLECTION-TYPE PARAMETRIC AMPLIFIER

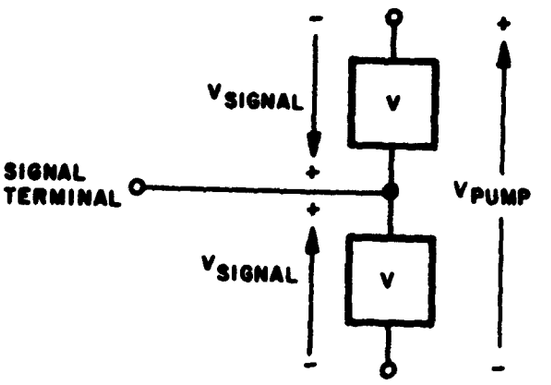

FIGURE VI-2. PHASING AND POLARITIES IN BALANCED PARAMP

$$I_2^* = I_2'^* = I_2''^* \quad \text{(VI-3)}$$

$$V_2^* = V_2'^* + V_2''^* \quad \text{(VI-4)}$$

$$I_3 = I_3' = I_3'' \quad \text{(VI-5)}$$

$$V_3 = V_3' + V_3'' \quad \text{(VI-6)}$$

$$V_1' = Z_{11} I_1' + Z_{12} I_2'^* + Z_{13} I_3' \quad \text{(VI-7)}$$

Equation VI-7 can be rewritten:

$$V_1 = Z_{11} I_1' + Z_{12} I_2^* + Z_{13} I_3 \quad \text{(VI-8)}$$

$$V_1'' = Z_{11} I_1'' + Z_{12} I_2''^* + Z_{13} I_3'' \quad \text{(VI-9)}$$

Equation VI-9 can be rewritten:

$$V_1 = Z_{11} I_1'' + Z_{12} I_2^* + Z_{13} I_3 \quad \text{(VI-10)}$$

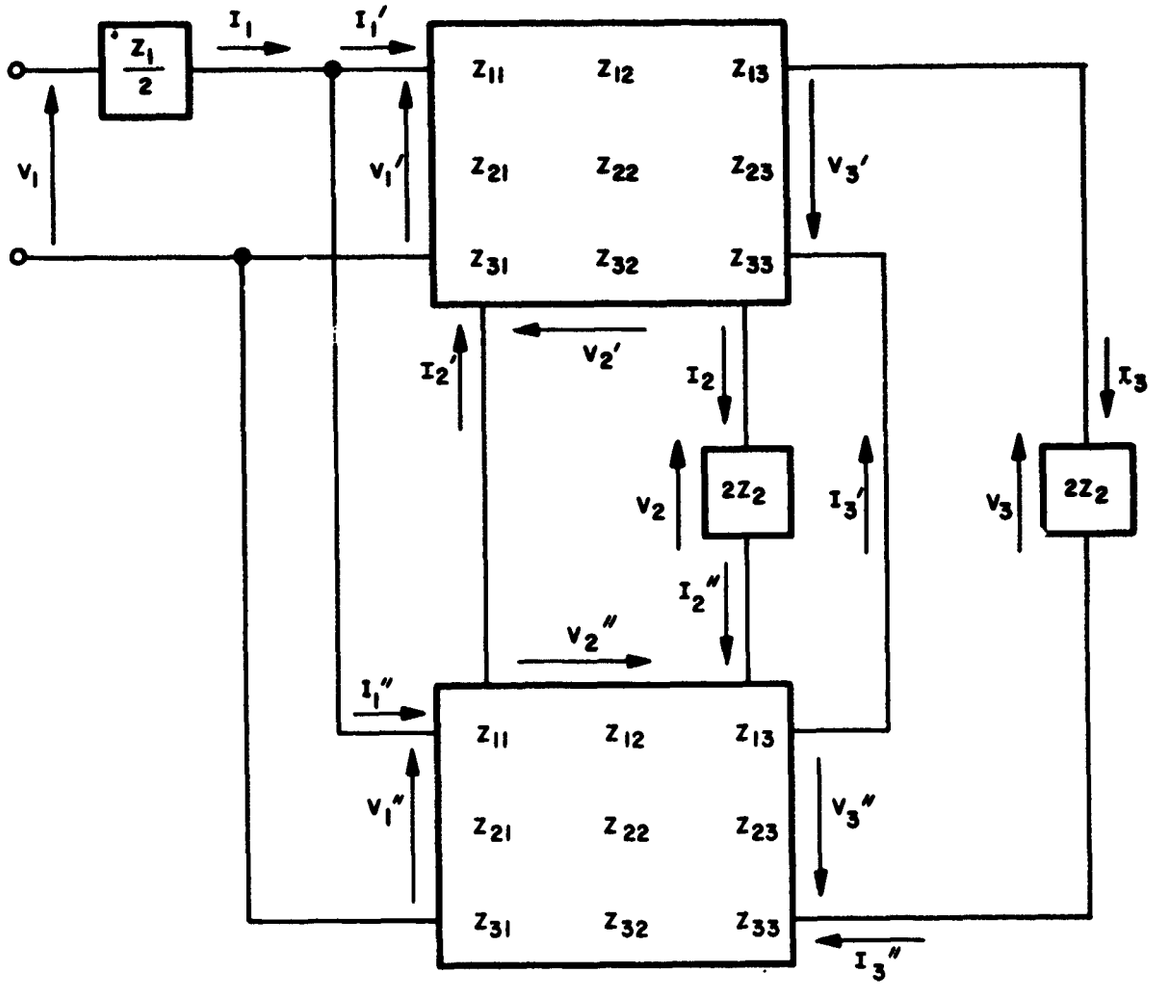

FIGURE VI-3. BALANCED CONFIGURATION IN IMPEDANCE NOTATION

Adding equation VI-8 to equation VI-10 yields:

$$2V_1 = Z_{11}(I_1' + I_1'') + 2Z_{12} I_2^* + 2Z_{13} I_3 \qquad \text{(VI-11)}$$

Therefore,

$$V_1 = \frac{1}{2} Z_{11} I_1 + Z_{12} I_2^* + Z_{13} I_3 \qquad \text{(VI-12)}$$

In a like manner, V_2^* and V_3 can be derived:

$$V_2^* = Z_{21} I_1 + 2 Z_{22} I_2^* + 2 Z_{23} I_3 \qquad \text{(VI-13)}$$

$$V_3 = Z_{31} I_1 + 2 Z_{32} I_2^* + 2 Z_{33} I_3 \qquad \text{(VI-14)}$$

From equations VI-12, VI-13, and VI-14, a general impedance matrix can be written for the balanced varactor configuration:

$$\begin{bmatrix} V_1 \\ V_2^* \\ V_3 \end{bmatrix} = \begin{bmatrix} \frac{1}{2}Z_{11} & Z_{12} & Z_{13} \\ Z_{21} & 2Z_{22} & 2Z_{23} \\ Z_{31} & 2Z_{32} & 2Z_{33} \end{bmatrix} \begin{bmatrix} I_1 \\ I_2^* \\ I_3 \end{bmatrix} \qquad \text{(VI-15)}$$

From this impedance matrix, the input impedance and the gain of the balanced paramp can be derived.

If the loadings at the three ports of the amplifier are taken into the matrix, the input impedance can be written directly from equation II-32 in Appendix II.

$$Z_{inB} = \frac{1}{2}(Z_{11} + Z_1) - \frac{Z_{12}\left[Z_{21} - \dfrac{Z_{23} Z_{31}}{(Z_{33}+Z_3)}\right]}{\left[2(Z_{22} + Z_2) - \dfrac{2Z_{23} Z_{32}}{(Z_{33}+Z_3)}\right]} - \frac{Z_{13}\left[Z_{31} - \dfrac{Z_{21} Z_{32}}{(Z_{22}+Z_2)}\right]}{\left[2(Z_{33} + Z_3) - \dfrac{2Z_{23} Z_{32}}{(Z_{22}+Z_2)}\right]} \qquad \text{(VI-16)}$$

From equation VI-16 it can be seen that Z_{inB} is exactly one-half of Z_{in} for a single varactor.

Neglecting the S_2 contribution, as in the earlier analysis, equation VI-16 reduces to:

$$Z_{inB} = \frac{1}{2}(Z_{11} + Z_1) - \frac{Z_{12}Z_{21}}{2(Z_{22}+Z_2)} - \frac{Z_{13}Z_{31}}{2(Z_{33}+Z_3)} \qquad \text{(VI-17)}$$

For ease of manipulation, Z_1 in this balanced analysis is equal to $2Z_1$ in the single-diode analysis, and Z_2 and Z_3 in this analysis are equal to $\frac{1}{2}Z_2$ and $\frac{1}{2}Z_3$, respectively, in the single-diode analysis.

From equation II-50 in Appendix II, equation VI-17 can be written in elastance terminology:

$$Z_{inB} = \frac{1}{2}\left[R_D + j2\Delta\omega_1 L_1 - \frac{S_1^2/\omega_1\omega_2}{R_{22} - j2\Delta\omega_2 L_2} + \frac{S_1^2/\omega_1\omega_3}{R_{33} + j2\Delta\omega_3 L_3}\right] \qquad \text{(VI-18)}$$

Since at mid-band

$$\Delta\omega_1 = \Delta\omega_2 = \Delta\omega_3 = 0$$

the mid-band input impedance is:

$$Z_{inB,m} = \frac{1}{2}\left[R_D - \frac{S_1^2}{\omega_1\omega_2 R_{22}} + \frac{S_1^2}{\omega_1\omega_3 R_{33}}\right] \qquad \text{(VI-19)}$$

The magnitude of the mid-band voltage gain is given by:

$$|\Gamma_o| = \left|\frac{Z_{inB,m} - Rg}{Z_{inB,m} + Rg}\right| \qquad \text{(VI-20)}$$

Substituting equation VI-19 into equation VI-20,

$$\left|\Gamma_o\right| = \left| \frac{\frac{1}{2}\left[R_D - 2Rg - \frac{S_1^2}{\omega_1\omega_2 R_{22}} + \frac{S_1^2}{\omega_1\omega_3 R_{33}} \right]}{\frac{1}{2}\left[R_D + 2Rg - \frac{S_1^2}{\omega_1\omega_2 R_{22}} + \frac{S_1^2}{\omega_1\omega_3 R_{33}} \right]} \right| \qquad \text{(VI-21)}$$

Therefore,

$$\left|\Gamma_o\right| = \left| \frac{1 - 2K_o - \frac{M^2}{f_1 f_2(1+K_2)} + \frac{M^2}{f_1 f_3(1+K_3)}}{1 + 2K_o - \frac{M^2}{f_1 f_2(1+K_2)} + \frac{M^2}{f_1 f_3(1+K_3)}} \right| \qquad \text{(VI-22)}$$

Since, as was stated before, $\frac{1}{2} R_D$ is substituted for R_D and $2 R_{22}$ and $2 R_{33}$ are substituted for R_{22} and R_{33}, respectively, equation VI-22 can be rewritten in a form which allows it to be compared with equation II-58 in Appendix II:

$$\boxed{\left|\Gamma_o\right| = \left| \frac{1 - K_o - \frac{M^2}{f_1 f_2(1+K_2)} + \frac{M^2}{f_1 f_3(1+K_3)}}{1 + K_o - \frac{M^2}{f_1 f_2(1+K_2)} + \frac{M^2}{f_1 f_3(1+K_3)}} \right|} \qquad \text{(VI-23)}$$

The mid-band gain of the balanced parametric amplifier is, therefore, exactly the same as that of the single-diode amplifier. The condition for gain is also the same as for the single-diode paramp:

$$\boxed{\frac{M^2}{f_1 f_2(1+K_2)} > 1 + \frac{M^2}{f_1 f_3(1+K_3)}} \qquad \text{(VI-24)}$$

APPENDIX VII

DERIVATION OF GAIN-BANDWIDTH PRODUCT FOR BALANCED REFLECTION-TYPE PARAMETRIC AMPLIFIER WITH SUM-FREQUENCY PROPAGATION

The constraints on this analysis are high gain and narrow bandwidth. The technique of analysis is the same as that used in Appendix III. Equation III-12 in Appendix III is of the form,

$$Z_{SB} = Rg + Z_{inB} = \frac{1}{2}\left\{ R_D + 2Rg + \frac{S_1^2}{\omega_1\omega_3 R_{33}} - \frac{S_1^2}{\omega_1\omega_2 R_{22}} + j\left[2\Delta\omega_1 L_1 + \frac{S_1^2 2Q_2}{R_{22}\omega_1\omega_2}\left(\frac{\Delta\omega_2}{\omega_2}\right) - \frac{S_1^2 2Q_3}{R_{33}\omega_1\omega_3}\left(\frac{\Delta\omega_3}{\omega_3}\right)\right]\right\} \quad \text{(VII-1)}$$

Equation VII-1 can be rewritten:

$$\frac{2Z_{SB}}{R_D} = 1 + 2K_o + \frac{M^2}{f_1 f_3(1+K_3)} - \frac{M^2}{f_1 f_2(1+K_2)} + j\,X\left[\frac{Q_{1U}}{f_1} + \frac{M^2 Q_2}{f_1 f_2^2(1+K_2)} - \frac{M^2}{f_1 f_3^2(1+K_3)}\right] \quad \text{(VII-2)}$$

Equating the real and imaginary parts of equation VII-2 to solve for the 3-db bandwidth of the balanced paramp yields:

$$X_{3db} = \frac{1 + 2K_o + \frac{M^2}{f_1 f_3 (1+K_3)} - \frac{M^2}{f_1 f_2 (1+K_2)}}{\frac{1}{B_{1U}} + \frac{M^2}{f_1 f_2 (1+K_2)} \left(\frac{1}{B_2}\right) - \frac{M^2}{f_1 f_3 (1+K_3} \left(\frac{1}{B_3}\right)} \qquad \text{(VII-3)}$$

Multiplying equation VII-3 by equation VI-22 of Appendix VI yields:

$$|\Gamma_o| \; X_{3db} = \frac{4K_o}{(1+2K_o)\left[\frac{1}{B_1} + \frac{1}{B_2}\right]\left[1 - \frac{f_2(1+K_2)}{f_3(1+K_3)}\right] - \frac{1}{B_3}\left[\frac{f_3(1+K_3)}{f_2(1+K_2)} - 1\right]} \qquad \text{(VII-4)}$$

Since, as in Appendix VI, $\frac{1}{2} R_D$ is substituted for R_D and $2R_{22}$ and $2R_{33}$ are substituted for R_{22} and R_{33}, respectively, equation VII-4 results in the same expression as for the single-varactor amplifier:

$$|\Gamma_o| \; X_{3db} = \left[\frac{2}{1 + \frac{1}{K_o}}\right]\left[\frac{B_1}{1 + \frac{B_1}{B_2}[U] - \frac{B_1}{B_3}[V]}\right] \qquad \text{(VII-5)}$$

where

$$U = \left[\frac{1}{1 - \frac{f_2(1+K_2)}{f_3(1+K_3)}}\right]$$

and

$$V = \left[\frac{1}{\frac{f_3(1+K_3)}{f_2(1+K_2)} - 1}\right]$$

Equation VII-5 is the gain-bandwidth product of balanced reflection-type parametric amplifier when sum-frequency propagation is allowed.

This result is reasonable, because the Q's of all of the resonant circuits are taken to be the same as in the single-diode paramp and, therefore, all bandwidth relations will be the same.

Although, ideally, the gain-bandwidth products are the same in the single-diode and balanced configurations, the physical realization of the balanced configuration yields a greater gain-bandwidth product. Figure VII-1 is a photograph of a single-diode paramp showing the varactor in a chuck that is a capacitive stub in the idler circuit. This additional capacitance increases the Q of the idler circuit (Q_2) and, therefore, decreases the gain-bandwidth of the single-diode paramp.

Figure VII-2 illustrates that the idler stub is unnecessary in a balanced paramp, because the two varactors can be biased and excited by the signal through a thin piece of metal foil that is crushed between the two varactors. In reference 6, relations are given for the gain-bandwidth products of a single-diode parametric amplifier, accounting for the idler stub with no sum propagation, and of a balanced paramp with no sum propagation.

For a single varactor paramp,

$$\left|\Gamma_o\right| X_{3db} = \left[\frac{C_1\sqrt{f_1 f_2}}{C_o}\right]\left[\frac{2}{\left(1+\frac{C_S}{C_o}\right)\left[\frac{f_2}{M}\left(\frac{f_2}{f_1}\right)^{1/2}+\frac{M}{f_2}\left(\frac{f_1}{f_2}\right)^{1/2}+\frac{\pi}{\sqrt{2}}\right]}\right] \qquad \text{(VII-6)}$$

where $\left|\Gamma_o\right| X_{3db}$ = mid-band voltage gain-bandwidth product

C_o and C_1 = fourier coefficients of C(t)

C(t) = time varying capacitance of pumped varactor

C_s = stray case capacitance

f_1 = signal frequency

f_2 = idler (difference) frequency

M = varactor figure-of-merit.

For a balanced paramp,

$$\left|\Gamma_o\right| X_{3db} = \left[\frac{C_1\sqrt{f_1 f_2}}{C_o}\right]\left[\frac{2}{(1+\frac{C_s}{C_o})\left[\frac{f_2}{M}\left(\frac{f_2}{f_1}\right)^{1/2} + \frac{M}{f_2}\left(\frac{f_1}{f_2}\right)^{1/2}\right]}\right] \quad \text{(VII-7)}$$

The term $\frac{\pi}{\sqrt{2}}$ in equation VII-6 is the degradation in gain-bandwidth product due to the idler stub. Typically, the gain-bandwidth product of the balanced paramp is about 30 per cent greater than that of the single-diode paramp.

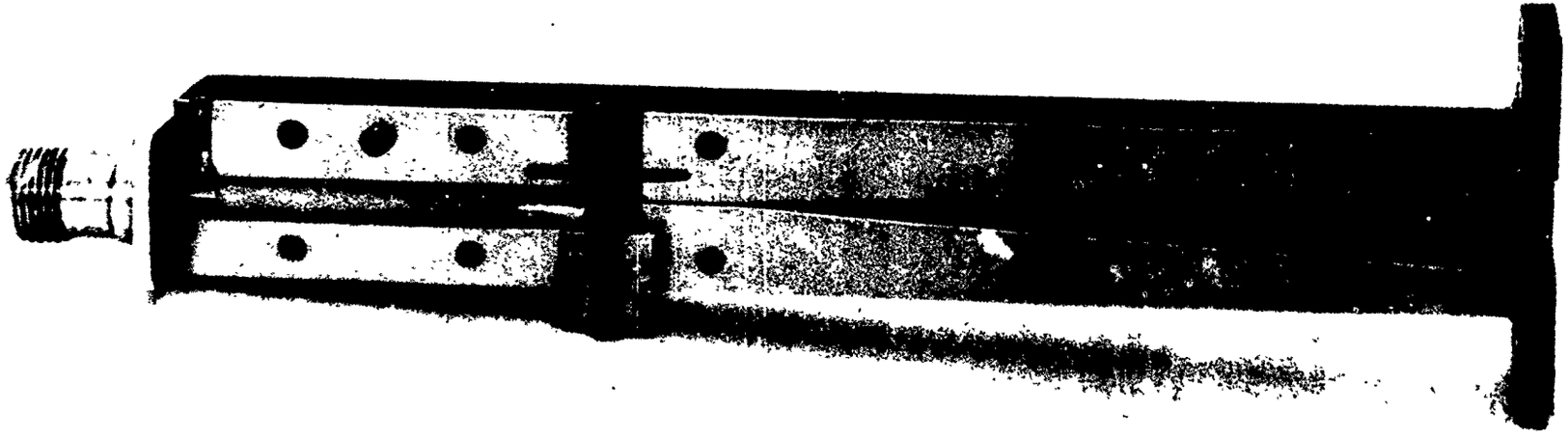

FIGURE VII-1. SINGLE DIODE PARAMETRIC AMPLIFIER

FIGURE VII-2. BALANCED PARAMETRIC AMPLIFIER

APPENDIX VIII

DERIVATION OF NOISE TEMPERATURE FOR BALANCED REFLECTION-TYPE PARAMETRIC AMPLIFIER WITH SUM-FREQUENCY PROPAGATION

A. INTRODUCTION

The technique of derivation will be the same as that used in Appendix IV. The model that will be used in the balanced paramp analysis is:

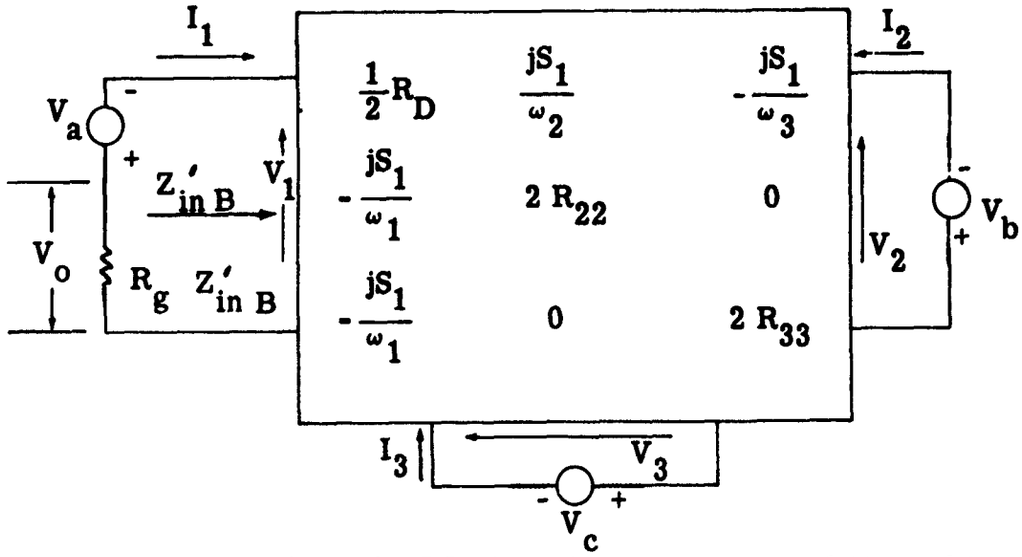

As in Appendix IV, the noise output power delivered to a matched load through a circulator, exclusive of the noise contributed by the generator, can be calculated by considering separately the contributions to I_1 of each of the three noise generators and then adding them by linear superposition.

B. NOISE OUTPUT POWER DUE TO V_a

$$V_o = \frac{V_a R_g}{R_g + Z'_{inB,\,m}} = \frac{V_a R_g 2}{R_D \left[1 + 2K_o + \frac{M^2}{f_1 f_3 (1+K_3)} - \frac{M^2}{f_1 f_2 (1+K_2)} \right]} \quad \text{(VIII-1)}$$

The term $Z'_{inB,\,m}$ was derived in Appendix VI.

$$\left|N_{oa}\right| = \frac{\overline{\left|V_o\right|^2}}{R_g} = \left| \frac{\overline{\left|V_a\right|^2}\ 4}{R_D^{\,2}\left[1 + 2K_o + \frac{M^2}{f_1 f_3 (1+K_3)}\ \frac{M^2}{f_1 f_2 (1+K_2)}\right]^2} \right| \qquad \text{(VIII-2)}$$

where N_{oa} = noise output due to V_a.

C. NOISE OUTPUT POWER DUE TO V_b

$$\begin{bmatrix} -V_o \\ -V_b^* \\ 0 \end{bmatrix} = \begin{bmatrix} \frac{1}{2}R_D & Z_{12} & Z_{13} \\ Z_{21} & 2R_{22} & 0 \\ Z_{31} & 0 & 2R_{33} \end{bmatrix} \begin{bmatrix} I_{1B} \\ I_2^* \\ I_3 \end{bmatrix} \qquad \text{(VIII-3)}$$

Solving equation VIII-3 for I_{1b}:

$$I_{1b} = \frac{V_b^*\, Z_{12} R_{33}}{2R_g R_{22} R_{33} + R_D R_{22} R_{33} - R_{22} Z_{13} Z_{31} - R_{33} Z_{12} Z_{21}} \qquad \text{(VIII-4)}$$

Substituting back in elastance notation,

$$I_{1b} = \frac{j\ V_b^*\, R_{33}\, \frac{S_1}{\omega_2}}{\left(R_D R_{22} R_{33} + 2R_g R_{22} R_{33} - R_{22}\, \frac{S_1^{\,2}}{\omega_1 \omega_3} + R_{33}\, \frac{S_1^{\,2}}{\omega_1 \omega_2}\right)} \qquad \text{(VIII-5)}$$

$$\left|N_{ob}\right| = \left|I_{1b}\right|^2 R_g \qquad \text{(VIII-6)}$$

$$\left|N_{ob}\right| = \left| \frac{\overline{\left|V_b\right|^2}\ R_g M^2}{f_2^{\,2} R_{22}^{\,2}\left[1 + 2K_o - \frac{M^2}{f_1 f_3 (1+K_3)} + \frac{M^2}{f_1 f_2 (1+K_2)}\right]} \right| \qquad \text{(VIII-7)}$$

Similarly,

$$\left|N_{oc}\right| = \left|I_{1c}\right|^2 R_g = \left| \frac{\overline{\left|V_c\right|^2}\, R_g M^2}{f_3^2 R_{22}^2 \left[1 + 2K_o - \frac{M^2}{f_1 f_3 (1+K_3)} + \frac{M^2}{f_1 f_2 (1+K_2)}\right]^2} \right| \qquad \text{(VIII-8)}$$

By linear superposition,

$$\left|N_o\right| = \left|N_{oa}\right| + \left|N_{ob}\right| + \left|N_{oc}\right| \qquad \text{(VIII-9)}$$

$$\left|N_o\right| = \left| \frac{R_g}{\left[1 + 2K_o - \frac{M^2}{f_1 f_3 (1+K_3)} + \frac{M^2}{f_1 f_2 (1+K_2)}\right]^2} \right. \qquad \text{(VIII-10)}$$

$$\left. \cdot \left[\frac{4\overline{\left|V_a\right|^2}}{R_D^2} + \frac{\overline{\left|V_b\right|^2} M^2}{R_{22}^2 f_2^2} + \frac{\overline{\left|V_c\right|^2} M^2}{R_{33}^2 f_3^2} \right] \right|$$

Since,

$$\overline{\left|V_a\right|^2} = 2\,k\,T_o\,X_{3db}\,R_D$$

$$\overline{\left|V_b\right|^2} = 8\,k\,T_o\,X_{3db}\,R_{22}$$

$$\overline{\left|V_c\right|^2} = 8\,k\,T_o\,X_{3db}\,R_{33}$$

$\left|N_o\right|$ can be rewritten:

$$\left|N_o\right| = \left| \frac{8k\,T_o\,X_{3db}\,K_o}{\left[1 + 2K_o + \frac{M^2}{f_1 f_3(1+K_3)} - \frac{M^2}{f_1 f_2(1+K_2)}\right]^2} \right. \qquad \text{(VIII-11)}$$

$$\left. \cdot \left[1 + \frac{M^2}{f_2^{\,2}(1+K_2)} + \frac{M^2}{f_3^{\,2}(1+K_3)}\right] \right|$$

The effective noise temperature of the paramp (T_e) is given by:

$$T_e = \frac{|N_o|}{k\,|\Gamma_o|^2\,X_{3db}} \qquad \text{(VIII-12)}$$

Substituting equation VIII-11 into equation VIII-12:

$$T_e = \frac{8\,T_o K_o}{\left[1 - 2K_o + \frac{M^2}{f_1 f_3(1+K_3)} - \frac{M^2}{f_1 f_2(1+K_2)}\right]^2} \qquad \text{(VIII-13)}$$

$$\cdot \left[1 + \frac{M^2}{f_2^{\,2}(1+K_2)} + \frac{M^2}{f_3^{\,2}(1+K_3)}\right]$$

Using the high-gain condition of,

$$\frac{M^2}{f_1 f_2(1+K_2)} - \frac{M^2}{f_1 f_3(1+K_3)} = 1 + 2K_o$$

equation VIII-13 reduces to:

$$T_e = \frac{T_o}{2K_o}\left[1 + \frac{M^2}{f_2^{\,2}(1+K_2)} + \frac{M^2}{f_3^{\,2}(1+K_3)}\right] \qquad \text{(VIII-14)}$$

Normalizing the resistors to those used in the single-diode analysis ($\frac{1}{2}R_D$ is substituted for R_D, $2R_{22}$ for R_{22}, and $2R_{33}$ for R_{33}) yields:

$$T_e = \frac{T_o}{K_o}\left[1 + \frac{M^2}{f_2^{\,2}(1+K_2)} + \frac{M^2}{f_3^{\,2}(1+K_3)}\right] \qquad \text{(VIII-15)}$$

Equation VIII-15 gives the mid-band noise temperature of a balanced reflection-type parametric amplifier when sum frequency propagation is allowed.

Unclassified
Security Classification

DOCUMENT CONTROL DATA - R&D

(Security classification of title, body of abstract and indexing annotation must be entered when the overall report is classified)

1. ORIGINATING ACTIVITY (Corporate author) Airborne Instruments Lab	2a. REPORT SECURITY CLASSIFICATION Unclassified 2b GROUP

3 REPORT TITLE
Preferred Circuit Techniques for Reflection-Type Parametric Amplifiers

4. DESCRIPTIVE NOTES (Type of report and inclusive dates)
Interim Technical Report

5. AUTHOR(S) (Last name, first name, initial)
Kaye, David

6. REPORT DATE	7a. TOTAL NO. OF PAGES	7b. NO. OF REFS
June 1966	140	13

8a. CONTRACT OR GRANT NO.	9a. ORIGINATOR'S REPORT NUMBER(S)
AF30(602)-3583 b. PROJECT NO. 4540 c. TASK: 454002 d.	9b. OTHER REPORT NO(S) (Any other numbers that may be assigned this report) RADC-TR-66-306

10. AVAILABILITY/LIMITATION NOTICES
This document is subject to special export controls and each transmittal to foreign governments or foreign nationals may be made only with prior approval of RADC (EMLI), GAFB, N.Y. 13440.

11. SUPPLEMENTARY NOTES	12. SPONSORING MILITARY ACTIVITY
None	RADC (EMCVI-1) Griffiss AFB, N.Y. 13440

13. ABSTRACT

This report describes the development and analysis of preferred circuit techniques for the reduction of certain RFI effects in reflection - type parametric amplifiers.

Emphasis is placed on reducing spurious responses and increasing the saturation power of paramps. Some of the preferred-circuit techniques are incorporated in experimental models and extensive measurements are reported which support the theoretical predictions of the effects of intermodulation products on paramp performance and the effect of the balanced configuration on spurious responses. Many additional characteristic of the models are described.

DD FORM 1 JAN 64 1473

Unclassified
Security Classification

14. KEY WORDS	LINK A		LINK B		LINK C	
	ROLE	WT	ROLE	WT	ROLE	WT
Solid State Components RFI Parametric Amplifiers						

INSTRUCTIONS

1. ORIGINATING ACTIVITY: Enter the name and address of the contractor, subcontractor, grantee, Department of Defense activity or other organization *(corporate author)* issuing the report.

2a. REPORT SECURITY CLASSIFICATION: Enter the overall security classification of the report. Indicate whether "Restricted Data" is included. Marking is to be in accordance with appropriate security regulations.

2b. GROUP: Automatic downgrading is specified in DoD Directive 5200.10 and Armed Forces Industrial Manual. Enter the group number. Also, when applicable, show that optional markings have been used for Group 3 and Group 4 as authorized.

3. REPORT TITLE: Enter the complete report title in all capital letters. Titles in all cases should be unclassified. If a meaningful title cannot be selected without classification, show title classification in all capitals in parenthesis immediately following the title.

4. DESCRIPTIVE NOTES: If appropriate, enter the type of report, e.g., interim, progress, summary, annual, or final. Give the inclusive dates when a specific reporting period is covered.

5. AUTHOR(S): Enter the name(s) of author(s) as shown on or in the report. Enter last name, first name, middle initial. If military, show rank and branch of service. The name of the principal author is an absolute minimum requirement.

6. REPORT DATE: Enter the date of the report as day, month, year; or month, year. If more than one date appears on the report, use date of publication.

7a. TOTAL NUMBER OF PAGES: The total page count should follow normal pagination procedures, i.e., enter the number of pages containing information.

7b. NUMBER OF REFERENCES: Enter the total number of references cited in the report.

8a. CONTRACT OR GRANT NUMBER: If appropriate, enter the applicable number of the contract or grant under which the report was written.

8b, 8c, & 8d. PROJECT NUMBER: Enter the appropriate military department identification, such as project number, subproject number, system numbers, task number, etc.

9a. ORIGINATOR'S REPORT NUMBER(S): Enter the official report number by which the document will be identified and controlled by the originating activity. This number must be unique to this report.

9b. OTHER REPORT NUMBER(S): If the report has been assigned any other report numbers *(either by the originator or by the sponsor)*, also enter this number(s).

10. AVAILABILITY/LIMITATION NOTICES: Enter any limitations on further dissemination of the report, other than those imposed by security classification, using standard statements such as:

(1) "Qualified requesters may obtain copies of this report from DDC."

(2) "Foreign announcement and dissemination of this report by DDC is not authorized."

(3) "U. S. Government agencies may obtain copies of this report directly from DDC. Other qualified DDC users shall request through

_____.

(4) "U. S. military agencies may obtain copies of this report directly from DDC. Other qualified users shall request through

_____."

(5) "All distribution of this report is controlled. Qualified DDC users shall request through

_____."

If the report has been furnished to the Office of Technical Services, Department of Commerce, for sale to the public, indicate this fact and enter the price, if known.

11. SUPPLEMENTARY NOTES: Use for additional explanatory notes.

12. SPONSORING MILITARY ACTIVITY: Enter the name of the departmental project office or laboratory sponsoring *(paying for)* the research and development. Include address.

13. ABSTRACT: Enter an abstract giving a brief and factual summary of the document indicative of the report, even though it may also appear elsewhere in the body of the technical report. If additional space is required, a continuation sheet shall be attached.

It is highly desirable that the abstract of classified reports be unclassified. Each paragraph of the abstract shall end with an indication of the military security classification of the information in the paragraph, represented as *(TS), (S), (C), or (U)*

There is no limitation on the length of the abstract. However, the suggested length is from 150 to 225 words.

14. KEY WORDS: Key words are technically meaningful terms or short phrases that characterize a report and may be used as index entries for cataloging the report. Key words must be selected so that no security classification is required. Identifiers, such as equipment model designation, trade name, military project code name, geographic location, may be used as key words but will be followed by an indication of technical context. The assignment of links, rules, and weights is optional